AN ABSTRACT OF THE THESIS OF

David W. Wendland for the degree of Master of Science in

Geology presented on April 1, 1988.

Title: Castle Rocks: a Late Miocene Eruptive Center at the North

End of Green Ridge, Jefferson County, Oregon

Redacted for privacy

Abstract approved:

Dr. Edward M. Taylor

Castle Rocks is 12 miles east of Mt. Jefferson, in the central Cascades of Oregon. The area contains volcanic rocks ranging from mid-Miocene to Holocene in age. These rocks record alternating periods of tholeiitic and calc-alkaline volcanism.

The oldest rocks in the area range from basaltic andesite lava flows to fayalite-bearing dacite breccias, and are best exposed near the confluence of the Metolius and Whitewater rivers. Petrographic and compositional evidence indicates that the dacites are highly differentiated products of a tholeiitic fractionation trend. The dacites were apparently derived from basalt by the fractionation of olivine, clinopyroxene and plagioclase.

The most prominent feature of the thesis area is the remnant of a calc-alkaline composite volcano of late Miocene age. The center of the volcano is marked by a pyroxene andesite plug near the north end of Green Ridge. This "Castle Rocks Volcano" produced andesitic lava flows and pyroclastic rocks characterized by abundant hornblende phenocrysts. Compositional trends are consistent with fractionation

of hornblende, clinopyroxene and possibly plagioclase.

The Castle Rocks Volcano is unconformably overlain by ash-flow tuffs and basaltic andesite lavas of the Deschutes Formation. The unconformity represents a period of change from compressional to extensional tectonics. Deschutes Formation rocks show tholeiitic compositional trends, apparently produced by the fractionation of olivine, clinopyroxene and plagioclase.

North-south normal faulting on the Green Ridge fault system terminated deposition of the Deschutes Formation at about 5.4 Ma. Three parallel faults in the thesis area are spaced about 0.5 miles apart. Maximum displacement is about 2200 ft, in the southern part of the thesis area, and decreases to a negligible amount at the confluence of the Metolius and Whitewater rivers.

High Cascade rocks representing two magma types erupted after the episode of normal faulting. Subduction-related, calc-alkaline basaltic andesites are confined to the area west of the Green Ridge fault scarp. They show compostional patterns very similar to those of the Castle Rocks Andesites, but are less phyric and lack hornblende. Diktytaxitic basalts spread east to the north of the Green Ridge fault scarp to form Metolius Bench. Younger diktytaxitic basalts flowed down the canyon of the Metolius River.
The diktytaxitic basalts are unrelated to the High Cascade basaltic andesites. Instead, they are similar to extension-related high alumina olivine tholeiites of the northwestern Great Basin.

Castle Rocks: a Late Miocene Eruptive Center at the
North End of Green Ridge, Jefferson County, Oregon

by

David W. Wendland

A THESIS

submitted to

Oregon State University

in partial fulfillment of
the requirements for the
degree of

Master of Science

Completed April 1, 1988

Commencement June 1989

APPROVED:

Redacted for privacy

Associate professor of Geology in charge of major

Redacted for privacy

Head of Department of Geology

Redacted for privacy

Dean of Graduate School

Date thesis is presented ___1 April, 1988___

Table of Contents

LIST OF FIGURES

LIST OF TABLES

CASTLE ROCKS: A LATE MIOCENE ERUPTIVE CENTER AT THE NORTH END OF GREEN RIDGE, JEFFERSON COUNTY, OREGON

Introduction

Location and geologic setting

Castle Rocks is a 520 foot (158 m) vertical cliff of hornblende andesite tuff-breccia on the north end of Green Ridge, in Jefferson County, Oregon. Because Castle Rocks itself is not accessible, or generally visible from any road, the name "Castle Rocks" is often mistakenly applied to an imposing, but unnamed plug of pyroxene andesite one mile to the north. Both plug and breccia are products of a late Miocene volcano, centered within the bend of the Metolius River, as seen in Figure 1. This volcano is informally referred to in this paper as the "Castle Rocks Volcano". Lavas and pyroclastic rocks from the Castle Rocks Volcano underlie most of the 31 mi^2 (80 Km^2) mapped in this study.

The southern part of Green Ridge is composed of lavas and pyroclastic rocks of the Deschutes Formation. This study concerns the northern end of Green Ridge, where the Deschutes Formation banks up against older andesites from the Castle Rocks Volcano. The west face of Green Ridge is a fault scarp, and marks the boundary between the Deschutes Basin and the High Cascades. West of the Metolius River, most Deschutes Formation rocks have been downfaulted and buried by Quaternary lavas of the High Cascades.
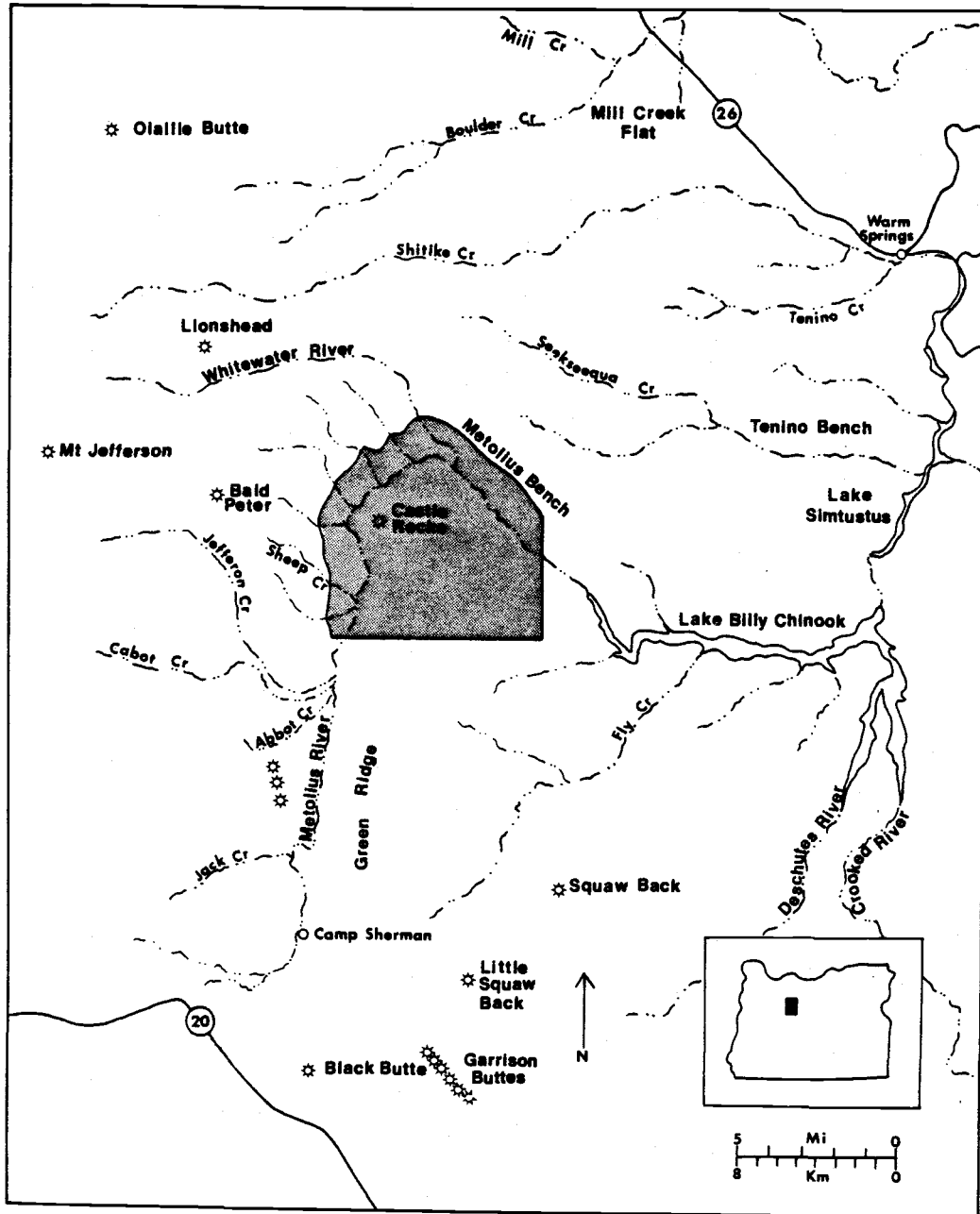
Figure 1. Location map.

Relief, exposure and access

Maximum elevation in the study area is 5160 ft (1573 m), at the top of Green Ridge. The minimum elevation is 2080 ft (634 m), along the Metolius River, making the total relief 3080 ft (940 m). Local relief encountered from the crest of the ridge west to the river, averages 2200 ft (670 m), over a distance of about 1.25 miles (2 km). West of the river, gently dipping High Cascades lavas form a bench at about 3600 ft elevation (1100 m), 1200 ft (366 m) above river level.

Topography on the east side of Green Ridge is gentler, dropping 2000 ft (610 m) in about 3 miles (4.8 km). The east side of Green Ridge is covered with pine forests, and exposures are limited. Exposures are better on the steeper western face. All but the steepest of north-facing slopes are covered with douglas fir forests, while south-facing slopes support dense manzanita thickets. The general effect is one of isolated cliffs and ledges separated by brush-or-forest covered talus slopes. As a result, actual contacts are rarely seen.

All of the land within the bend of the Metolius is under U.S. Forest Service management. The crest of Green Ridge and its eastern slopes are accessible by Forest Service roads or fire trails. Two river-level roads follow the Metolius along the eastern and western flanks of Green Ridge, but do not meet at its northern end. The steep northern and western slopes are accessible only on foot.

The area west and north of the Metolius is part of the Warm

Springs Indian Reservation. Permission to travel must be granted by tribal authorities. Logging roads lead to the canyon rim, but access to the Metolius and Whitewater canyons is on foot only.

Previous work

C.E. Dutton (1889) was the first geologist to describe the Metolius River Canyon. Dutton found little of interest, commenting only on the difficulty of access and the curious north-south course of the river.

Hodge (1928) was the first to suggest a reason for the river's behavior, hinting at a fault in the area. Later, he referred to "a fault on the west side of Green Ridge", and speculated that it might be related to faults near Hood River and Klamath Falls (Hodge, 1938).

In 1942, Hodge discussed the Pliocene "Dalles Formation". Noting that this prism of volcanic debris thickened towards the Cascades, Hodge postulated that its source area must have been in that direction. In the same paper, Hodge described the diktytaxitic olivine basalts of the Metolius Canyon, and recognized them as intracanyon flows. No mention was made of a Green Ridge Fault.

Williams (1957) showed a fault on the west face of Green Ridge. He also described the complex of pyroxene and hornblende-andesite lavas and dikes at the north end of the ridge, believing them to be "pre-Pliocene".

The compilation map of Wells and Peck (1961) shows a "Metolius Fault" on the west face of Green Ridge, curving to the southeast and extending to Bend. The same map shows a northwest-trending fault

passing through the intersection of the Metolius and Whitewater Rivers. The same fault is shown, extended to the southeast, on a map by Waters (1968).

Wells and Peck (1961) misidentified the diktytaxitic intracanyon flows as Columbia River Basalt. Dacites, andesites and basaltic andesites at the junction of the Whitewater and Metolius Rivers are identified as a "mafic intrusive" on the same map.

Hales (1975) was the first to map the north end of Green Ridge in detail, recognizing that the area was the former site of a "hornblende andesite stratovolcano", centered on a plug in T11S, R10E, Sec 6. According to Hales, products of this volcano show a progressive change from early, hornblende-rich to later, pyroxene-rich andesites. Hornblende was believed absent from the youngest rocks, due to a progressive pressure reduction in the magma chamber.

Hales also carried out a program of radiometric dating, in which the hornblende-andesite volcano was dated as late Miocene (8.1 $\pm$0.6 Ma). Other radiometric dates established the age of activity on the Green Ridge Fault. Hales dated the youngest rocks cut by the fault at 4.5 $\pm$0.4 Ma (recalculated to 4.7 $\pm$ 0.4 Ma by Fiebelkorn and others, 1982). Hales believed that motion on the Green Ridge Fault separated High Cascade volcanism from Deschutes activity.

Several OSU MS theses on adjacent areas have recently been completed. Conrey (1985) studied the part of Green Ridge immediately to the south of the thesis area. Yogodzinski (1985) studied the Deschutes-High Cascade transition in the Whitewater canyon (Fig. 1). Dill (in prep.) mapped in the Deschutes Basin immediately to the east. Some units of Castle Rocks age are found in the lowest parts of

the section studied by Yogodzinski (1985).

Purpose of study

One end product of a field oriented geologic study is an accurate geologic map. On Green Ridge, such a map would answer several questions: first, how much motion has occured on this segment of the Green Ridge Fault?; second, does the Green Ridge Fault continue north of the Metolius River?; third, what is the evidence for a northwest-trending fault in the lower Whitewater canyon?

Another objective was to chemically and petrographically characterize rocks from the Castle Rocks Volcano. If Castle Rocks was a Deschutes Formation source volcano, it might be possible to recognize its products in the sedimentary section.

Field and analytical methods

Mapping was done in the field on advance-print topographic maps at a scale of 1:24,000. Elevations were determined to ±20 feet using a Thommen pocket altimeter. Aerial photographs at a scale of 1:62,000 were used for route finding and location of outcrops. A flux-gate magnetometer was used to determine magnetic polarity of oriented samples.

Thin sections of 140 rocks were prepared, and used to determine texture and modal mineralogy. Modes of selected samples were determined by point-counting at least 700 points, using a mechanical

stage. The relationship between accuracy and the number of points counted is discussed by Van Der Plas and Tobi (1965). Plagioclase feldspar compositions were estimated optically, using the Michel-Levy, Carlsbad-albite and A-Normal methods.

Major-element chemical analyses were performed on 86 samples. X-ray Fluorescence Spectrometry (XRF) was used to determine contents of Fe, Ti, Ca, K, Si and Al. Na and Mg contents were determined by Atomic Absorption Spectrophotometry(AA). All major element XRF analyses were performed by the author. AA analyses were performed by the author or by E.M. Taylor. Richard Conrey of Washington State University analyzed fifteen samples for Cr, Ni, Sc, Va, Ba, Rb, Sr, Zr, Y, Nb, Ga, Cu and Zn, using XRF methods, and also performed the microprobe analyses shown in Tables 1 and 2. Details of analytical procedures can be found in Appendix 1.

Nomenclature of Rocks and Map Units

The International Union of Geological Sciences Commission of Petrology has proposed a system of igneous rock nomenclature based on modal mineralogy (Streckeisen, 1979). Such a system is difficult to apply to volcanic rocks, because of their fine-grained or glassy groundmass. Complex plagioclase zoning, and presence of more than one type of plagioclase make application of a mineralogical classification even more difficult. This paper uses instead, a classification based on the weight percent SiO_2 of chemically

analyzed rocks (Taylor, 1978) as follows:

     Basalt...............48-53%

     Basaltic andesite....53-58%

     Andesite.............58-63%

     Dacite...............63-68%.

     Rhyodacite............>68%

     Rhyolite..............>73%, and K_2O >4%

Pyroclastic deposits are named according to Fisher (1966).
Petrographic terminology is often inconsistently applied in earth
science literature. This paper follows the usage of Bates and
Jackson (1980).

Map units are grouped under several major headings: Quaternary
(Q), High Cascade (HC), Deschutes Formation (DF), Pre-Deschutes
Formation rocks of uncertain affinity (PDF), Castle rocks (CR), and
Pre-Castle Rocks (PCR). The prefixes Q (Quaternary) and T (Tertiary)
indicate age. Individual map units are numbered, mainly for purposes
of identification. Although map units are numbered and described in
an overall older to younger sequence, a strict stratigraphic
succession is not implied.

Cenozoic Volcanism in the Cordillera

Subduction-related, calc-alkaline rocks dominate the early Cenozoic volcanic history of the Cordillera. These rocks were erupted onto an Andean-type continental margin, established in the mid Triassic (Dickinson, 1976). In late Oligocene, subduction related volcanism ceased in New Mexico and Arizona, to be replaced by bimodal basalt and rhyolite related to extension. The locus of change migrated northwest in the United States, reaching Oregon by mid Miocene (Christiansen & Lipman, 1972). Subduction-related activity has continued into historical time in the Cascades, contemporaneous with bimodal volcanism east of the mountains. Space-time patterns of Cenozoic magmatism in the Pacific Northwest are summarized below.

Paleocene

Volcanic rocks of this age are rare in the Pacific Northwest. Late Paleocene basalts are found in the southern Oregon Coast Range and on Vancouver Island. Inland, volcanic rocks are confined to scattered areas such as the Adel and Little Rocky Mountains in Montana, dated at 65 and 66-58 Ma, respectively (Ewing, 1980), and the Black HIlls of Wyoming, 59-50 Ma (Armstrong, 1978).

Eocene

The Eocene was a period of widespread arc volcanism on the

continent, and marine activity off of the coast.

Eocene volcanic rocks of the Coast Ranges are found today from southern Vancouver Island to southern Oregon. In Oregon, tholeiitic pillow basalts and marine sediments of the lower Eocene Roseburg Formation and Siletz River Volcanics are capped by terrestrial alkalai basalts (Magill, et al, 1981; Snavely, et al, 1968). In the Olympic mountains, Eocene pillow basalts of the Crescent Formation appear correlative. The exact origin of these rocks is still unclear, but it is generally believed that they represent oceanic islands or seamounts accreted to the North American plate (Snavely & McLeod, 1974; Cady, 1975). Accretion was probably complete by mid-Eocene (Magill, et al, 1981).

On the continent, Eocene magmatism is represented by intrusive rocks in northern British Columbia, with volcanics becoming more common in the central part of the province. Continuing south, the volcanic belt widens, including the Sampoil Volcanics of northeast Washington, the Challis Volcanics in Idaho and the Absaroka Volcanics in Montana. This wide zone of Eocene calc-alkaline volcanism is known as the "Challis Arc". The inward sweep of volcanism was apparently in response to high Farallon/North American plate convergence rates, and slab dips as low as 10° (Coney & Reynolds, 1977).

Activity on the Challis Arc began about 53 Ma, reached its peak at about 51-48 Ma, and had nearly ceased by 42Ma (Ewing, 1980). Although some activity continued until about 36 Ma (Armstrong, 1978), the locus of volcanism had begun a westward shift to the Cascades. The demise of the Challis Arc and westward shift of volcanism

coincided with a decrease in convergence rate, and an increase in slab dip (Coney & Reynolds, 1977).

The Clarno Formation of central Oregon is intermediate in both age and location between the Challis and Cascade arcs. Clarno activity began about 46 Ma (Enlows & Parker, 1972), and ended at about 36 Ma (Taylor, 1981a).

The Clarno consists of calc-alkaline volcanic and volcanogenic rocks, apparently originating from vents along the Blue Mts. uplift (Robinson, et al, 1984). Chemically and petrographically somewhat enigmatic, the Clarno has features common to both island arc and continental margin suites (Rogers & Novitsky-Evans, 1977). It is generally believed to have formed on thin continental crust, and may represent an intermediate position of the migrating volcanic front (Wells, et al, 1984).

Late Eocene-Oligocene

By late Eocene, arc volcanism had shifted from the Challis arc to the north-south belt of the Cascades. Magmatism in the north is represented by belts of plutons in British Columbia and northern Washington. Volcanic rocks become common farther south in the Cascades. Volcanic rocks of this age in Washington include the 41-39 Ma Naches Fm. (Ewing, 1980); the 36-30 Ma Ohanapecosh Fm.; and the 29-22 Ma Stevens Ridge Fm. (Wells, et al, 1984).

The oldest rock yet dated in the Cascades of Oregon is a basaltic andesite of 41 Ma from the Western Cascades (Lux, 1982). The Oligocene of the Western Cascades is characterized by abundant

silicic tuffs. The base of this sequence in the southern Oregon Cascades has been dated at 35 Ma (Smith, 1980).

John Day volcanism in north-central Oregon was partly coincident with activity in the Cascades, beginning about 37 Ma. John Day vents between the Cascades and Blue Mts. produced alkaline rhyolites, while alkalai-olivine basalts and trachyandesites erupted farther east (Robinson, et al, 1981).

During the early Oligocene, calc-alkaline volcanism of the Western Cascades was coeval with alkaline activity to the east. By about 25 Ma, alkaline volcanism east of the Cascades had ceased. John Day deposition continued until about 18 ma. Andesitic to dacitic airfall tuffs of early Miocene age in central Oregon apparently came from vents near the Cascade axis (Robinson, et al. 1984).

Miocene-Present

The Miocene was a time of major change in tectonic and volcanic regimes. The change from subduction to bimodal, extension related volcanism actually began in the Great Basin at about 29 Ma, with the collision of the East Pacific Rise and the North American Trench. Activation of the San Andreas Fault produced two triple junctions, which migrated northwest and southeast along the coast (Atwater, 1970). Since then, bimodal volcanism has spread northwest and southeast, due to extension associated with the lengthening San Andreas Fault system. Currently, the Pacific/Juan deFuca/North American triple junction is located west of Cape Mendocino,

California, and calc-alkaline volcanism in the western United States has been extinguished south of Mt. Lassen. Subduction related volcanism continued in the Cascades north of Mt. Lassen, modified by extension behind the arc.

Huge sheets of tholeiitic Columbia River Basalt were erupted between 17 and 13 Ma (Swanson, et al, 1979). Columbia River Basalt dike swarms trend between N10°W and N30°W, as do post-Oligocene dikes in the Great Basin (Taubeneck, 1970). This suggests that Basin-Range extension was active behind the Cascades Arc. The Steens and Owyhee Basalts of southeast Oregon were erupted at about the same time, but are alkali-olivine and high-alumina basalts, rather than tholeiites. They are associated with silicic tuffs, flows and domes (Walker, 1970), and are the first manifestations of bimodal volcanism as defined by Lipman and others (1972) in the Pacific Northwest.

Eruption of high-alumina and alkaline basalts, silicic lavas and ash flows has continued into the Holocene in the northwest Great Basin and Modoc Plateau. In the Modoc Plateau, the high-alumina olivine-tholeiites of this association show a general westward decrease in age (McKee, et al, 1983; Hart, et al, 1984). MacLeod, et al, (1975) noted a similar westward decrease in age of bimodal rhyolites between the Harney Basin and Newberry Caldera.

Activity has continued into historic times in the Cascades, with the production of isolated andesite-to-dacite stratovolcanoes.

Cascade Stratigraphy and the Deschutes Formation

Stratigraphy

Russel (1897) noted that the Cascade Range could be divided into
an older eroded range in the west and a series of younger, less
dissected peaks to the east. This two-fold division is still the
basis of Cascade stratigraphy. The Oregon Cascades can be divided
into Western Cascade and High Cascade physiographic provinces as
shown in Figure 2. The Western Cascades are composed of late Eocene
to early Pliocene volcanic rocks which are folded, altered and deeply
eroded. The High Cascades are late Pliocene to Holocene, and are
unconformable on the Western Cascades. High Cascade rocks are
relatively undeformed and unaltered.

Stratigraphic nomenclature of the Cascades (Thayer, 1939; Peck
et al, 1964; Hammond, 1979; White, 1980a) may be confusing, with
terms such as "Sardine Formation" and "Outerson Formation" being
inconsistently applied. Priest and others (1983) have provided an
excellent summary of Cascade stratigraphy and introduced a system of
informal time catagories for Cascade volcanism, summarized in Figure
3. Priest and others noted that the volcanic history of the central
Oregon Cascades can be divided into "episodes", during which the
overall composition of volcanic rocks was relatively constant.
Changes in overall composition seem to be separated by periods of
inactivity. This informal system has the advantage of avoiding the
confusing rock-stratigraphic nomenclature previously used in the
Cascades.
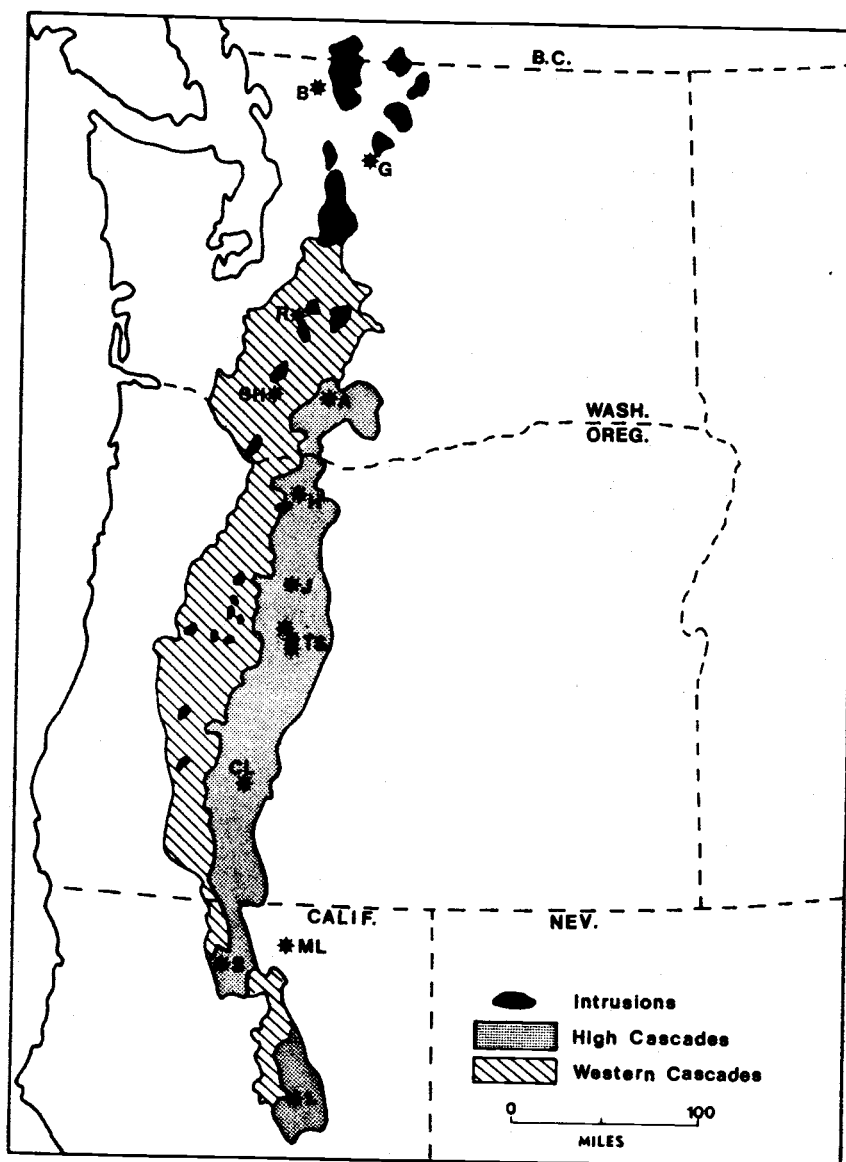
Figure 2. Generalized geologic map of the volcanic Cascade Range. B=Mt. Baker, G=Glacier Peak, R=Mt. Rainier, H=Mt. Hood, J=Mt. Jefferson, TS=Three Sisters, CL=Crater Lake, ML=Medicine Lake, S=Mt. Shasta, L=Mt. Lassen. After Hammond (1979).

THIS PAPER	PRIEST AND OTHERS	AGE	MAG	TIME m y

HIGH CASCADE

LATE HIGH CASCADE

DESCHUTES FORMATION

EARLY HIGH CASCADE

PRE-DESCHUTES
? ?

CASTLE ROCKS

? ?

PRE-CASTLE ROCKS

LATE WESTERN CASCADE

Pleistocene

Pliocene

Miocene

1
2
3
4
5
6
7
8
9
10
11
12
13
14
15
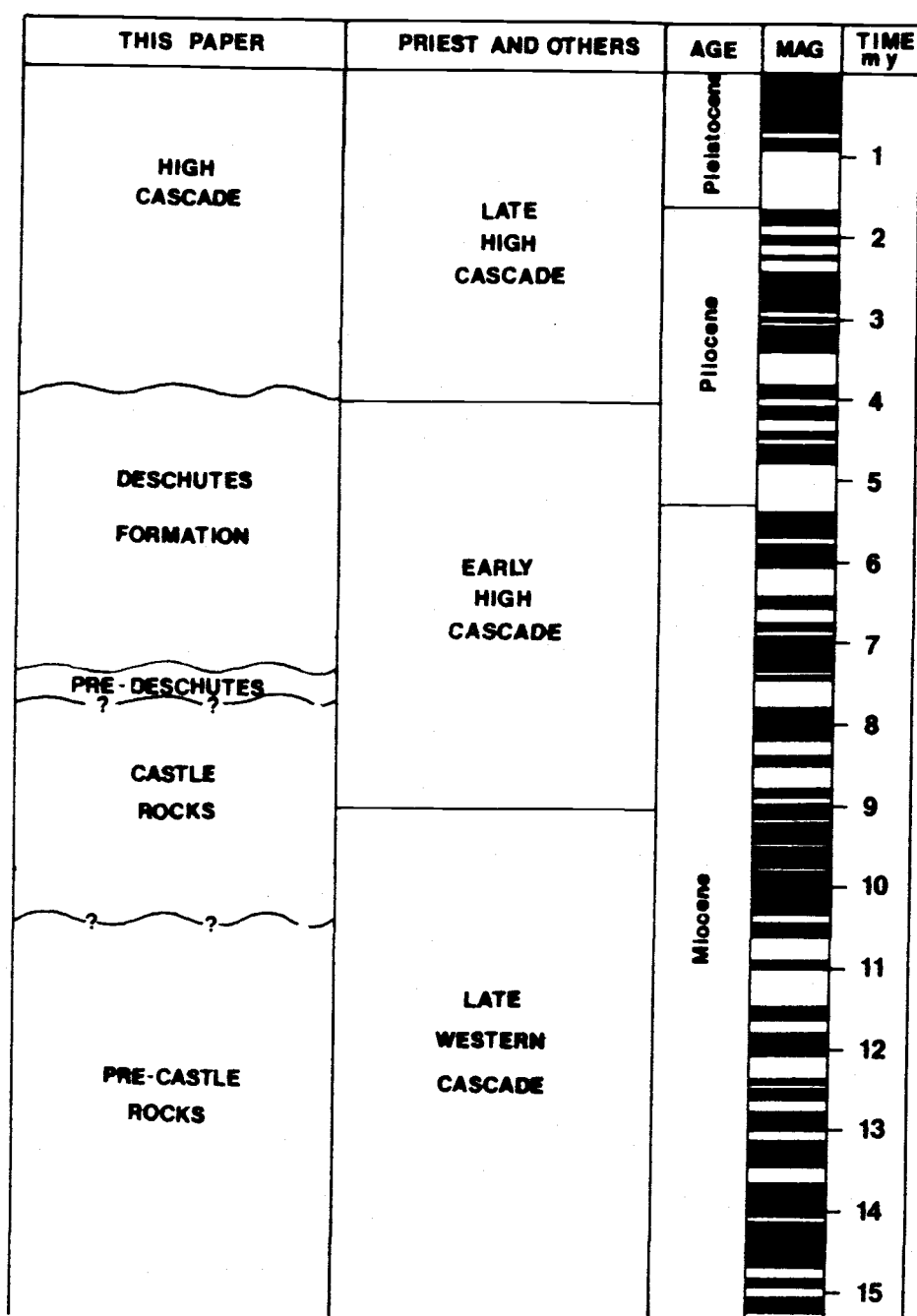
Figure 3. Stratigraphy used in this report compared to the nomenclature of Priest and others (1983), the geologic time scale, the magnetic time scale (Harland and others 1982), and the absolute time scale (Palmer, 1983).

Priest and others retain the basic "Western Cascades" and "High Cascades" division. The boundary between the two is placed at about 9 Ma, when a change from silicic to mafic volcanism coincided with an eastward shift of the volcanic axis.

Western Cascade volcanism can be divided into early and late episodes. The Early Western Cascades episode lasted from 40 to 18 Ma, and was dominantly silicic. Subordinate mafic lavas were strongly tholeiitic. Predominantly intermediate, calk-alkaline volcanism of the Late Western Cascades episode lasted until 9 Ma.

The Early High Cascades episode was marked by mafic volcanism. Many of these units were displaced by widespread normal faulting at 5-4 Ma. The Late High Cascades Episode began at about 4 Ma, after the faulting. Priest and others believe that Early and Late High Cascade rocks are compositionally similar. Late High Cascade rocks post-date faulting, and their distribution is contolled by current topography.

The Deschutes Formation

The Deschutes Formation is named for its type area, the Deschutes Basin, where it consists of volcaniclastic sediments and ash flows, with interbedded lava flows. Hodge (1942) suggested that its source was toward the Cascade range because it thickened markedly in that direction. In addition, the proportion of sediments decreases toward the Cascade axis, and basaltic andesite lava flows become predominant. Indicators of transport direction in Deschutes sediments also suggest a source to the west.

Various ages have been assigned to the Deschutes Formation. McBirney (1974) assigned the Deschutes Formation an age of 11-9 Ma, and equated it with the Sardine Formation of the Western Cascades. Farooqui and others, (1981) believed it to be mid-Miocene to Pliocene. Mid-Miocene ages for the Deschutes Formation are based on a K-Ar date of 15.9 $\pm$3.0 Ma for the Pelton Basalt (Armstrong, et al, 1975), near the base of the Deschutes Formation. A recent $^{40}Ar/^{39}Ar$ date (Smith & Snee, 1983) of 7.6 $\pm$0.3 Ma for the Pelton Basalt, and the presence of late Miocene fossils directly above it, suggest that the base of the Deschutes Formation is actually late Miocene.

The youngest Deschutes Formation lavas on Green Ridge are about 4.5 million years old (Hales, 1975). Shortly after their emplacement, normal faulting terminated deposition. Apparently, most Deschutes volcanism took place between about 7.5 and 4.5 Ma, during the Early High Cascades Episode of Priest and others (1983).

The oldest rocks yet dated from the High Cascade platform are about 4.3 million years old (Yogodzinski, 1983), and postdate the faulting which marked the end of Deschutes volcanism. Taylor (1981b) has postulated an earlier range of volcanoes, the "Plio-Cascades", as the source for the Deschutes Formation. The "Plio-Cascade" axis would have been near that of the High Cascades. This earlier range subsided along range-bounding faults, and must now lie buried beneath rocks of the High Cascades. One such boundary fault is the Green Ridge Fault. Taylor (1981b) suggested that the Castle Rocks Volcano may be the only Deschutes Formation source still exposed.

Description of Map Units

Pre-Castle Rocks Units

The oldest rocks on the north end of Green Ridge are reverse polarity lavas and pyroclastic breccias with minor associated epiclastic sedimentary rocks. Hales (1975) referred to these rocks as "Brown Glassy Dacites". This is a misnomer however, as compositions actually range from glassy dacite to holocrystalline basaltic andesite. In this paper, the more general term "Pre-Castle Rocks" will be used for units which are unconformably overlain by products of the Castle Rocks volcano.

The most extensive Pre-Castle Rocks outcrops are near the confluence of the Whitewater and Metolius rivers; isolated exposures are found both up and downstream. North of the Whitewater, discontinuous exposures extend from river level to an elevation of 3140 feet (957 m), a vertical distance of 900 feet (275 m).

Pre-Castle Rocks units can be divided into three chemical types: basaltic andesite, andesite and dacite. Each is distinct from younger rocks of similar silica content. Stratigraphic relationships are unclear because contacts are not exposed. Individual outcrops consist of only one rock type, and outcrops are usually small and widely separated.

Basaltic andesite, andesite and dacite are all found in the deep canyon traversing Section 4, T.11S., R.10E. (locally known as Hubbards Draw). Although no contacts are exposed, basaltic andesite is topographically lowest and dacite is highest. Units will be

presented in this order, although stratigraphic significance is
uncertain.

Basaltic Andesite

Basaltic andesites are exposed in only two locations; both are
near river level on opposite sides of the Metolius River (Plate 1).

Basaltic Andesites north of the Metolius (TPCR 1)
Map unit TPCR1 is a single flow unit, with neither top nor bottom
exposed. Jointing is hackly at river level, becoming crudely platy
near the top of the outcrop. Exposed thickness is 60 feet (19 m),
with the top of the unit obscured by hornblende andesite talus.

Hand specimens are dark gray, dense, and glomeroporphyritic.
Plagioclase phenocrysts make up 20% of the mode, and may be assigned
to three populations. Clear plagioclases have a seriate size distri-
bution, from 3 mm down to groundmass size. Most show continuous
normal zoning, from labradorite at the core to andesine at the rim.

Sieve-textured plagioclases are highly variable. Most have
clear cores, surrounded by a band rich in glass inclusions. Clear
rims, if present, are less calcic than the cores. Other crystals
have an inclusion-rich core, oval in shape, surrounded by a clear
band with continuous normal zoning. Some large (up to 7 mm) sieve
textured plagioclase phenocrysts lack bands or cores charged with
tiny glass inclusions. Instead, bodies of glass and pyroxene follow
cleavages throughout the crystals, giving them a somewhat "graphic"
appearance.

A third type of plagioclase phenocryst is large, anhedral and lacks both inclusions and polysynthetic twinning. The cores of these phenocrysts have patchy zoning, surrounded by a band of complex oscillatory zoning. Crystal margins are deeply embayed, and the embayments filled with groundmass material.

Subhedral to anhedral clinopyroxene crystals up to 3 mm long make up about 5% of the mode. Many of these are prominently twinned, and poikilitically enclose plagioclase, olivine relicts and opaque Fe-Ti oxides.

Orthopyroxene phenocrysts are less common than clinopyroxene, and usually less than 1 mm long. These are subhedral and often rimmed with clinopyroxene.

Almost no olivine is present, but pseudomorphs after euhedral olivine make up about 1% of the rock. Pseudomorphs are up to 1.5 mm in diameter and are composed of fibrous olive-green bowlingite. A few have unaltered cores, and some of these show optic angles of about 90°. Opaque Fe-Ti oxides form equant microphenocrysts up to 0.5 mm in diameter.

Glomerocrysts are up to 7 mm in diameter, and contain most phenocryst phases. Orthopyroxene crystals are rimmed with clino-pyroxene only where in contact with the groundmass, and contain symplectic intergrowths of opaque Fe-Ti oxides. Clinopyroxene and olivine crystals are identical with those outside the glomerocrysts. Sieve textured plagioclases do not occur in glomerocrysts with pyroxene and olivine, although they tend to form clumps with other sieve-textured plagioclase.

The groundmass is a holocrystalline, felty mass of plagioclase

microlites with subordinate clinopyroxene, opaque Fe-Ti oxide granules and tiny rods of apatite.

Basaltic Andesites south of the Metolius (TPCR 2)

Map unit TPCR2 is a single outcrop of basaltic andesite exposed in Hubbards Draw. A ten foot exposure of crudely columnar basaltic andesite is vesicular near the top, and is overlain by 3 feet of scoriacious autobreccia. Like TPCR1, the outcrop consists of a single flow unit with neither top nor bottom exposed.

Hand specimens are dark gray, with phenocrysts of plagioclase and olivine. In contrast to TPCR1, no pyroxene phenocrysts are present. Vesicles are lined with a green clay mineral. In thin section, samples are porphyritic and hypohyaline. Plagioclase phenocrysts make up 10-15% of the mode, and two populations can be identified. Clear plagioclase phenocrysts are free of inclusions, up to 1.5 mm long, and show continuous normal zoning. Sieve-textured plagioclases are larger, up to 7 mm long, and crowded with tiny inclusions of glass and minor pyroxene along cleavage planes. Most sieve-textured plagioclase phenocrysts have a clear core surrounded by an inclusion-rich band. A thin, clear outer rim is usually present, with a lower An-content than the core.

Subhedral to anhedral olivine phenocrysts make up about 3% of the mode. Phenocrysts range from 0.1 to 1.5 mm in diameter and are usually altered to orange-red iddingsite. A few of the larger crystals have unaltered cores with a 2V of about 90°.

The groundmass is a turbid mass of plagioclase microlites, rods of clinopyroxene and minor brown glass. Abundant tiny orange blebs

appear to be opaque oxides, altered to hematite.

Andesite

Outcrops of Pre-Castle Rocks andesite generally parallel the course of the Metolius River around the north end of Green Ridge (Plate 1). Exposures are poor, and all andesites are treated here as members of two units. Map unit TPCR3 includes isolated outcrops of tuff-breccia, pyroclastic breccia, rare stringers of lava and a dike. Unit TPCR4 is a lava flow.

Breccias with Associated Lavas and Dike (TPCR 3)

Tuff-breccias dominate TPCR3 near the mouth of Rainy Creek, and on the northeast side of Green Ridge at the end of Forest Service road 113. Outcrops are generally poorly sorted, unstratified and composed of dense subangular blocks, usually in clast support. Block-sized clasts make up about 70% of the outcrop. The matrix is composed of lapilli and ash of similar lithology. From a distance, outcrops appear to be mudflow deposits. However, the lack of sedimentary structures and grading, and the uniform magnetic polarity, and monolithologic nature of the blocks suggest otherwise. These tuff-breccias appear to be near-vent airfall deposits.

Some pyroclastic breccias are over 90% subangular to subrounded blocks. Rarely, what appear to be broken pieces of single blocks form "trails" in the deposit. These outcrops probably represent autobrecciated lava flows, and often contain thin stringers of coherent lava less than 6 feet (2 m) thick.

Andesites of unit TPCR 3 can be divided into two petrographic types based on phenocryst content. Two-pyroxene andesites contain phenocrysts of orthopyroxene, clinopyroxene, plagioclase and olivine. In contrast, single-pyroxene andesites contain only clinopyroxene and plagioclase phenocrysts. Microphenocrysts of opaque Fe-Ti oxides are present in both types.

Total phenocryst content of two-pyroxene andesites varies from 4% to 30%. Plagioclase phenocrysts total between 3% and 21% of the rock, and have a seriate size distribution from about 4 mm to 0.25 mm long. Sieve-textured cores are usually surrounded by clear rims. Composition of the cores is about An_{55}; the normally zoned rims range from about An_{45} to An_{40}.

Subhedral olivine relicts make up less than 1% of the rocks. Iddingsite rims crystals and lines cracks, wheras cores of the same crystals are altered to yellowish-green bowlingite. Pyroxene phenocrysts total 3% or less. Orthopyroxene is euhedral to subhedral, prismatic and less than 1.5 mm long. Clinopyroxene forms stubby subhedral to anhedral phenocrysts less than 1 mm in length.

Opaque Fe-Ti oxides are present as equant microphenocrysts up to 0.25 mm in diameter. A few biotite microphenocrysts are present in DW381. Pseudohexagonal in outline, they are about 0.3 mm in diameter, and pleochroic in yellow-brown, golden-brown, and pale green. Extinction angles are about 3°.

Groundmass textures are intergranular to intersertal, with clinopyroxene needles, opaque Fe-Ti oxide grains and subordinate brownish glass occupying space between plagioclase microlites. Hyalopilitic to pilotaxitic groundmass textures are common.

Vesicles and fractures are lined with radial aggregates of fibrous, pale green material of low relief and low birefringence; probably celadonite or nontronite.

Single-pyroxene andesites usually contain 7-15% phenocrysts. Plagioclase is most common, serially distributed from 3 mm to 0.5 mm in length. Most have sieve-textured cores, with thin, clear, normally zoned rims.

The only other phenocryst phase is clinopyroxene, making up less than 2% of the mode. Clinopyroxenes are euhedral to anhedral, and less than 1 mm in length.

Groundmass textures are intersertal to intergranular. Samples from lava flows are hyalopilitic and trachytoid, wheras dikes show no preferred orientation. Anhedral clinopyroxene grains and brown glass occupy the spaces between plagioclase grains in lava flows. Glass is rare in dikes.

Near the confluence of the Metolius and Whitewater Rivers, a 2.5 foot (0.8 m) thick dike of Pre-Castle Rocks andesite striking S60°E and dipping 60°NE cuts sedimentary rocks and andesitic breccias. Although it is included in map unit TPCR3, the dike has a unique mineralogy. The phenocryst assemblage is similar to that of the single-pyroxene andesites, except that euhedral augite phenocrysts are rimmed with another clinopyroxene. Figure 4 shows an example. On the basis of its small optic angle, the rim pyroxene is identified as pigeonite.

Lava Flow (TPCR 4)

Map unit TPCR4 is exposed in the unnamed canyon draining southwest,
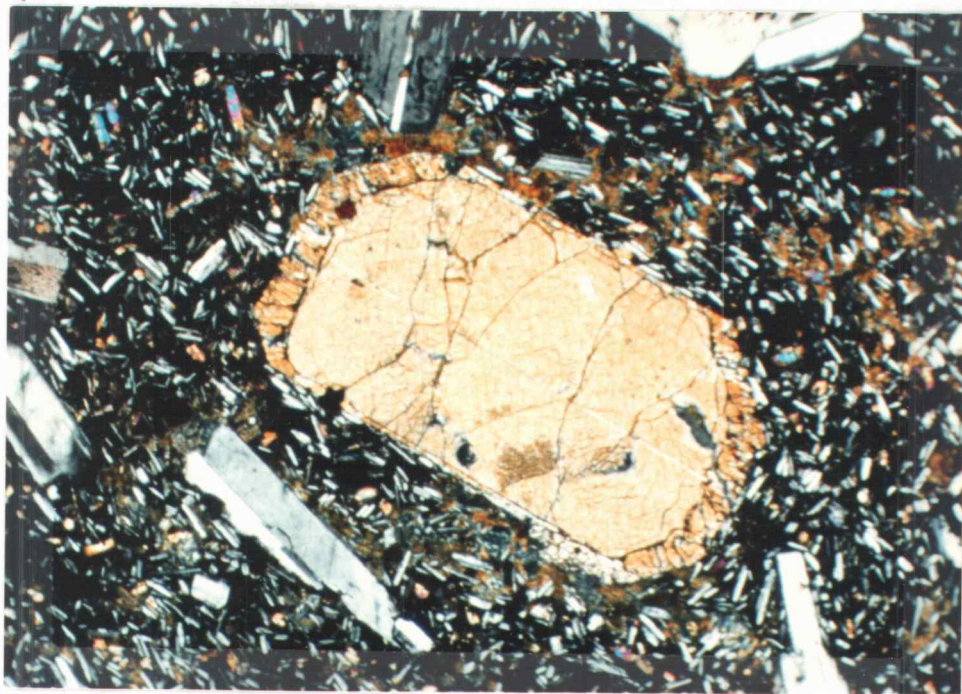
Figure 4. Photomicrograph of clinopyroxene phenocryst with clino-pyroxene overgrowth. Andesite dike (map unit TPCR 3, sample 104). NE1/4 Sec. 26, T.10S., R.10E. Field of view 3.3 mm., crossed polars.

below Castle Rocks. Platy jointed andesite forms a prominent ledge 60 feet (18 m) thick. Platy joints are spaced at about 1 inch (2 cm), and show well developed ramping near the top of the outcrop.. Flow breccias 15 feet (4.5 m) thick overlie and underlie the lava flow. Similar rocks are exposed downstream, through gaps in the alluvial cover.

Hand specimens are dark greenish gray, with phenocrysts of plagioclase and pyroxene. In thin section, rocks are glomero-porphyritic, hypohyaline and intergranular. Plagioclase phenocrysts make up 20% of the rock, and have a seriate size distribution from 3.0 to 0.3 mm. Cores show weak continuous normal zoning, with a maximum An content of about 50. Unzoned outer rims usually have lower An contents than the core. Blebs of glass are sometimes present along cleavages.

Anhedral clinopyroxene up to 1.2 mm long is the most common ferromagnesian phenocryst. Orthopyroxenes are subhedral, and less than 1.2 mm long. Many are rimmed with clinopyroxene, and often have irregular, resorbed outlines.

Fe-Ti oxides are unusually large and abundant. Equant to highly irregular opaque microphenocrysts make up 1% of the mode. Most are about 0.25 mm in diameter, but some are up to 0.8 mm. Isolated opaque phenocrysts are rimmed with aggregates of fine, columnar crystals of moderate birefringence which are probably clinopyroxene.

Glomerocrysts contain plagioclase, clinopyroxene, orthopyroxene, opaque Fe-Ti oxides and orange-red pseudomorphs, apparently after olivine. Some orthopyroxene crystals contain symplectic intergrowths of an opaque mineral. Opaque Fe-Ti oxides are similar in size and

shape to those in the groundmass, but lack clinopyroxene rims. Apparently these rims result from a reaction with the groundmass. If so, the rims are likely to be pigeonite.

The groundmass is a felty mass of plagioclase microlites, with minor granules of clinopyroxene. Tiny opaque Fe-Ti oxide grains are uniformly distibuted throughout the groundmass.

Dacite

Pre-Castle Rocks dacites appear very similar to andesites in the field, and a chemical analysis or thin section is required to make the distinction. Outcrops are limited and lateral continuity is nil, so all dacites are mapped as unit TPCR5.

Tuff-breccia is the most common rock type, with about 70% block and lapilli-sized fragments. Clasts are porphyritic and medium gray, with reddish-brown flow bands. The matrix is composed of comminuted clast material. Deposits are massive and completely unsorted, with blocks up to 1.5 m in diameter, and appear to represent airfall explosion breccias.

A few outcrops are pyroclastic breccias, composed of about 95% dense subangular blocks similar to those found in the tuff-breccias. These deposits are also massive and unsorted, and were probably formed by autobrecciation of lava flows.

Lava flows are uncommon, and usually occur as pods within pyroclastic breccias. These flows are less than 10 feet (4 m) thick, with platy jointing. Prominent flow bands are parallel to the platy joints.

Most dacites contain about 10% phenocrysts. Plagioclase is most

common, with a seriate size distribution from 2.5 mm to 0.25 mm. Although a few are sieve textured, most are clear, with oscillatory zoned andesine cores and slightly more calcic rims. Table 2 summarizes microprobe data on plagioclase phenocrysts from a Pre-Castle Rocks dacite.

Sparse Olivines are euhedral to subhedral, and less than 1 mm long. Olivines are altered to red-orange iddingsite on crystal rims and along cracks. The cores of most olivines are altered to pale green, fibrous bowlingite. A few fresh cores remain, but are rarely oriented to obtain optic-axis interference figures. In one grain, the optic angle was estimated at about 60°, corresponding to a composition of Fo_{30}. Microprobe analyses summarized in Table 1 indicate a composition of about Fo_{32}.

Clinopyroxene phenocrysts up to 2 mm long are subhedral to anhedral, colorless, and tend to form glomerocrysts with opaque oxides. A limited number of microprobe analyses indicate that the clinopyroxene phenocrysts are ferroaugite (Table 1). Equant microphenocrysts of opaque Fe-Ti oxides up to 0.5 mm in diameter make up less than 1% of the rocks, and are found both in glomerocrysts and isolated in the groundmass. Microprobe analyses of opaque oxides (Table 1) indicate that they are unusually rich in TiO_2 and poor in MgO.

Groundmass textures are intersertal and hyalopilitic. Brownish glass and opaque oxides are evenly distributed between aligned oligoclase microlites. Needle-like crystallites of apatite are common in the groundmass, and may form microphenocrysts up to 0.15 mm

TABLE 1

Microprobe analyses from Pre-Castle Rocks Dacite
Sample DW2

	OL1	OL2	OL3	PX1	PX2	PX3	OP1	OP2
				Oxide wt. %				
SiO_2	33.32	33.35	33.19	50.64	51.15	51.13	00.18	00.36
CaO	00.32	00.31	00.28	17.73	17.50	17.60	00.05	00.05
Al_2O_3	00.02	00.03	00.01	00.82	00.99	01.20	01.37	02.36
Cr_2O_3	00.00	00.01	00.01	00.04	00.00	00.00	00.02	00.00
$FeO*$	52.62	52.09	52.27	17.52	18.16	17.98	71.54	60.64
TiO_2	00.01	00.07	00.06	00.12	00.36	00.40	20.97	29.74
MgO	13.75	14.17	13.79	10.78	10.87	10.87	00.36	00.13
NiO	00.00	00.01	00.02	00.00	00.00	00.01	00.01	00.01
MnO	01.35	01.22	01.23	00.72	00.65	00.63	01.18	00.66
				Normative Composition				
Fo	31.22	32.14	31.46					
Fa	68.78	67.86	68.54					
Wo				37.75	37.00	37.25		
En				31.92	31.96	31.99		
Fs				30.33	31.04	30.75		

OL1:   Core of Olivine phenocryst
OL2:   Core of Olivine in glomerocryst
OL3:   Rim of OL2
PX1:   Core of clinopyroxene in glomerocryst
PX2:   Rim of PX1
PX3:   Clinopyroxene in glomerocryst
OP1:   Opaque in glomerocryst
OP2:   Opaque in groundmass

TABLE 2

Microprobe analyses of plagioclase from Pre-Castle Rocks Dacite
Sample 109

	PL1	PL2	PL3	PL4	PL5	PL6	PL7
				Oxide wt. %			
SiO_2	55.87	56.44	58.39	56.78	58.45	57.95	58.07
Al_2O_3	28.33	27.58	26.61	27.18	25.93	26.66	26.38
CaO	10.51	09.98	08.83	09.90	08.27	09.03	08.85
FeO*	00.32	00.46	00.36	00.31	00.34	00.33	00.37
K_2O	00.24	00.27	00.34	00.29	00.36	00.33	00.34
Na_2O	05.43	05.77	06.29	05.92	06.50	06.31	06.01
BaO	00.05	00.04	00.00	00.07	00.04	00.02	00.04
				Molecular Composition			
Ab	47.67	50.34	55.22	51.10	57.49	54.78	54.03
Or	01.37	01.53	01.94	01.67	02.10	01.90	01.99
An	50.96	48.13	42.84	47.23	40.41	43.33	43.98

PL1:   Plagioclase in glomerocryst
PL2:   Plagioclase in glomerocryst
PL3:   Plagioclase core
PL4:   Mantle on PL3
PL5:   Core of oscillatory zoned plagioclase
PL6:   Outer core of PL5
PL7:   Core of plagioclase in glomerocryst
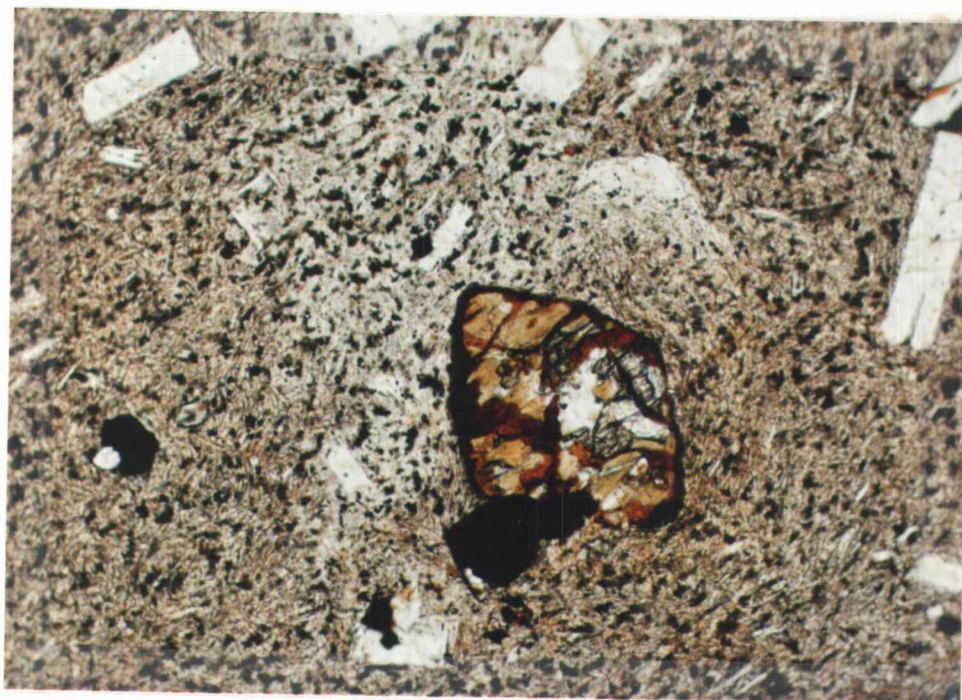
Figure 5. Olivine phenocryst in Pre-Castle Rocks dacite (map unit TPCR 5, Sample 109). SE1/4, Sec. 29, T.11.S., R.10E. Field of view 1.3 mm, plane light.

long. Reddish banding is due to concentrations of opaques, oxidized to hematite.

Sedimentary Rocks

Near the confluence of the Metolius and Whitewater rivers, pumice-rich tuff-breccias and interbedded sedimentary rocks form discontinuous bodies within the andesite sequence. Stratified tuff-breccias are up to 6 feet (1.8 m) thick and medium bedded. Bedding is planar, and both normal and reverse grading are present. Clasts sizes range from ash to blocks. Subangular pumice predominates, with subordinate dense andesite and reddish scoria. Glassy margins surround some andesite blocks. Heavy mineral separates from pumice clasts contain olivine (fo_{85}), apatite, magnetite and rare ilmenite, orthopyroxene and clinopyroxene (E.M. Taylor, pers. comm.)

Laminated to very thin bedded, coarse sandstones form beds less than 10 feet (3 m) thick. Subangular sand grains are dense andesite and scoria, with rounded pumice lapilli. Planar bedding predominates, but cross bedding is also common. Sandstones are well sorted, with both normal and reverse grading. Pumice fragments are often concentrated at the tops of individual beds and laminae.

Sandstones and pumice-rich breccias form bodies of limited lateral extent, usually less than 75 feet (23 m). Tops are planar, and lower contacts are irregular and trough-shaped. These units apparently filled shallow topographic lows. Lack of sags beneath blocks, and association with sandstones in low spots indicate that the pumice-rich tuff-breccias have been reworked.

Sedimentary units have dips as high as 35°, with variable strikes. Hales (1975) believed that the sandstones were surge deposits, and that the dips were initial rather than tectonic. However, all the beds within an outcrop (whether sediments or volcanic breccia) have the same dip. The dips must be due to faulting or slumping, but exposures are too poor to distinguish between the two. A few small normal faults strike north-south. Fault planes dip both east and west, with displacements less than 2 feet (0.6 m).

Composition

Figures 6 through 10 are major-element variation diagrams for all rock types in the thesis area. Variability is relatively low in the more mafic rocks, but Pre-Castle Rocks units have a strongly tholeiitic composition quite distinct from that of younger units.

Pre-Castle Rocks samples are enriched in K_2O, TiO_2 and FeO^*, and depleted in Al_2O_3, CaO and MgO, relative to those from younger units. Iron enrichment is pronounced, with FeO^*/MgO as high as 14 in more silicic rocks. Results of a limited number of minor and trace element analyses are listed in Appendix 2a, and show that Pre-Castle Rocks samples are high in P, Rb, Nb, Ba and Zr.
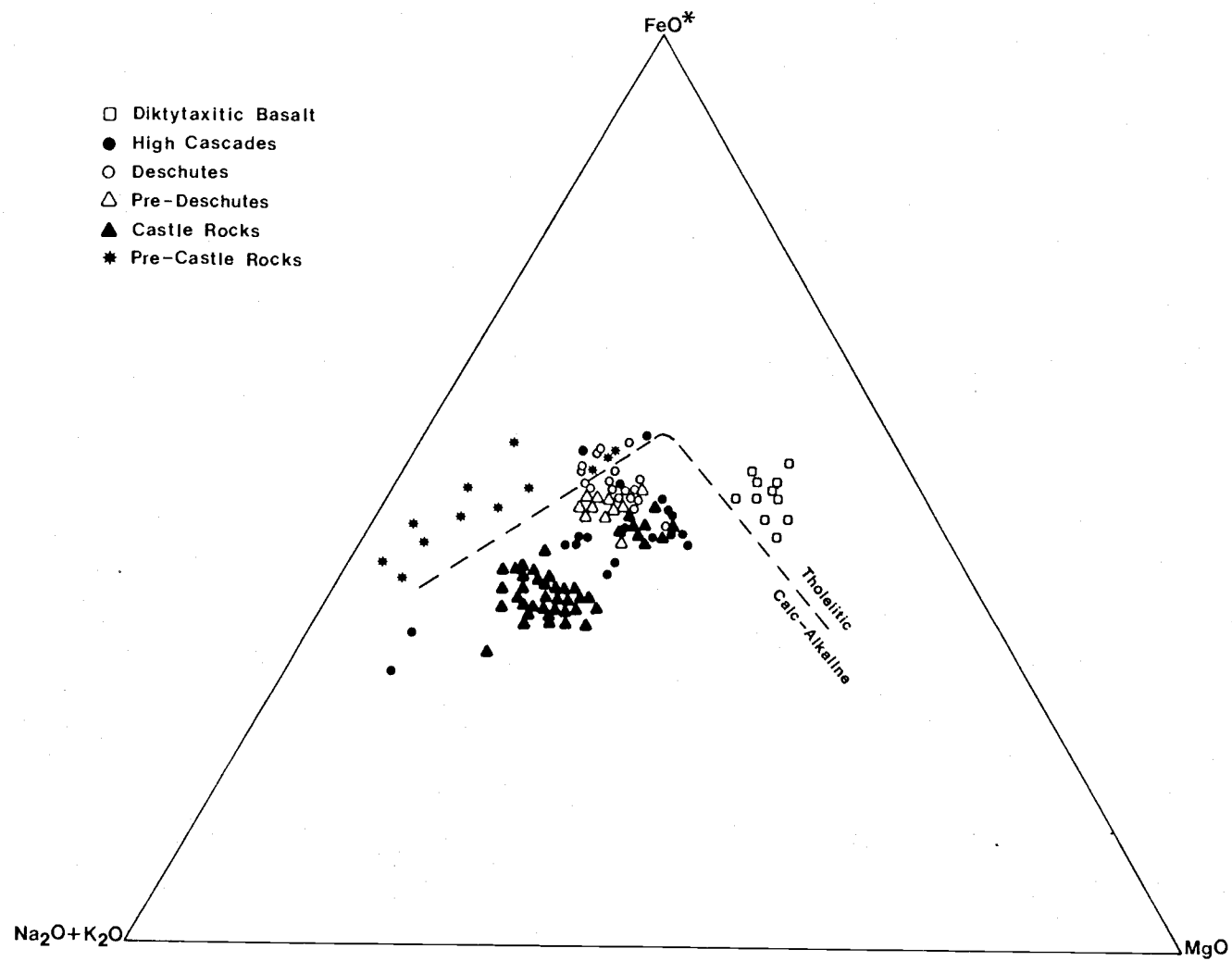
Figure 6.   AFM diagram. Tholeiitic and calc-alkaline fields from
Irvine and Baragar (1970).
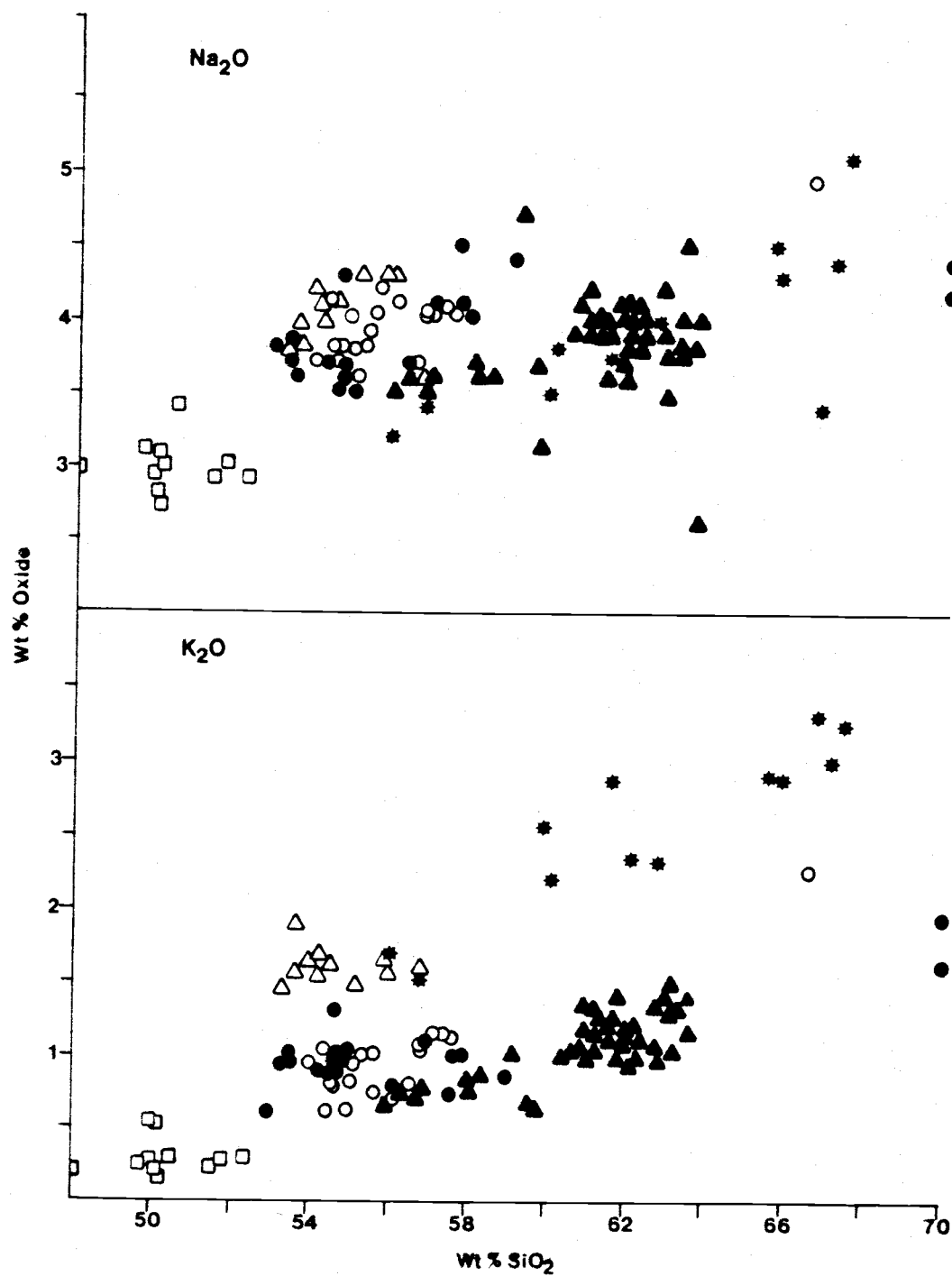
Figure 7.   Silica variation diagram for Na_2O and K_2O.   Symbols as in
figure 6.
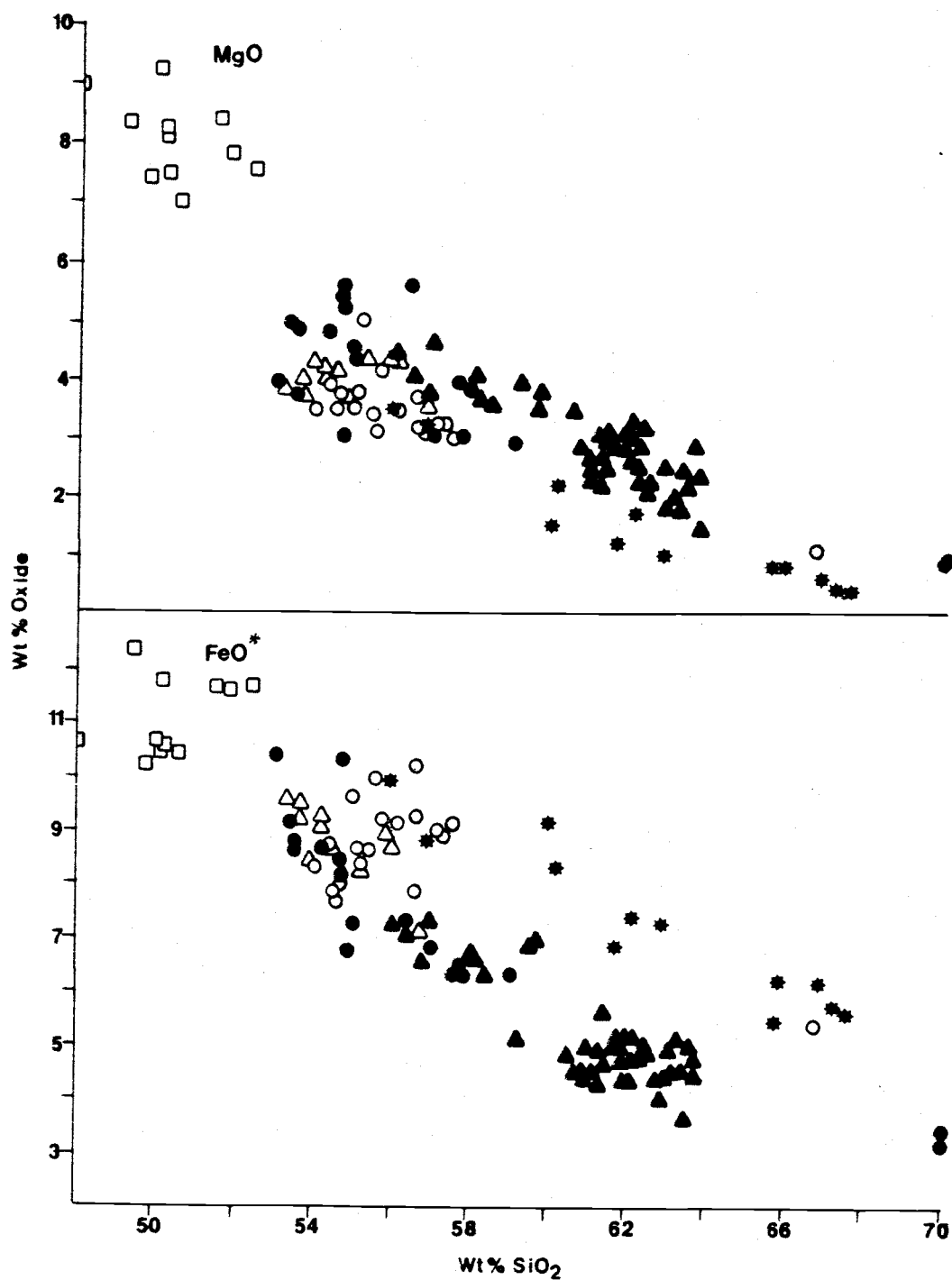
Figure 8. Silica variation diagram for MgO and FeO*. Symbols as in figure 6.
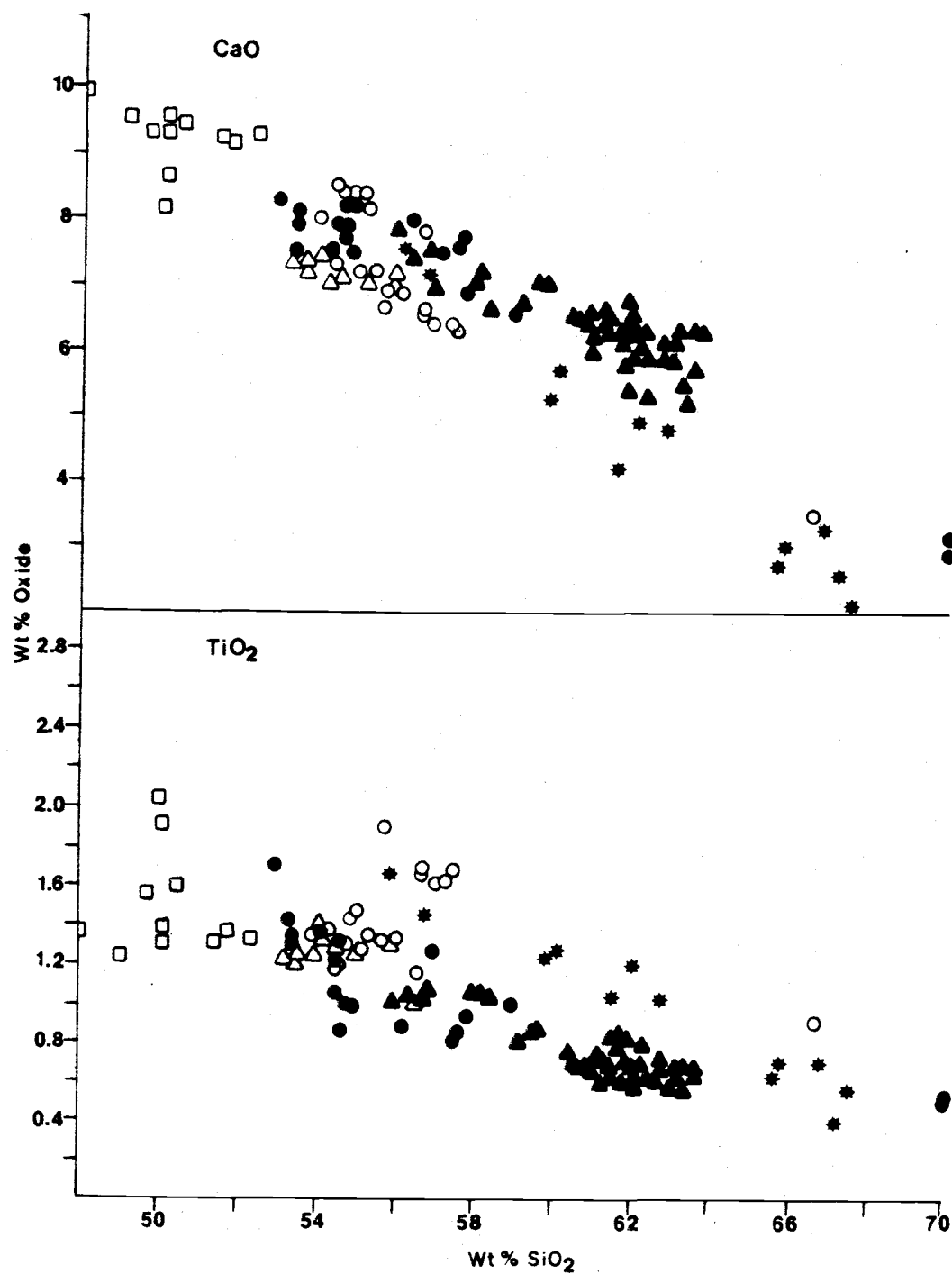
Figure 9. Silica variation diagram for CaO and TiO_2. Symbols as in figure 6.
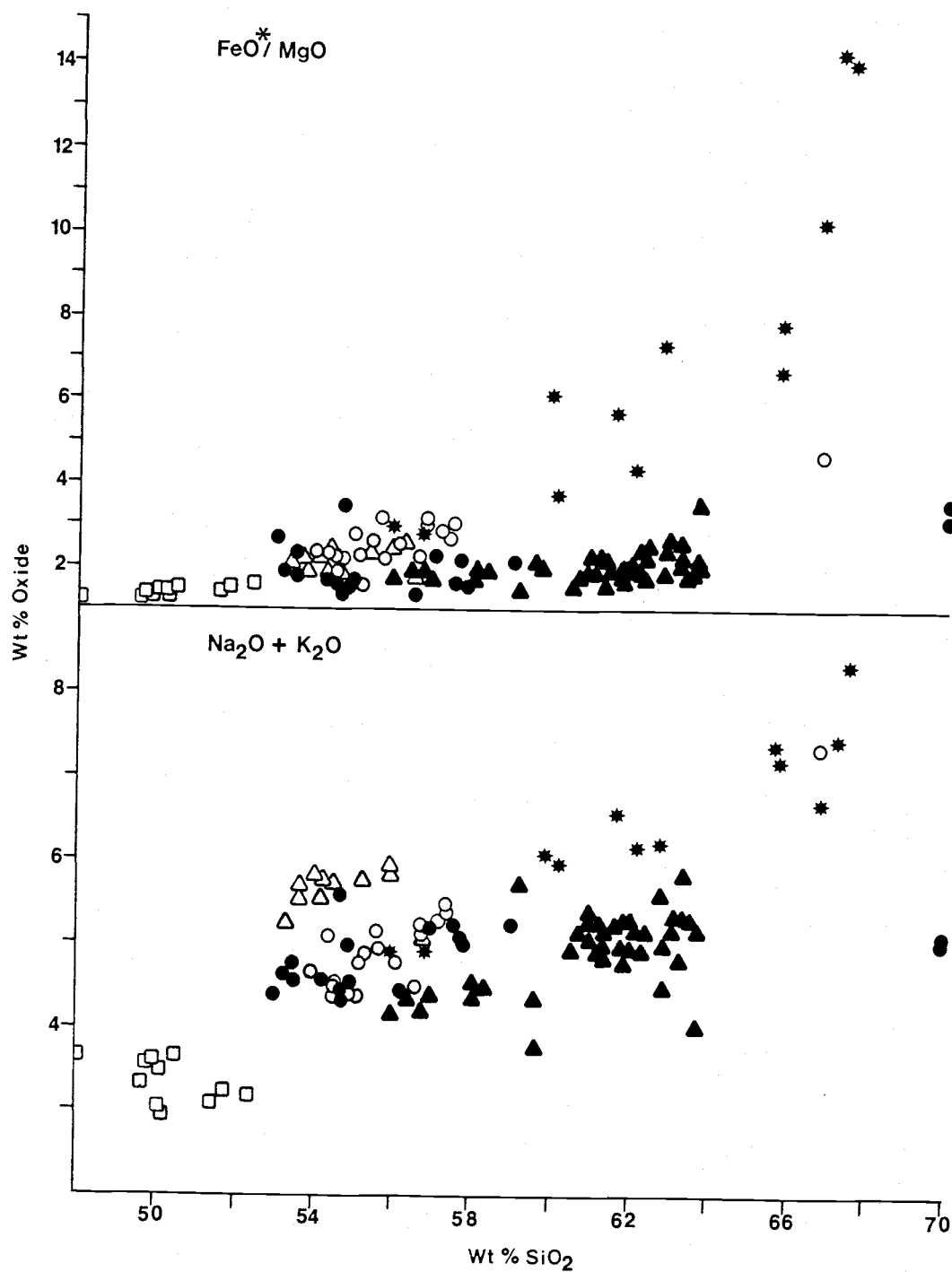
Figure 10. Silica variation diagram for Fe/Mg and Na_2O + K_2O. Symbols as in figure 6.

Discussion

Phenocryst assemblages in Pre-Castle Rocks samples commonly show evidence of disequilibrium. Plagioclase phenocrysts with embayed margins, and sieve-textured plagioclase with anhedral outlines and clear, more sodic rims indicate crystal/melt disequilibrium. The presence of euhedral olivine phenocrysts in dacite is surprising. However, intermediate to felsic rocks containing ferroaugites and fayalitic olivines are found in the upper part of layered mafic intrusions (Wager and Brown, 1967), and in iron-rich volcanic sequences known as "Icelandites" (Carmichael, 1964). Fayalitic olivines also observed in ash-flow tuffs (Noble, et al., 1970; R.M. Conrey, pers. comm.). The significance of these iron-rich minerals is discussed in the section on petrology.

Definite age relationships cannot be established among Pre-Castle Rocks units, although dacites tend to be topographically higher than other rock types. The prevalence of unsorted air-fall deposits containing abundant block-sized clasts suggests that the Pre-Castle Rocks eruptive center was nearby. Measurable strikes and dips are scarce, and most reflect faulting or slumping, but they appear to have a radial pattern, dipping away from the north end of Green Ridge. This suggests that the eruptive center may have been somewhere near Castle Rocks. Whatever its location, it must have been a major edifice, as its distal deposits retain 900 feet (275 m) of relief, and strata of Castle Rocks, Deschutes and High Cascade age bank up against them.

Alternatively, the few available attitudes may not represent a

radial pattern of initial dips. Instead, Pre-Castle Rocks units may have been faulted, and tilted toward the north before the deposition of younger rocks.

Sedimentary rocks are consistent with deposition from small streams. There are no coarse sediments to indicate that the ancestral Metolius River passed through the field area.

No radiometric dates are available for Pre-Castle Rocks units. The oldest reliably dated overlying rock is a hornblende andesite, dated by Hales (1975) at 8.3 ±0.6 ma. This appears to be one of the youngest Castle Rocks lavas. Based on this date, and their reverse magnetic polarity, it appears that Pre-Castle Rocks units are at least 11 million years old.

Except for Columbia River Basalt, volcanic rocks dated as mid-Miocene are rare in central Oregon. The Simtustus Formation (Smith, 1986a) is mid Miocene in age, and could contain sediment derived from Pre-Castle Rocks volcanics. Pre-Castle Rocks volcanism might have been contemporaneous with that of the John Day formation, which ended about 18 ma. Several dacite domes of presumed John Day age are scattered about the Deschutes basin; including Eagle Butte, Long Ridge and Forked Horn Butte. Pre-Castle Rocks dacites are lithologically and petrographically different from these domes. Major element composition (Weidenheim, 1981; G. Smith, pers. comm.) is equivocal.

Priest and others (1983) have described several epidsodes of Cascade volcanism. The Early Western Cascades Episode ended at about 18 ma (Fig. 3), when tholeiitic volcanism ceased and was replaced by calc-alkaline activity. In the Western Cascades near the town of

Detroit, the end of the Early Western Cascades Episode was marked by eruption of the tholeiitic, iron-enriched Scorpion Mountain Lavas (White, 1980b). The Scorpion Mountain Lavas have been dated at 27-19 ma, and have major element composition similar to that of Pre-Castle Rocks basaltic andesites.

If Pre-Castle Rocks volcanism was indeed part of the Early Western Cascades Episode, these rocks are probably early Miocene in age. If so, the unconformity above them would represent the passage of about 10 million years. Pre-Castle Rocks volcanism was tholeiitic, producing highly evolved rocks rich in incompatible elements and lacking hydrous minerals. Such rocks are generally believed to form during periods of extensional tectonics. Volcanism resumed with the production of strongly calc-alkaline hornblende-andesites from the Castle Rocks volcano.

Castle Rocks Andesites

Pre-Castle Rocks units are unconformably overlain by lava flows, pyroclastic rocks and mudflows; all with compositions distinctly different from the older rocks. These younger rocks are strongly porphyritic hornblende, hornblende-pyroxene or pyroxene andesites. In contrast to Pre-Castle Rocks units, these andesites have normal magnetic polarity. Most dip radially away from a pyroxene andesite plug in NE1/4NE1/4 sec. 6, T.11S., R10E. This plug was the center of a late Miocene composite volcano, referred to by Hales (1975) as the "hornblende andesite volcano".

Porphyritic hornblende-pyroxene andesites and associated rocks unconformably overlying Pre-Castle Rocks units are here discussed under the general heading of "Castle Rocks Andesites". Unfortunately, the geographic feature known as Castle Rocks is a large outcrop of tuff-breccia, and not actually the center of the volcano. Because the term "Castle Rocks Volcano" is already in informal use, and the plug itself is unnamed, the term will be retained here. For lack of a better name, the pyroxene andesite plug is refered to as "the plug". Map units TCR 6,7,9 and 10 are distinctive orthopyroxene andesites and hornblende dacites, some of which may have issued from a seperate vent. Their chemical and mineralogical compositions are similar to Castle Rocks andesites, and they are discussed together.

According to a strict chemical classification, some products of the Castle Rocks Volcano are basaltic andesites (56 wt% SiO_2), wheras others are dacites (63.7 wt% SiO_2). For the sake of simplicity the

term "Castle Rocks Andesites", as used in this paper, includes these.

Mudflows (TCR 1)

One of the oldest products of the Castle Rocks volcano is a mudflow exposed in a small, unnamed canyon in the NW1/4 Sec.11, T.11S., R.10E. The deposit is poorly sorted, with clast sizes ranging from ash to blocks 10 feet (3 m) in diameter, usually in matrix support. The largest blocks are concentrated near the base of the deposit, producing a crude grading. All clasts are subangular, dense, and lack visible jointing. The clasts show random paleomagnetic polarity, indicating that the deposit was cold when emplaced. A variety of lithologies are present, but all are porphyritic hornblende-pyroxene andesites typical of the Castle Rocks volcano.

This unit is identified as a mudflow on the basis of its lack of sorting or stratification and the presence of a variety of lithologies. Paleomagnetic evidence that the deposit was emplaced at near ambient temperatures also favors deposition by a mudflow. The base of unit TCR 1 is somewhere below road level at 2160 ft (658 m) elevation. Similar rocks are exposed at 2620 ft (799 m) in NE1/4NE1/4 Sec. 10, where the maximum clast size is 0.5 ft (0.15 m). Due to poor exposures, no estimate of the number or thickness of individual mudflows is possible.

Pyroclastic-Flow Deposits (TCR 2)

A single pyroclastic-flow deposit from the Castle Rocks volcano is found about 1.25 mi (2 km) north of the pyroxene andesite plug (Plate 1). Most of the slope is talus covered, and the outcrop is too small to map. Less than 6 feet (2 m) of unsorted and ungraded lapilli-tuff is exposed.

Subangular blocks of dense andesite make up about 5% of the deposit. Mineralogy of the blocks is typical of Castle Rocks andesites. Subhedral clinopyroxene and orthopyroxene phenocrysts each make up about 2 % of the mode, with subordinate hornblende. Hornblende phenocrysts have a rounded, anhedral outline and are rimmed with "opacite".[1] Plagioclase phenocrysts comprise about 20% of the rock, and can be divided into two populations based on zoning and inclusions. The petrography of hornblende-pyroxene andesites is discussed more thoroughly in the section on hornblende-pyroxene andesite lavas. Yellowish pumice lapilli with euhedral pyroxene and anhedral hornblende crystals make up about 25% of the deposit. The ashy matrix is light pink. The deposit is poorly welded, with no evidence of compaction of pumice lapilli.

---

[1] The term "opacite" is used for the opaque mass of fine mineral grains often found as rims on volcanic hornblende and biotite phenocrysts. Opacite apparently forms by dehydration, and consists of fe-ti oxides, pyroxene, and plagioclase. Washington (1896) was the first to describe the process.

Hornblende-Pyroxene Andesites

Castle Rocks Tuff-Breccia (TCR 3)

Map unit TCR3 is an andesitic tuff-breccia which forms Castle Rocks. Figure 11 shows the vertical 660 foot (200 m) north face of Castle Rocks. The deposit is crudely stratified, with layering defined by variations in block size. Stratification is not apparent at the outcrop, but is recognizable from a distance. Dips are southwest at about 35°, making the exposed thickness of the deposit approximately 540 feet (165 m). Faint stratification is visible in Figure 11, as are widely spaced vertical joints which cut through the entire deposit. Vertical or overhanging cliffs make a thorough examination of Castle Rocks impossible, but one traverse was made from 150 feet (45 m) above the base to the top. Evidence from this traverse suggests a slight coarse-tail grading in the Castle Rocks Breccia. Maximum block diameter appears to decrease from 3 feet (1 m) near the bottom of the deposit to less than 1 foot (30 cm) at the top. Blocks are subangular and non-vesicular. Some blocks, especially the larger ones, show radial prismatic jointing.

During the traverse, blocks were collected at various points. Because safety was the primary concern, sampling intervals are variable. Petrography of the blocks is constant, although the degree of alteration varies. Plagioclase is the most common phenocryst, forming 30-32% of the mode. Most plagioclase phenocrysts are andesine, with weak continuous normal zoning. A few have highly sieve-textured cores and thin, clear rims of lower An-content.

Highly altered hornblende phenocrysts up to 3 mm long make up 4

Figure 11. Castle Rocks, seen from the northwest. Cliff is 660 feet
high. Note crude stratification and vertical joints.
NE1/4 Sec. 7, T.11S., R.10E.

to 6% of the rock. Two types of magmatic alteration are found, often in the same thin section. In the first type, cores of amphibole are surrounded by opaque rims of fine grained Fe-Ti oxide and granular pyroxene. Characteristic amphibole cleavage, yellow to dark reddish-orange pleochroism, and extinction angles of less than 10^0 identify the core mineral as oxyhornblende.[2] In the second type, the oxyhornblende core and its opaque rim are surrounded by an aggregate of small orthopyroxene, clinopyroxene, plagioclase, and opaque oxide crystals. Often, the amphibole core is lacking, and all that remains is an amphibole-shaped aggregate of orthopyroxene, clinopyroxene, plagioclase, and opaque oxides.

Orthopyroxene phenocrysts make up 4-5% of the mode, and are subhedral, prismatic, and generally less than 0.75 mm in length. Stubby, subhedral phenocrysts of clinopyroxene are less common, making up 1-1.5% of the rock. The groundmass is a felty mass of plagioclase laths, with tiny prisms of pyroxene and equant opaque oxides.

Although clast mineralogy is constant throughout the breccia unit, the degree of alteration varies with stratigraphic position. In clasts near the bottom of Castle Rocks, orthopyroxene phenocrysts are completely replaced by dark aggregates of opaque oxides, and clinopyroxene phenocrysts are surrounded by brown rims. Higher in

---

[2] Oxyhornblende is simply common hornblende which has been heated to at least 800^0C in an oxidizing environment (Barnes, 1930). Under these conditions, hydrogen is driven off and Fe^{+2} is converted to Fe^{+3}. This reaction is accompanied by an increase in refractive indices, a decrease in extinction angle, and a change in pleochroic colors. Oxyhornblende is also referred to as "basaltic hornblende" and "lamprobolite". The name "basaltic hornblende" is particularly misleading, since the mineral is most common in intermediate rocks.

the section, orthopyroxene phenocrysts are cloudy and brown, but translucent. At the same level, the brown rim surrounding clinopyroxene phenocrysts is thin, or sometimes absent. Near the top of Castle Rocks, both types of pyroxene are unaltered, and orthopyroxenes show normal pink pleochroism. Clasts from the base of Castle Rocks probably cooled more slowly than those near the top, resulting in increased oxidation of pyroxene phenocrysts.

The ashy matrix of the breccia contains about 25% crystals or crystal fragments. Plagioclase crystals are generally less than 1 mm in length, and appear fresh. Many are broken, with the pieces still in contact. Pyroxene crystals are completely replaced by aggregates of dark opaque oxides. Their shapes suggest that both orthopyroxene and clinopyroxene were present. Oxyhornblende is present as anhedral, deep reddish-orange fragments. Subrounded oxhyhornblende fragments are surrounded by opacite. As seen in Figure 12, other fragments are partially rimmed with opacite, but have angular, broken surfaces which lack them. Apparently the opaque rims formed prior to brecciation. Crystal fragments are set in a cryptocrystalline matrix with low birefringence.

Chemical analyses were performed on 6 clasts, collected over a 520 foot (158 m) elevation interval. Composition (Appendix 2b) is typical of Castle Rocks Andesites, and shows no variation with stratigraphic position.

Stratification and uniform dips suggest that the Castle Rocks Breccia is a subareal fallout deposit. Its great thickness, lack of lateral continuity, and absence of vesicular material are unusual for an airfall deposit. These constraints, and the striking chemical and
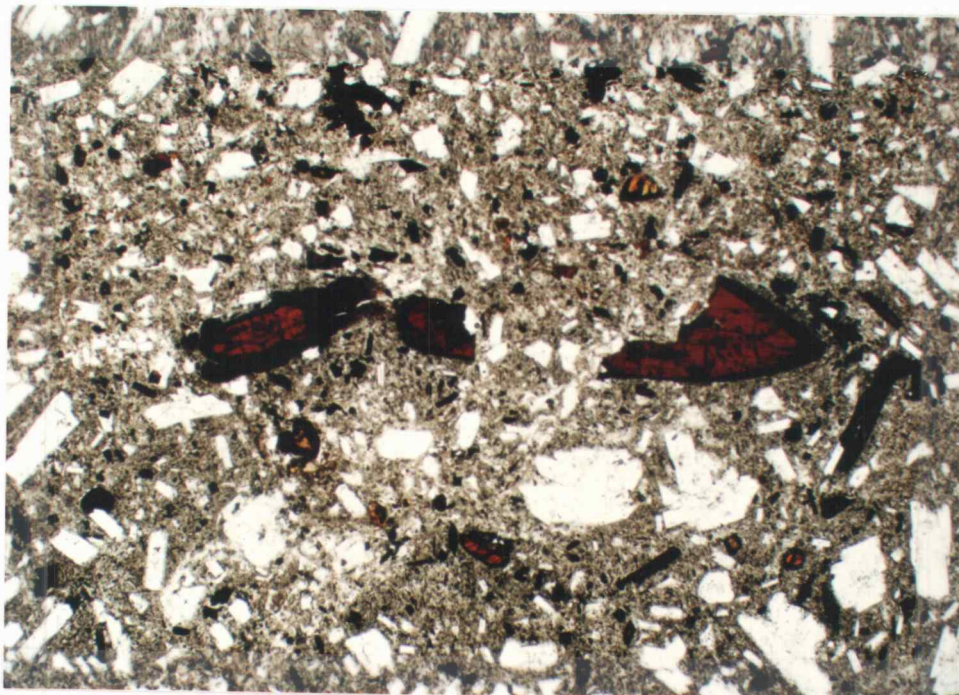
Figure 12. Photomicrograph of matrix of Castle Rocks breccia (Map unit TCR 3). Broken oxyhornblende crystal with partial opacite rim. Plane polarized light, field of view 6.7 mm.

lithological uniformity of the Castle Rocks Breccia suggest an origin by explosive disruption of a dome or lava flow.

Hornblende-Pyroxene Andesite Tuff-Breccias (TCR 4)

Tuff-breccias are especially common on the west face of Green Ridge, and are mapped as a single unit. These deposits are monolithologic, unstratified and poorly sorted. Most breccia units are ungraded, although weak normal and reverse grading are sometimes found. Dense, angular blocks of andesite make up 25-75% of the deposits, and may be up to 15 ft (4.5 m) in diameter. Pumice is absent, and the matrix consists of light-colored ash with broken phenocrysts similar to those found in the clasts.

Uniform magnetic polarity of the clasts indicates that these breccias were hot when emplaced. In addition, radial prismatic jointing is common in breccia clasts. Often, broken blocks are only loosely held together, indicating that the joints formed after the block came to rest. As seen in Figure 13, block fragments are commonly partially separated, with matrix material filling the gaps.

The breccia unit in NW 1/4NW1/4 Sec.5, T.11S., R.10E., contains unusual interbeds of lapilli tuff. Wave forms and cross beds indicate that these are surge deposits. Figure 14 shows a typical example - a small patch of lapilli tuff within the breccia unit.

Breccia clasts have mineralogies similar to hornblende-pyroxene andesite lava flows. The matrix of most breccias is soft and white, and consists mostly of fragmented clast material.

These tuff-breccias are very similar to "hot avalanche deposits" described by Francis and others (1974) on a historically active

Figure 13. Radial prismatic jointing in breccia clast, map unit
TCR 4. NW1/4 Sec.33, T.10S., R.10E. Hammer for scale.

Figure 14. Surge deposit in hornblende-pyroxene andesite tuff breccia (map unit TCR 4). NE1/4 Sec. 26, T.11S., R.10E.

volcano in Chile. There, the deposits can be traced back to prominent collapse scars, where andesite flows failed on steep slopes. Wright and others (1980) refer to these "hot avalanche deposits" as one type of "block and ash deposit". These are products of pyroclastic flows, which may be initiated in several ways: collapse of a vertical eruptive column, explosive collapse of a lava flow or dome, or gravitational collapse of a lava flow or dome (Wright, et al, 1980).

The hornblende-pyroxene andesite tuff-breccias have several features in common with deposits of block and ash flows: poor sorting, lack of stratification, lack of vesicular material, radial prismatic jointing, and monolithologic composition. Airfall deposits from vulcanian explosions may share these characteristics, especially near the vent.

Although most hornblende-pyroxene andesite tuff breccias are massive and unstratified, one small outcrop of planar bedded tuff breccia is exposed 600 feet (183 m) southeast of the plug, at 3900 feet (1190 m) elevation. The outcrop, seen in Figure 15, is 65 feet (20 m) thick, strikes N50°E, and dips 28°SE. Bedding is gradational, and individual beds of tuff breccia are less than 2 feet (60 cm) thick. Grading in individual beds may be normal, reverse, symmetric, or absent. Sorting is poor, with clast size varying from ash to blocks 1 foot (30 cm) in diameter. Most clasts are dense angular to subangular lithic fragments. Lithic fragments are all hornblende-pyroxene andesite. Crystal fragments are scarce, and pumice lapilli are vary rare. A few of the larger blocks show prismatic jointing. The outcrop is too small to exhibit any lateral variations, and its

Figure 15. Vent-facies of the Castle Rocks Volcano. Massive tuff
breccia at upper right overlies planar bedded tuff
breccia at lower center. Hornblende-pyroxene andesite
dike cuts breccia at right center. Pyroxene andesite
plug at left.

base is not exposed.

The bedded tuff breccias are a subaerial fallout deposit, probably produced by a fluctuating eruption column. It is surprising that only one outcrop of this type was found.

Hornblende-Pyroxene Andesite Lavas and Dikes (TCR 5)

Porphyritic andesite lavas are the most common rock type in the upper part of the Castle Rocks section. Hand specimens are usually medium gray with prominent hornblende phenocrysts up to 2 cm long. Inspection of hornblende phenocrysts with a hand lens reveals that most are partially altered to granular aggregates of plagioclase and pyroxenes. Each lava flow has a distinctive phenocryst assemblage, but extensive talus deposits prevent tracing individual flows. All hornblende-pyroxene andesite lava flows are included in map unit TCR5. Where visible, contacts between lava flows are indicated on Plate 1 by dashed lines. Precise attitudes are difficult to obtain, but dips have a radial pattern, away from the pyroxene andesite plug.

Hornblende-pyroxene andesite lava flows are up to 200 ft (60 m) thick. Columnar jointing is common, frequently the only type seen in an outcrop. Thicker flows often have a columnar jointed base, a platy center and a top with columnar or irregular jointing. The most siliceous lavas tend to have only platy jointing. Most outcrops are surrounded by extensive talus aprons. Occasionally an underlying breccia is visible, with clast mineralogy identical to that of the lava flow above. These are interpreted as autobreccias. A particularly well-exposed autobrecccia is found in SW1/4NW1/4 Sec.1, T.11S., R10E., and was mapped by Hales (1975) as a mudflow.

Like other Castle Rocks units, hornblende-pyroxene andesite lava flows are highly porphyritic, with phenocrysts making up as much as 45% of the rock. Plagioclase is the most common phenocryst phase, up to 35% of the mode. Two populations of plagioclase phenocrysts can be identified. About one-third of the plagioclase phenocrysts have sieve textured cores of labradorite, with poorly developed twinning. Cores generally have irregular outlines suggesting resorption, and are surrounded by thin clear rims of andesine. Sieve-textured plagioclase may be up to 2 mm in length. The more common, clear plagioclase are smaller and often show a seriate size distribution. These lack inclusions, and usually show continuous normal zoning, from labradorite to andesine.

Orthopyroxene is the most common mafic phenocryst phase, usually making up 3-9% of the mode. Phenocrysts are euhedral to subhedral, and less than 1 mm long. Pink pleochroism is well developed. Orthopyroxene phenocrysts commonly contain inclusions of opaque oxides, and are sometimes jacketed with clinopyroxene. Clinopyroxene phenocrysts are less abundant, usually forming less than 2.5% of the mode. Phenocrysts of clinopyroxene are subhedral to anhedral, and in a given lava flow are larger than those of orthopyroxene. Hornblende or hornblende relicts are present in variable amounts, ranging from a trace, to over 10% of the mode.

Microphenocrysts of biotite up to 0.25 mm in diameter are rarely present. Equant microphenocrysts of opaque oxide make up as much as 1% of some rocks, often as inclusions in orthopyroxene phenocrysts.

Tightly packed plagioclase microlites are the most common groundmass constituent. In some cases, granular clinopyroxene and

prismatic orthopyroxene microlites can be identified. More commonly, the groundmass contains irregular grains of moderate relief, too small for identification. These are probably pyroxenes. Needle-like microlites of somewhat lower relief may be apatite. Opaque oxides occur as tiny equant grains, or as dark "dust" scattered throughout the groundmass. Biotite is occasionally present in trace amounts, and is pleochroic in pale yellow to pinkish-brown. The groundmass of many andesites contains dendritic patches of low relief material with a birefringence of about 0.03. These patches appear to result from devitrification.

A striking feature of Castle Rocks hornblende-pyroxene andesites is the variety of hornblende alteration. Various examples are shown in Figures 16 through 19. The simplest form of hornblende alteration is replacement by fine-grained aggregates of pyroxene and opaque oxides known as "opacite". Replacement begins on crystal rims and along cleavages (Fig. 16). Smaller crystals are often completely replaced by opacite (Fig. 17). Hornblende phenocrysts are often replaced by roughly equigranular aggregates of clinopyroxene, orthopyroxene, clear plagioclase and finer grained opaque oxides. In some cases, hornblende relicts rimmed with opacite are found at the center of the aggregates (Fig. 18). Often, no trace of the original mineral remains, except in the typical hornblende-shaped cross section of the aggregate. In the least common form of alteration, proxene-plagioclase-opaque oxide aggregates are surrounded by coarser-grained "necklaces" of clinopyroxene and orthopyroxene, with minor plagioclase and opaque oxide. References to this type of alteration are scarce, but MacGregor (1939) described similar
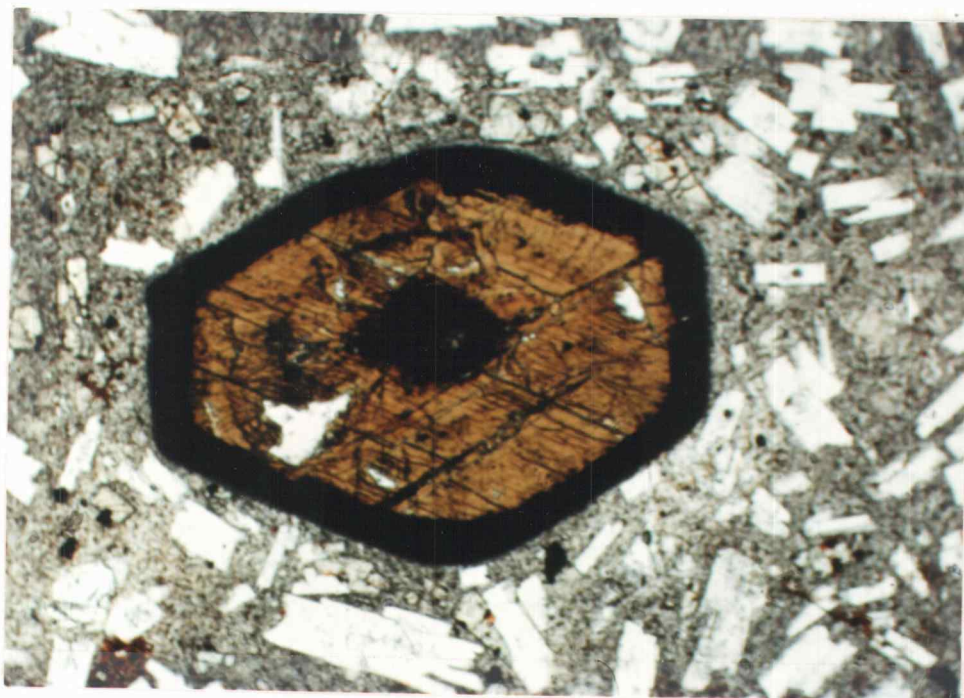
Figure 16. Photomicrograph of a hornblende phenocryst, partly
replaced by opacite (map unit TCR 5). SW1/4 Sec. 34,
T.10S., R.10E. Plane polarized light, field of
view 3.3 mm.
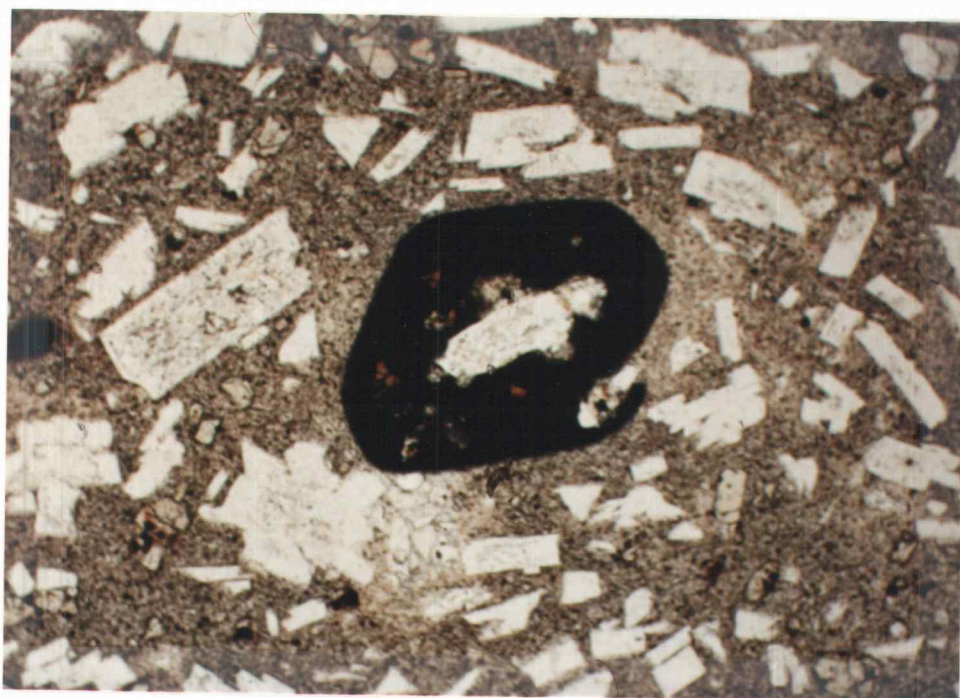
Figure 17. Photomicrograph of a hornblende relict, completely
replaced by opacite (map unit TCR 5). SW1/4 Sec. 34,
T.10S., R.10E. Plane polarized light, field of
view 3.3 mm.

Figure 18. Photomicrograph of a hornblende relict at the center of crystal aggregate (map unit TCR 5). SW1/4 Sec. 34, T.10S., R.10E. Plane polarized light, field of view 6.7 mm.

"pyroxenic" rims on hornblende from Martinique. Occasionally all three alteration types are found in one pseudomorph, as seen in Figure 19. In these cases, pseudomorphs are always zoned, from hornblende/opacite in the center to pyroxene "necklaces" around the rim. The equigranular aggregates and coarser grained necklaces probably formed by reaction of hornblende phenocrysts with the enclosing magma at depth. Opacite formation (refered to as "black" alteration in the older literature), on the other hand, results from dehydration of the magma under low-pressure, near-surface conditions. Zoned pseudomorphs represent three stages in magmatic history: first, the crystalization of hornblende at depth; second, the slow reaction of hornblende with the magma at lower pressure, perhaps in a higher level magma chamber; and third, extrusion, with loss of volatiles and formation of opacite.

Dikes are exposed only on the west face of Green Ridge, due to the deeper erosion there. Only one of these, in SW1/4NW1/4, Sec. 5, has mineralogy and composition similar to the abundant hornblende-pyroxene andesite lava flows. Plate 1 and Fig. 15 show that, unlike other dikes, it is not radial to the pyroxene andesite plug. The dike is up to 20 feet thick, with glassy chill margins and an irregularly jointed interior. Large, relatively fresh hornblende crystals are the only phenocrysts visible in hand specimen.

In thin section, samples are holocrystalline and porphyritic. Hornblende phenocrysts up to 7 mm in length make up 2-3 % of the rock. Hornblende phenocrysts have anhedral, rounded outlines, and are rimmed with opacite. Clinopyroxene phenocrysts are rare, and appear to be broken fragments of larger crystals. Tabular
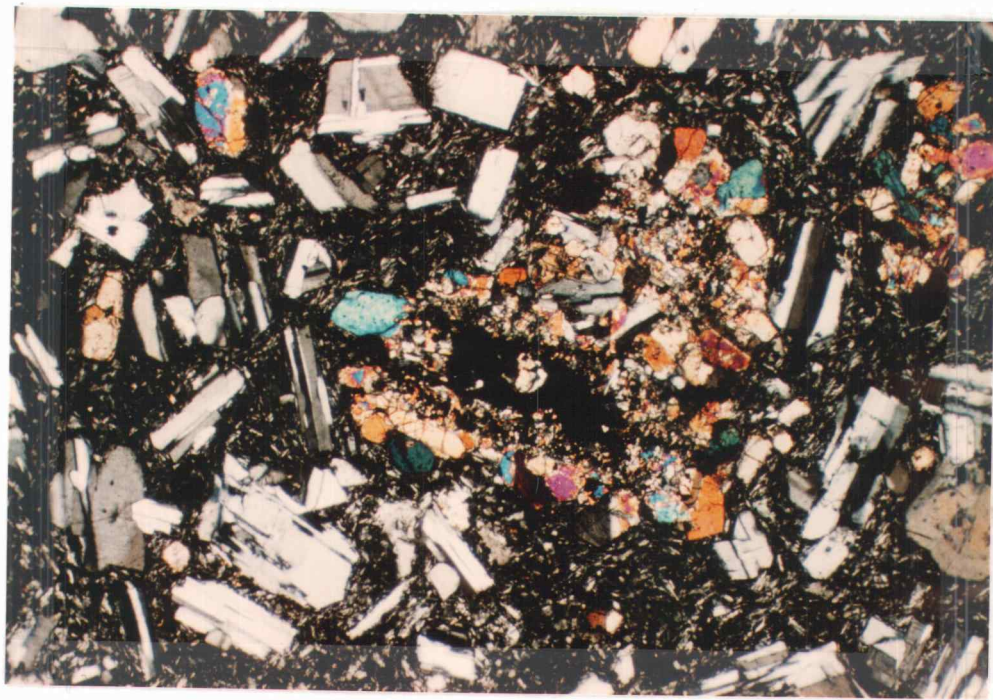
Figure 19. Photomicrograph of a hornblende relict showing
an opacite core, an intermediate zone of replacement by
equigranular pyroxene/plagioclase/opaque oxide, and an
outer rim of coarse pyroxene (map unit TCR 5, sample 124).
Plane polarized light, field of view 3.3 mm.

microphenocrysts of orthopyroxene less than 0.75 mm in length make up about 2 % of the rock. Plagioclase crystals have a seriate size distribution, ranging from microphenocrysts 1.5 mm in diameter to groundmass size. The groundmass consists of clinopyroxene, orthopyroxene, plagioclase and opaque oxide grains.

High-Silica Pyroxene Andesites

Pyroxene Andesite Dome (TCR 6)

A distinctive body of pyroxene andesite caps the hill immediately east of the plug. The unit is 470 feet (145 m) thick, and dips to the south or southeast. Sparse ledges of platy jointed andesite protrude through extensive talus deposits. The crude joints are curved, producing characteristic dish-shaped plates.

Hand specimens are unusual among Castle Rocks andesites, in that they lack prominent pyroxene or amphibole phenocrysts. Hand samples are light gray to nearly white, with clear plagioclase microphenocrysts and sparse needles of greenish-brown orthopyroxene less than 1 mm in length.

In thin section, samples are porphyritic and holocrystalline. Plagioclase phenocrysts are unusually abundant, making up nearly 50% of the mode. Most plagioclases are less than 0.7 mm in length, clear, and tabular in shape. These generally display continuous normal zoning, from labradorite (An_{60}) at the core to andesine (An_{45}) at the rim. A second population of plagioclase phenocrysts is slightly larger, up to 1 mm in length. These have anhedral outlines and highly sieve-textured cores, with continuous normal zoning. Many

have clear rims, with compositions similar to those of the rims of the clear plagioclase.

Orthopyroxene phenocrysts make up about 3% of the mode, and are euhedral to subhedral. Most are less than 1 mm in length, and display distinct pink pleochroism. Euhedral opaque oxide inclusions are common within the orthopyroxenes. Stubby clinopyroxene phenocrysts are less than 0.75 mm in length, and make up less than 1 % of the mode. A few anhedral microphenocrysts of amphibole are present. These are less than 0.30 mm in diameter, and have irregular, "shreddy" outlines. Crystals of amphibole are optically positive, with an optic angle of approximately 70°, pale brown/pale green/colorless pleochroism, and extinction angles of 17°. Equant grains of opaque oxide up to 0.15 mm in diameter make up less than 1 % of the rock. The groundmass is a tightly-packed mass of plagioclase microlites and anhedral quartz, with very sparse opaque oxide dust.

The identity of the amphibole phenocrysts is uncertain. Their positive optic sign and pleochroism are not those of common hornblende. Only two monoclinic amphiboles are optically positive, pargasite and cummingtonite. Pleochroism of the amphiboles in these samples is similar to that of pargasite, and the multiple twinning characteristic of cummingtonite is absent. Pargasite is not normally found in volcanic rocks. Cummingtonite is occasionally found as phenocrysts in felsic pyroclastic rocks (Ewart and others, 1971; E.M. Taylor, pers. comm.).

High-silica pyroxene andesites post-date the hornblende-pyroxene andesites which form the bulk of the Castle Rocks volcano. In

NW1/4NW1/4, Sec. 5, the large orthopyroxene andesite dike (apparently an apophysis of the plug) has a glassy chill margin adjacent to high-silica pyroxene andesite. The great thickness and limited areal extent of the high-silica pyroxene andesites suggest that they may have formed as part of a dome. The presence of low-angle platy joints throughout the section, and the holocrystalline, quartz-bearing groundmass of samples also support emplacement as a dome.

Orthopyroxene Andesites

Lava flows and dikes in which orthopyroxene is the predominant mafic phenocryst are referred to as orthopyroxene andesites. As seen in Appendix 2b, strict adherence to a chemical classification would result in some samples being called basaltic andesite. Because of their petrographic uniformity, and lack of resemblance to typical basaltic andesites, all are refered to as andesite. No contacts between flows of orthopyroxene andesite and hornblende-pyroxene andesite are exposed, and their relationships are unclear. Orthopyroxene andesite dikes cut hornblende-pyroxene andesite flows and breccias, however, and are radial to the plug. It appears that the orthopyroxene andesite lavas issued from the Castle Rocks volcano, probably after the hornblende-pyroxene andesites. Orthopyroxene andesites crop out in two widely separated areas. Rocks from the two areas are petrographically similar, but chemically distinct.

Orthopyroxene Andesite Lava Flows and Dikes (TCR 7)

Orthopyroxene andesite lava flows and dikes are exposed west of the plug, on both sides of the Metolius River canyon. Exposures on Green Ridge are poor, usually consisting only of float. West of the Metolius River, sparse outcrops of columnar, blocky or platy jointed andesite are found. Mineralogy and chemistry of samples are uniform over the entire outcrop area, but heavy talus and forest cover prevent determination of flow thickness or the number of lava flows .

Hand specimens have a medium gray matrix, with prominent phenocrysts of white plagioclase and brownish-green pyroxene imparting a speckled appearance. In thin section, flow rocks are porphyritic and holocrystalline to hypohyaline. Phenocrysts make up about 35 % of most rocks, with plagioclase being the most common. Two types of plagioclase phenocryst can be recognized. Sieve-textured plagioclases have irregular outlines, patchy zoning and obscure twinning. Clear plagioclases are tabular, and usually continuously zoned from about An_{65} to An_{45}. As the unit name inplies, orthopyroxene is the most common mafic phenocryst. Euhedral to subhedral orthopyroxene crystals make up 6-8 % of the mode, and range from 4 mm to 0.25 mm in length. Opaque oxide inclusions are common, and orthopyroxene phenocrysts are sometimes jacketed with clinopyroxene. Rarely, orthopyroxene phenocrysts have thin rims of fibrous greenish uralite. Anhedral clinopyroxene phenocrysts make up less than 0.5 % of the mode, and most are less than 1 mm in diameter. Some thin sections contain one or two amphibole relicts, completely replaced by opaque oxides. Opaque oxide microphenocrysts up to 0.15 mm in diameter are present in trace amounts. The groundmass usually

consists of plagioclase microlites, with intergranular clinopyroxene and opaque oxides. Apatite needles are often included within plagioclase microlites.

As seen on Plate 1, orthopyroxene andesite dikes are found on the west face of Green Ridge, and are radial to the central plug. Most dikes are less than 15 ft (5 m) thick, and may project 30 ft (9 m) above ground. Dikes commonly have horizontal joints perpendicular to the chill margin, producing the "cordwood" appearance seen in Figure 20. Dike mineralogy is similar to that of the lava flows, except that hornblende crystals may have fresh cores, with only the rims replaced by opacite.

Orthopyroxene Andesites near Reservation Point (TCR 8)

Orthopyroxene andesite lava flows are also found 0.3 mi (0.5 km) southeast of Reservation Point, at about 3950 ft (1200 m) elevation, in SE1/4 Sec.18, T.11S., R.10E. Concentrations of float at 3200 ft (975 m) in SW1/4SE1/4 Sec.7 (along the abandoned Reservation Point Trail) appear to be from the same unit. Outcrops above Reservation Point are small and widely separated, but appear to be columnar jointed lava flows. Appendix 2b shows that samples from opposite ends of the outcrop area (samples 154 & 155) are identical. This, along with the thinness of the unit, suggests that only one lava flow is present.

Hand specimens are similar to those from unit TCR 7, except that pyroxene phenocrysts in TCR 8 are fewer and larger. Chemically, Reservation Point pyroxene andesites are higher in SiO_2 and lower in TiO_2 than those from TCR 7.

In thin section, these andesites are holocrystalline and porphyritic. Plagioclase phenocrysts make up about 25% of the mode, and two types are recognized. As in other units, the most common type of plagioclase is clear and tabular, with well-developed twinning. Most of the clear plagioclases show continuous normal zoning, from labradorite to andesine. The second type is anhedral to subhedral and somewhat larger, up to 4 mm in length. Patchy zoning is common in the cores of these phenocrysts, and the cores are often surrounded by an oscillatory zoned outer portion. Twinning is obscure, and glass inclusions are confined to thin bands concentric to the crystal margin.

Euhedral to subhedral orthopyroxenes make up 12-15% of the rock, and are up to 4 mm in length. Equant opaque oxide inclusions are common within orhtopyroxene phenocrysts. Clinopyroxene phenocrysts are scarce, less than 0.5% of the mode, and anhedral. Plagioclase microlites make up most of the groundmass, with common intergranular clinopyroxene and opaque oxides. The groundmass also contains a few shreds of brown biotite.

The orthopyroxene andesites near Reservation Point are isolated 2.6 mi (4.2 km) from the vent of the Castle Rocks volcano, and no similar rocks are found nearer the vent. A local source is a possibility, but there is no direct evidence. The float found along the Reservation Point trail and the outcrops above Reservation Point are separated by a north-south normal fault (Plate 1). If the float found along the trail is roughly in place, displacement on the fault must be about 750 ft (230 m).
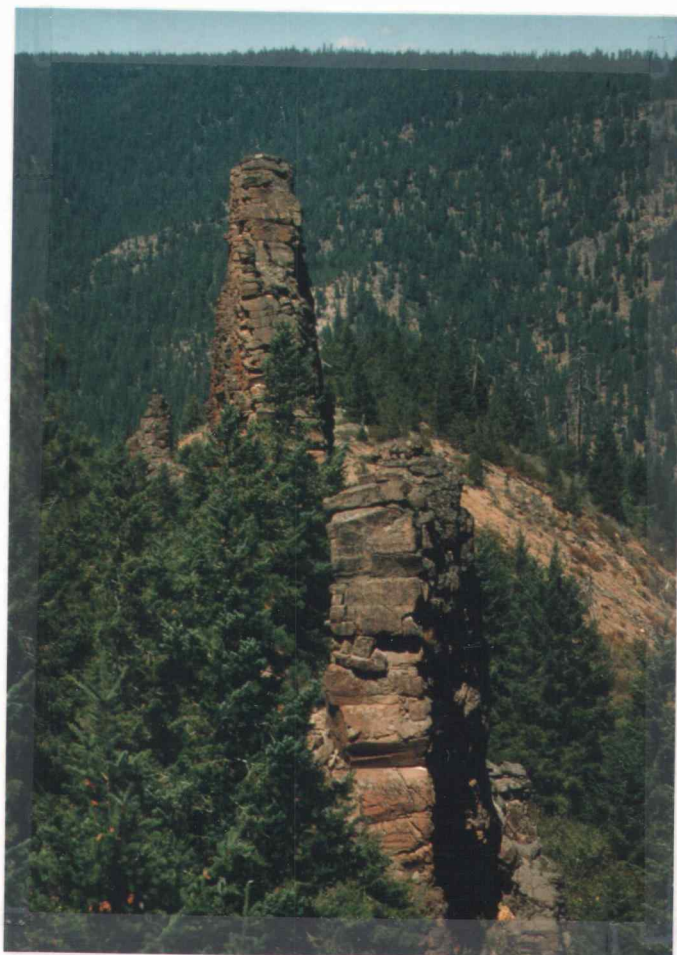
Figure 20. Orthopyroxene andesite dike (map unit TCR 5) trending
N40°W. SW1/4, Sec. 32, T.10S., R.10E.

Pyroxene Andesite Plug (TCR 9)

A cylindrical plug of normally polarized pyroxene andesite in NE 1/4NE1/4 Sec.6, T.11S., R10E. marks the center of the Castle Rocks volcano. The plug is approximately 350 ft (106 m) in diameter, and 200 ft (60 m) high. Near the contact with the country rock, the plug forms rubbly outcrops with irregular, vertical platy joints spaced at about 1 in (2.5 cm). The impressive vertical walls are produced by a combination of two joint sets; horizontal joints spaced at about 1 foot (30 cm) and well-developed vertical joints.

Hand samples from the interior of the plug are phaneritic, and light gray with greenish-brown orthopyroxene crystals up to 7 mm in diameter. Samples from the plug margins are darker and finer grained. In thin section, plug rocks are holocrystalline, hypidiomorphic, and medium-grained phaneritic with a seriate size distribution. Orthopyroxene crystals make up 5-7 % of most samples, and range from 7 mm to 0.2 mm in diameter. Most show pink pleochroism, and tend to occur in glomerocrysts. Anhedral clinopyroxene crystals make up about 1 % of the mode, and are less than 0.5 mm long. Plagioclase crystals range from 2 mm to 0.1 mm in length, and occur in two populations. Anhedral plagioclases have patchy zoned, sometimes sieve-textured cores with obscure twinning. Most have clear rims, with continuous normal or oscillatory normal zoning. Clear, tabular plagioclases have well developed twinning. Continuous normal zoning is common, from about An_{55} at the core to An_{40} at the rim. Equant opaque oxide grains make up less than 1 % of the mode. These range in size from 0.25 mm to 0.02 mm, and show a

slight tendency to occur in glomerocrysts with orthopyroxene.

Accessible parts of the plug show a uniform mineralogy. Figure 21 however, shows a block found at the foot of a cliff on the west side of the plug. It appears to indicate mixing of two magmas or assimilation of cognate xenoliths. The east margin of the plug is cut by a few dikes containing about 5% anhedral hornblende phenocrysts up to 7 mm long.

Southeast of the plug is a 75-ft.-thick dike of identical mineralogy and chemistry. The two bodies are not connected at the surface, but were probably emplaced together.

The mineralogy of the plug is similar to that of the orthopyroxene andesite lava flows, but their composition is quite different. As seen in Appendix 2b, composition of the plug is typical of hornblende-pyroxene andesites.

Hornblende Andesites and Dacites

Two units mapped in the southern part of the thesis area are discussed along with the Castle Rocks Andesites, even though they apparently did not issue from the same vent. They are treated as Castle Rocks Andesites because they share the distinct petrographic and chemical characteristics of that eruptive period.

Hornblende Dacite Dome (TCR 10)

Porphyritic hornblende dacites form the large promontory in NW1/4NW1/4 Sec.18, T.11S., R.10E., known as Reservation Point. Patches of similar rock are found on both sides of the Metolius

Figure 21. Hand sample from pyroxene andesite plug (map unit TCR 9)
showing evidence of assimilation or mixing.

River, some up to 4 miles (6.5 km.) from Reservation Point. Field
relationships are unclear, and all outcrops are mapped as unit TCR
10. At Reservation Point, the section is 1100 feet (335 m.) thick.
A north-trending normal fault displaced down-to-the-west passes
through the saddle just east of Reservation Point. The fault·
separates two outcrops of hornblende dacite. The tops of the two
outcrops are offset by about 350 ft (105 m), but the actual
displacement across the fault is unknown. Some of the thickness of
the Reservation Point exposure may be due to faulting, but there is
no direct evidence.   The slopes of Reservation Point are largely
talus-covered, with isolated ledges of dacite less than 10 feet
thick. Curved plates are the most common joint type. Irregular
blocky joints are fairly common, wheras crude columns are rare. No
single outcrop displays more than one joint type. In contrast to the
other porphyritic rock types associated with the Castle Rocks
Volcano, hornblende dacites show reverse magnetic polarity.

Hornblende dacites are distinctive in hand specimen, with about
10% glossy black hornblende phenocrysts in a light gray to nearly
white matrix. Hornblende phenocrysts are up to 5 mm in length,
usually strongly aligned, and are the only mafic phase visible. Hand
specimens from all outcrops are similar, except those from SW1/4 Sec.
1, T.11S., R.10E. Clasts from the rubbly outcrops there are
argillically altered to soft white clay with greenish phenocrysts.

In thin section, hornblende dacites are porphyritic and
holocrystalline to hypohyaline. Plagioclase phenocrysts make up
about 25% of the mode. Most plagioclase phenocrysts are clear,
tabular in shape and less than 1 mm in length. Continuous normal

zoning, from An_{50} at the core to An_{40} at the rim, is typical. Sieve-textured plagioclases are anhedral, and may be up to 2 mm in length. Most sieve-textured plagioclases show continuous normal zoning, commonly with a thin, clear rim.

Hornblende phenocrysts up to 2 mm in diameter and 5 mm in length make up 10-15% of the mode, and are much fresher than in other rock units. Most are euhedral, with thin opacite rims and olive green to brown pleochroism. Equant opaque oxide micropenocrysts up to 0.15 mm in diameter make up 1-2% of the rock.

Plagioclase microlites make up most of the groundmass, with minor needle-like crystals of higher relief and tiny flecks of opaque oxide. Hypohyaline specimens have some intersertal glass, wheras holocrystalline rocks contain intergranular quartz up to 0.1 mm in diameter.

As seen in figs. 6 through 10 and Appendix 2b, major and trace element compositions of hornblende dacites are similar to those of other Castle Rocks units.

Reservation point appears to be an exogenous dome, based on its great thickness, limited areal extent and the presence of platy jointing throughout the section. A small patch of float at about 2700 ft (823 m) in SW1/4SW1/4 Sec. 13, T.11S., R.10E., is probably part of the Reservation Point dome.

Small outcrops of hornblende dacite are also found in SW1/4NW1/4 Sec.1, T.11S., R.10E., and in NE1/4SW1/4 Sec. 30, T.10S., R.10E. These outcrops are small, and less than 75 ft (23 m) in thickness. Although compositionally and petrographically similar to the Reservation Point dacites, they probably issued from another source.

The stratigraphic position of the hornblende dacites is difficult to assess, due to the almost complete lack of visible contacts with other units. Only one contact is exposed, at 3000 ft (915 m) in NE1/4SW1/4 Sec. 30, T.10S., R.10E., where a small outcrop of hornblende dacite lies above orthopyroxene andesite. In SE1/4SW1/4 Sec. 7, T.11S., R10E., float of hornblende dacite is seen above float of orthopyroxene andesite. The situation there is complicated by faulting and extensive talus deposits. Evidence suggests that the hornblende dacites were emplaced after the orthopyroxene andesites, and were thus one of the last products of Castle Rocks volcanism. Paleomagnetic studies support the field evidence, because all hornblende dacites show reverse magnetic polarity, wheras other Castle Rocks units are normally polarized.

Hornblende Andesite Tuff Breccia (TCR 11)

Tuff breccias in NW1/4SW1/4 Sec. 19, T.11S., R.10E. appear to be related to the Castle Rocks volcano, but are sufficiently different from other tuff breccias to be treated separately. Deposits are unstratified and unsorted, with clast sizes ranging from ash to blocks 2 ft (0.6 m) in diameter. The unit is exposed over a vertical distance of about 800 ft (240 m); its true thickness is unknown. Several breccia units are probably present, but no contacts are visible. These breccias support a distinct plant community of stunted and widely scattered douglas fir trees, with almost no shrubs. The absence of shrubs is (regretably) unique in the study area, as is the close correlation between vegetation and rock type.

Breccia clasts are typically light gray, with plagioclase

phenocrysts and dark, hornblende-shaped aggregates. In thin section, plagioclase phenocrysts make up about 15% of the mode. Plagioclases have a seriate size distribution, from 2.0 to 0.5 mm in length. As in rock types described earlier, the larger plagioclase phenocrysts tend to be anhedral in shape and sieve-textured. Glass inclusions may be evenly distributed throughout the crystal, or in a band surrounding a patchy zoned core. Sieve-textured plagioclase commonly have a clear rim of lower An content than the core. Clear, tabular plagioclase phenocrysts are generally smaller and have well-developed polysynthetic twinning. Most clear plagioclases show continuous normal zoning, from labradorite at the cores to andesine at the rims.

Hornblende-shaped aggregates of opacite up to 1.5 mm in length make up about 5% of the mode. Some samples contain microphenocrysts of brown orthopyroxene between 0.025 and 0.25 mm in length. The groundmass consists mainly of plagioclase microlites, with rods of brown orthopyroxene, clear apatite and sparse opaque oxide grains.

The affinity of these breccias is unclear. The hornblende dacites discussed in the last section also have amphibole as their only large mafic phenocryst phase, but they lack groundmass pyroxene. Major-element composition of the breccias is similar to that of the hornblende-pyroxene andesites, but the breccias in unit TCR 11 lack pyroxene phenocrysts.

These breccias resemble the block-and-ash flows discussed in the section on hornblende-pyroxene andesite tuff breccias, but are spatially isolated from them. There are no lava flows of comparable mineralogy, and it seems likely that these breccias had a source different from those of unit TCR 4.

Aphyric Andesites (TCR 12)

Hales (1975) mapped this group of distinctive platy jointed, aphyric lava flows exposed southeast of Reservation Point as "La", because of their lack of phenocrysts. Hand specimens are greenish-gray and nearly aphyric. Gently curved platy joints are pervasive, and hand samples dissagregate readily into heaps of small chips. Because of the platy jointing this unit is a slope-former, and good outcrops are seldom found. A few patches of float consist of medium gray fragments with poorly developed platy jointing. These clasts contain very sparse greenish-gray phenocrysts, less than 2 mm in length. Poor exposures preclude mapping these two rock types separately, and they are consolidated into unit TCR 12.

In thin section, aphyric andesites are holocrystalline, very sparsely porphyritic and highly pilotaitic. "Aphyric" samples actually contain a few (one or two per thin section) microphenocrysts of subhedral orthopyroxene less than 0.5 mm in length. The groundmass consists of strongly aligned plagioclase microlites, with intergranular orthopyroxene and opaque oxides. Sparsely phyric varieties have similar groundmass characteristics, but contain about 2% microphenocrysts. Subhedral to euhedral orthopyroxene crystals less than 0.5 mm in length make up about 1% of the mode; some are jacketed with clinopyroxene. Aggregates of opaque material pseudomorphed after hornblende also make up 1% of the mode. A few anhedral clinopyroxene crystals up to 0.5 mm in length are found, as are a few anhedral plagioclases. The plagioclases are up to 2 mm in

diameter, with highly sieve-textured cores and thin clear rims.

In the field, there is little to suggest that these aphyric andesites are related to the Castle Rocks Volcano, and Hales (1975) mapped them as part of the Deschutes Formation. The presence of hornblende relicts in the more phyric samples, however, suggests that they are not Deschutes lavas. Appendix 2b shows that their composition is not that of Deschutes formation rocks and is, in fact, typical of Castle Rocks Andesites.

Due to poor exposure, the relationship between these aphyric andesites and the orthopyroxene andesites of TCR 8 is unknown. Plate 1 suggests several possibilities. The aphyric andesites might actually consist of two units, one younger than the orthopyroxene andesites and one older. Alternatively the orthopyroxene andesite may be younger, with its outcrops representing the remnants of an intracanyon flow. A third possibility is that of a fault west of unit TCR 8, repeating the aphyric andesite section. Faulting is unlikely, however, as the orthopyroxene andesites do not repeat, and Deschutes lavas 1200 ft (365 m) north are not faulted.

Composition

Figures 6 through 10 show that Castle Rocks Andesites are generally lower in alkalais, TiO_2, and FeO* than other rocks in the area, and are higher in CaO and MgO. Castle Rocks Andesites have a typical calc-alkaline compositional range, with very little iron enrichment. Compared to underlying Pre-Castle Rocks units, Castle Rocks Andesites are markedly lower in incompatible elements.

Discussion

The presence of radial dikes, and quaquaversal dips away from the plug indicate that it was the center of the Castle Rocks Volcano. Products of this composite volcano include lava flows, domes, pyroclastic breccias and ash-flow tuffs. Ash-flow-tuffs are confined to one small outcrop, probably due to non-deposition near the vent. Products of the volcano extend at least 4 mi (6.5 km) from the plug, and are covered by rocks of the Deschutes Formation. No clasts with definite Castle Rocks mineralogy are found in Deschutes Formation sedimentary rocks (Smith G.A., pers. comm, Dill, T.D., pers. comm.).

Most Castle Rocks Andesites are easily distinguished from older Pre-Castle Rocks units by their markedly porphyritic character and by the common presence of prominent hornblende phenocrysts. Hornblende phenocrysts are partially to completely replaced by aggregates of other minerals, indicating that the phenocrysts were not in equilibrium with the melt. The presence of these hornblende-based "clots" may have a bearing on calk-alkaline magma genesis, and will be discussed in the section on petrogenesis. Large, sieve-textured plagioclase phenocrysts also were out of equilibrium with the melt. These appear to be an early phase, possibly cognate, and their relationship to the large hornblendes is unknown.

Hales (1975) described a progressive change in phenocryst content in products of the "Hornblende Andesite Volcano". According to Hales, early lava flows contain hornblende phenocrysts, wheras in younger rocks, pyroxene phenocrysts supplant hornblende. This change was ascribed to progressive depressurization and dehydration within

the magma chamber. Unfortunately, it is impossible to establish an accurate stratigraphic succession among all the products of a poorly-exposed composite volcano. On the Castle Rocks Volcano, only one clear stratigraphic succession is visible, between 2400 ft (731 m) and 4500 ft (1372 m) in SE1/4 Sec. 33 and SW1/4 Sec. 34, T.10S., R.10E. The sequence of lava flows in this area shows no progressive mineralogical or chemical change.

On a larger scale, Hales' generalization may be more accurate. The high-silica pyroxene andesites of unit TCR 6, for example, overlie hornblende-pyroxene andesites. Although the relationship between the orthopyroxene andesite lava flows of unit TCR 7 and hornblende-pyroxene andesites is unclear, the orthopyroxene andesite plug and its associated dikes are obviously younger than the hornblende-pyroxene andesites they cut. The plug itself, however, is cut by minor hornblende-rich dikes.

The youngest Castle Rocks units, the hornblende dacites, contain no pyroxene phenocrysts at all. The hornblende dacites may actually have originated from a separate magma chamber. Certainly, the abundance of fresh hornblende reflects different conditions, either in the source region or during the ascent of the magma. The difference in magnetic polarity suggests that hornblende dacites were erupted considerably later than other Castle Rocks units.

Hales (1975) dated the hornblende dacites at Reservation Point as 8.3 ± 0.6 Ma The apparent onset of Deschutes volcanism at about 7.6 ± 0.3 Ma (Smith & Snee, 1983) also suggests that the Reservation Point dome was one of the last products of the Castle Rocks episode. Unfortunately no radiometric dates are available for any other Castle

Rocks Andesites. The age and reverse magnetic polarity of the
Reservation Point dacites suggest that they were emplaced during
Chron 4Ar of the magnetostratigraphic time scale (Harland,et al,
1982). Chron 4Ar lasted from 8.2 to 8.4 Ma (Fig. 3). Other Castle
Rocks units, almost without exception, have normal magnetic polarity.
These rocks were probably emplaced during Chron 5; a period of
predominantly normal polarity which lasted from 9 to 10.3 ma
(Harland, et al, 1982).

Castle Rocks volcanism marked a return to calc-alkaline activity
following deposition of the tholeiitic, highly evolved Pre-Castle
Rocks suite. Castle Rocks activity seems to belong to the late
Western Cascade episode of Priest and others (1983), which lasted
from about 18 m.y.B.P. to 9 m.y.B.P., and was predominantly calk-
alkaline in character. Rocks from the Castle Rocks volcano are
similar in many ways to the Elk Lake lavas of White (1980b), dated at
11.2±0.8 ma (Fiebelkorn, et al, 1982).

Pre-Deschutes Rocks

Field relationships indicate that these rocks were erupted during the relatively brief interval between the end of Castle Rocks volcanism and the onset of Deschutes activity. Pre-Deschutes rocks are significantly different, both petrographically and compositionally, from both Castle Rocks and Deschutes lavas.

Basaltic Andesites

All rocks designated as "Pre-Deschutes" are basaltic andesites with distinctive alkalai-rich compositions (Appendix 2c). Units TPDF 1 through TPDF 4 are related pyroclastic rocks, lava flows, dikes and volcanic mudflow deposits - apparently associated with a single vent.

Lapilli Tuff and Tuff Breccia (TPDF 1)

Lapilli tuffs and tuff breccias are exposed in canyon bottoms in SE1/4, Sec.1, T.11S., R.9E., and are usually overlain by mudflow deposits. Deposits are composed of lapilli to block-sized fragments supported by a matrix of waxy yellowish palagonite. Smaller clasts tend to be scoriacious, wheras the larger blocks are generally dense or only slightly inflated. Beds are thinly laminated to very thick bedded, and individual beds are often trough-shaped. Individual beds are moderately sorted, and show poor normal, reverse or symmetrical grading. The wave-like structures seen in Figure 22

Figure 22. Wave forms in Pre-Deschutes lapilli tuff (map unit
TPDF 1). SE1/4 Sec. 1, T.11S., R.10E.

are fairly common in lapilli tuffs, and are apparently base-surge deposits. Generally, bedding dips to the west and the deposit thickens to the east, giving it a wedge-shaped geometry.

Blocks from these tuffs and breccias are petrographically and compositionally (Appendix 2c) identical to the basaltic andesite lava flows described in the next section.

Basaltic Andesite Lava Flows (TPDF 2)

Lava flows usually consist of irregularly jointed pods of basaltic andesite less than 15 ft (4.5 m) in diameter in a matrix of orange-red clinker. Fragments of solid basaltic andesite are dark gray in hand specimen, with tiny plagioclase crystals and larger, equant, greenish-brown olivine. All samples tested show reverse magnetic polarity.

In thin section, samples are porphyritic and hypohyaline. Olivine is the only phenocryst phase, and crystals display a well-developed seriate size distribution. Olivine makes up about 3% of the mode, with subhedral crystals ranging from 1.5 mm to 0.2 mm in diameter. Olivine crystals are usually replaced by reddish iddings-ite.

The groundmass is weakly pilotaxitic, and composed mainly of labradoritic plagioclase laths less than 0.5 mm in length. The remainder of the groundmass is intergranular olivine, pyroxene and opaque oxide granules. Some samples contain minor intersertal brown glass.

The basaltic andesites dip roughly southwest, and represent autobrecciated lava flows.

Mudflow Deposits (TPDF 3)

Extensive outcrops of mudflow deposits are found in SW1/4. Sec.1, T.11S., R.9E. Smaller exposures of the same material are also found directly across the Metolius River. Outcrops are massive, poorly sorted and ungraded. Subangular pebbles to boulders 5 ft (1.5 m) in diameter make up about 75% of most deposits. Clasts are supported in a matrix of sand-sized material and yellow palagonite. The clast population consists of two lithologies: porphyritic hornblende andesite/dacite similar to unit TCR 10, and dark gray basaltic andesite identical to unit TPDF 2. Both lithologies are represented among the pebbles and smaller cobbles, but the larger cobbles and boulders are always basaltic andesite.

Clasts have random magnetic polarity, indicating that these deposits were emplaced at near ambient temperatures. The lack of layering, presence of large boulders and common clay-sized component argue against a fluvial origin. These deposits represent mudflows, probably triggered by the eruption of basaltic andesites onto steep slopes composed of Castle Rocks Andesites.

Basaltic Andesite Dikes (TPDF 4)

Two dikes of unusual mineralogy and composition cut ortho-pyroxene andesites in SW1/4. Sec.31, T.10S., R.10E. In hand specimen the dike rocks are dark gray, with small plagioclase phenocrysts and greenish clinopyroxene. All samples show reverse magnetic polarity. Thin sections reveal a phenocryst assemblage unlike that of any other rock in the thesis area. Plagioclase phenocrysts make up 20% of the

mode, and show a seriate size distribution from 1.5 mm to 0.5 mm in length. A few plagioclases are sieve-textured, but most are clear labradorite with continuous normal or oscillatory zoning. Subhedral clinopyroxenes make up about 3% of the mode, and show a seriate size distribution, from 2 mm to 0.1 mm in length. Subhedral ortho-pyroxenes less than 1 mm in length make up about 2% of the mode. Trace amounts of olivine relicts are present as microphenocrysts less than 0.5 mm in diameter. These are euhedral and altered to red iddingsite along the rims, wheras the cores are composed of fibrous, pale green bowlingite. Biotite microphenocrysts less than 0.25 mm in diameter are also present in trace amounts. The groundmass is composed of plagioclase, with intergranular orthopyroxene, clino-pyroxene and opaque oxides, plus intersertal brown glass.

The presence of two pyroxenes plus olivine and biotite as phenocrysts is unique among rocks in the field area. Composition-ally, the dike rocks are also unusual. In general, their composition is similar to other Pre-Deschutes basaltic andesites, but they are lower in TiO_2 and FeO*. They are included here because they share the unusually high alkalai content and reverse magnetic polarity of the other Pre-Deschutes rocks. The phenocryst assemblage seems to be a combination of Castle Rocks and Pre-Deschutes basaltic andesite phenocrysts, and may result from contamination.

These dikes are clearly radial to the plug (Plate 1). If they are truly related to the other high alkalai basaltic andesites, all of the Pre-Deschutes units may have issued from a vent in that area.

Composition

The major element composition of Pre-Deschutes basaltic andesites is distinct from both Castle Rocks and Deschutes Formation units. Most striking is the enrichment in alkalais, especially K_2O (Fig. 7). Trace element composition is completely different from that of the Castle Rocks Andesites, with the Pre-Deschutes basaltic andesites being greatly enriched in incompatible elements. On the other hand, trace element compositions of these rocks are quite similar to those of Deschutes Formation lavas.

Discussion

Pre-Deschutes basaltic andesites represent a brief eruptive period, between the end of Castle Rocks volcanism and the beginning of Deschutes activity. Compositionally they are distinct from both, although they are petrographically similar to Deschutes basaltic andesites.

Field relations indicate that the eruption of these high-K_2O basaltic andesites began explosively, producing the lapilli tuffs and tuff breccias seen in the canyon bottoms. Subsequent eruption of basaltic andesite lavas triggered mudflows on slopes of poorly consolidated Castle Rocks Andesite. Lava flows are always highly autobrecciated, indicating that they were erupted onto steep slopes.

The location of the vent is uncertain. The dikes of unit TPDF 4 suggest that the vent was near that of the Castle Rocks volcano, and the lapilli tuffs and tuff breccias appear to thicken in that dir-

ection. Surge deposits within unit TPDF 1 are found at least 1.5 mi (2.5 km) from the plug. As a rule-of-thumb, base surges reach radial distances of about one vent-width from the vent (Wohletz & Sheridan, 1979). There are exceptions, of course, but this suggests that the vent was nearer than the plug. It seems likely that the high K_2O basaltic andesites erupted from a satellitic vent somewhere on the southwest slopes of the Castle Rocks volcano.

The presence of abundant clasts of hornblende andesite/dacite in the mudflows is puzzling, as none are exposed in the area of the presumed vent. Mudflows of unit TRDF 3 do overlie poorly exposed hornblende andesite/dacite west of the Metolius River, in section 2.

Deschutes Formation

The hiatus between Castle Rocks and Deschutes volcanism was apparently brief, as the hornblende dacites of Reservation Point have been dated at 8.3±0.6 ma (Hales, 1975, recalculated by Fiebelkorn, et al, 1983) and the base of the Deschutes Formation at about 7.6 ±0.3 ma (Smith and Snee, 1983). Evidence to be discussed later indicates that the base of the Deschutes Formation in the thesis area is younger, perhaps about 6.5 ma.

Deschutes strata bank up against Castle Rocks Andesites in sections 8, 9 and 10 of T.11S., R.10E., and cover most of the southeast corner of the thesis area. Eastward-dipping basaltic andesite lavas, with subordinate ash-flow tuffs, are the most common Deschutes Formation rock types in the area. The Deschutes Formation has a maximum apparent thickness of about 1000 ft (300 m) on the northern part of Green Ridge, and thickens to between 1200 ft (365 m) and 1400 ft (427 m) southward (Conrey, 1985). The Deschutes Formation thins abruptly to the north against the high of the Castle Rocks volcano, which was never completely buried by Deschutes strata. Most Deschutes Formation rocks in the thesis area have reverse magnetic polarity, with only a thin strip of normally polarized rock along the top of Green Ridge.
Rocks of the "Old Volcano" discussed below may actually be older than the Deschutes Formation, but are included here for the sake of simplicity.

Rocks of the "Old Volcano"

Basaltic Andesite Dikes (TDF 1)

Several basaltic andesite dikes cut hornblende andesite tuff breccias in SW1/4 Sec. 29, T.11s., R.10E. Dikes are near-vertical, less than 5 ft (1.5 m) in thickness, and trend N15°-30°W. Dike segments are less than 50 ft (4.5 m) in length.

Hand specimens are dark gray, with scattered olivine phenocrysts. In thin section olivine phenocrysts make up about 5% of the mode, and have a seriate size distribution from 1 mm to 0.05 mm. A few orthopyroxene microphenocrysts up to 0.75 mm in length are present. The groundmass consists of labradorite laths, with intergranular clinopyroxene, orthopyroxene, opaque oxides and apatite needles.

These dikes are radial to a volcanic center 0.6 mi (1 km) to the south, mapped by Conrey (1985) as the "Old Volcano". The age of this "Old Volcano" is uncertain, but Conrey believed it was older than the Deschutes Formation. Hales (1975) dated a rock apparently associated with this eruptive center at 9.4±0.6 ma (recalculated by Fiebelkorn, et al, 1983), which is before the presumed beginning of Deschutes volcanism. This is older than the 8.3 ma date for the hornblende dacites of Reservation Point. At first glance this appears to contradict field evidence, since these dikes cut the hornblende andesite breccias of unit TCR11 (Plate 1). There is, however, no direct evidence to connect the hornblende andesite beccias with Reservation Point, and they could be considerably older. If both

dates are correct, it implies that the "Old Volcano" and the Castle Rocks volcano were active at about the same time.

Subaerial Fallout Deposits (TDF 2)

Tuff breccias and lapilli tuffs are exposed in Sec. 24, T.11S., R.10E., where they are apparently interbedded with Deschutes Formation lava flows. Outcrops are medium to thick-bedded, massive, and dip generally westerly. Individual beds are moderately sorted, and show weak normal or reverse grading. Clasts are monolithologic, consisting of olivine-bearing mafic rock fragments ranging from ash-sized to blocks 1 ft (30 cm) in diameter, in a matrix of waxy yellow palagonite. Lapilli and ash-sized fragments are scoriacious, while blocks are less inflated. A few blocks are somewhat fusiform. All of the samples examined show normal magnetic polarity.

In thin section, clasts are sparsely porphyrytic. Olivine is the most common phenocryst, making up less than 3% of the mode. Olivine phenocrysts are euhedral to subhedral, less than 1 mm in diameter, and contain sparse equant opaque oxide inclusions. Plagioclase microphenocrysts, if present, are seriate with groundmass plagioclase. The goundmass is composed of plagioclase microlites with intergranular clinopyroxene, opaque oxide granules and abundant apatite, plus some intersertal brown glass.

One clast was analyzed, and its composition is shown in Appendix 2d (Sample 177). Composition of the clast is unusual for a basaltic rock; it is high in TiO_2, Na_2O, K_2O, FeO* and P_2O_5, and low in CaO and MgO. The rock was analyzed by Chemex Labs Inc., and the analysis

is suspect because of its low total (Chemex reported a 1.13% LOI).

These breccias appear to represent subaerial fallout from a volcanic center somewhere nearby. The eruptive center for the "Old Volcano" of Conrey is 0.6 mi (1 km) to the southeast, but composition (Conrey, 1985, p.132) indicates that the two are not related.

Ash-flow tuffs and Tuffaceous Sediments

Ash-flow tuffs of Deschutes age are uncommon in the thesis area. Ash-flow tuffs are more common farther south on Green Ridge, especially in the lower part of the Deschutes section (Conrey, 1985). Ash-flow tuffs are scarce in the thesis area because the topographic high of the Castle Rocks volcano diverted early Deschutes-age ash flows to the north or south. Only three exposures of Deschutes-age ash-flow tuff are found in the thesis area. Outcrops are poor, and the presence of ash-flow tuffs is indicated only by float or a change in soil color. Very little work was done on these ash-flow tuffs, and all exposures on Green Ridge are consolidated into one map unit; TDF 4. The Whitewater tuff, in the canyon of the Whitewater River, is better exposed and is mapped separately.

Whitewater Tuff (TDF 3)

A distinctive pink, moderately to strongly welded ash-flow tuff exposed in the canyon of the Whitewate River has been designated the "Whitewater Tuff" by Yogodzinski (1985). Outcrops near the junction of the Metolius and Whitewater Rivers (Plate 1) are less than 100 ft (30 m) thick, and show crude columnar jointing. The upper and lower

contacts are obscured by talus, but the deposits appear to represent a single flow unit. Pumice lapilli are pink to pinkish gray, and slightly flattened. Dense, glassy blocks of porphyritic dacite (Appendix 2d) show reverse magnetic polarity.

The Whitewater Tuff is the uppermost in a series of ash-flow tuffs exposed in the Whitewater canyon. The earlier ash-flow tuffs are confined to north to northeast-trending paleochannels, and are not exposed in the thesis area. Apparently, (Yogodzinski, 1985) the Whitewater Tuff represents the last explosive Deschutes eruption represented in the Whitewater River area.

Ash-Flow Tuffs, undiff. (TDF 4)

Ash-flow tuffs included in this unit crop out in three different areas on the east side of Green Ridge (Plate 1). Exposures are poor, but the three areas obviously represent different ash flows.

The ash-flow tuff mapped in Sec. 22 & 23, T.11S., R.10E. is the northern extremity of an "andesitic" ash-flow tuff mapped by Conrey (1985, p. 245). The most common constituent of the tuff is light gray, sparsely phyric, unflattened pumice. Cores of the pumice lapilli are often darker than the rims. Glassy, sparsely phyric lithic fragments show reverse magnetic polarity.

Another ash-flow tuff is exposed in Sec. 14 & 15, T.11S., R.10E. Pumice lapilli are pale gray to dark gray, nearly aphyric and unflattened. Dark glassy lithic fragments less than 5 mm in diameter make up about 10% of the deposit. Dark, sparsely phyric lithic blocks are scarce, and show reverse magnetic polarity..

A small exposure of ash-flow tuff is found in dense woods in

SE1/4 Sec. 34, T.10s., R.10e. This tuff is composed of unflattened angular pumice lapilli, medium gray to pinkish tan in color, in a medium gray matrix. Crystals are sparse, and consist of plagioclase and rare orthopyroxene. A distinctive feature of this deposit is the absence of lithic fragments. The deposit is about 100 ft (30 m) thick and its lateral extent is limited, indicating that it filled a rather narrow channel. Like other Deschutes Formation ash-flow tuffs in the thesis area, it shows reverse magnetic polarity.

Reworked Ash-Flow Tuffs (TDF 5)

Just south of the ash-flow tuff in Sec. 34 (Plate 1) is one of the few outcrops of sedimentary rock in the thesis area. The single outcrop is less than 30 ft (10 m) in thickness, and extends an unknown distance below road level. The sediments fill a channel cut into talus deposits composed of Pre-Castle Rocks and Castle Rocks clasts, and are covered with a thick layer of colluvium.

Individual beds are tabular to trough-shaped, with the trough beds being as much as 10 ft (3 m) thick. Both planar bedding and tabular cross beds are present. Sorting is good, with most of the deposit consisting of rounded pumice fragments less than 1 cm in diameter. Most beds show normal grading of pumice clasts, and rare cobbles of Pre-Castle Rocks dacite and Castle Rocks andesite are concentrated at the bottom of beds. Pumice fragments are identical to those found in the ash-flow tuff in SE1/4 Sec. 34, and these sediments represent a reworking of that unit.

Lava Flows

Lava flows of Deschutes age bank against the Castle Rocks volcano near the middle of the thesis area (Plate 1). The distinction between the two is easily made, because Castle Rocks lavas are medium to light gray and highly porphyrytic, with large phenocrysts of hornblende, pyroxene and plagioclase. Deschutes lavas are dark gray and sparsely phyric, with phenocrysts of plagioclase and subordinate olivine and pyroxene.

Deschutes Formation basaltic andesites are also exposed west of the Metolius River. Exposures there are very poor, due to heavy forest, extensive talus deposits and a thick blanket of colluvium. Contacts shown on Plate 1 are often based only on widely scattered pieces of float.

The bulk of Deschutes Formation lavas in the field area show reverse magnetic polarity. On Green Ridge, the transition to normal polarity is found at about 4700 ft (1433 m). West of the Metolius, a reverse-to-normal transition is found at about 3000 ft (915 m).

Very little work was done on the stratigraphy of Deschutes Formation basaltic andesites. For an exhaustive treatment of the subject, the reader is refered to Conrey (1985). In this thesis, Deschutes Formation lava flows are subdivided into three units: plagioclase megacryst-bearing basaltic andesites, basaltic andesite lavas, and aphyric lavas.

Plagioclase Megacryst-Bearing Basaltic Andesites (TDF 6)

Basaltic andesite lavas with distinctive plagioclase megacrysts

are found in Sec. 22 & 23, T.11S., R.10E. Lava flows are up to 120 ft (36 m) thick, with platy jointed centers. Hand samples collected from these lava flows contain sparse, but ubiquitous, rounded clear megacrysts ranging in length from 2 to 12 mm. In hand sample it is not obvious that the megacrysts are plagioclase, because polysynthetic twinning is not pronounced. Instead, the megacrysts display closely spaced, slightly curved fractures resembling the conchoidal fracture of quartz.

In thin section, the plagioclase megacrysts show clear, unzoned cores with poorly developed twinning. The core is usually surrounded by a band rich in glass inclusions and pyroxene needles. Most megacrysts have a thin, clear, normally zoned outer rim. The megacrysts often contain large apatite inclusions.

Although Conrey (1985) reports the presence of rare ilmenite megacrysts in some samples, plagioclase megacrysts were the only phenocryst phase observed in this study. The rest of the rock consists of plagioclase laths, with intergranular clinopyroxene, olivine and opaque oxides. The rounded outlines of the plagioclase megacrysts indicate that they were resorbed by the magma.

The origin of the megacrysts is unclear. It seems unlikely that they are early phases which later reacted with the magma, because the apatite and reported ilmenite would require a magma enriched in TiO_2 and P_2O_5. Conrey (1985) believed that they formed by assimilation of anorthosite by a basaltic andesite magma.

Basaltic Andesite Lavas (TDF 7)

Basaltic andesite lava flows included in this map unit range

from 15 ft (4.5 m) to 120 ft (36 m) in thickness. Thickness variations are partly due to the fact that many of the lava flows fill east-trending valleys.

Individual flows are not mapped, but three general types are recognized. Samples 184, 185 and 186 (Appendix 2d) are similar to Conreys' "feldspar-phyric basaltic andesite". Plagioclase phenocrysts make up about 20% of these rocks, and may be up to 2 mm in length. Sieve-textured plagioclases are usually larger, with poorly developed twinning, normal zoning, and clear rims. Clear plagioclases are labradoritic in composition, and may show weak normal zoning. Sparse olivine phenocrysts are less than 1 mm in diameter. Groundmass textures are intergranular, with clinopyroxene, opaque oxides, and minor olivine occupying space between plagioclase laths.

Olivine and pyroxene-bearing basaltic andesites are also common. Normally zoned plagioclase phenocrysts make up about 15% of most samples. Olivine and clinopyroxene phenocrysts each make up less than 5% of the mode, and trace amounts of orthopyroxene are sometimes found. The groundmass consists of plagioclase, with intergranular clinopyroxene, olivine and opaque oxides.

A few samples are sparsely phyric, with less than 2% phenocrysts of plagioclase (An_{75}) and olivine. Phenocrysts of olivine are euhedral to subhedral, with iddingsite rims. The groundmass consists of plagioclase with intergranular clinopyroxene and opaque oxide grains.

Basaltic andesite lava flows are sometimes interbedded with airfall pyroclastic deposits. These are generally thin bedded and

well sorted. Commonly, normally graded beds of red and black lapilli-sized scoria alternate with beds of scoriaceous ash. The matrix of both is yellowish palagonite. Deposits range from 2 ft (60 cm) to 60 ft (18 m) in thickness. Where contacts are visible, pyroclastic beds mantle the underlying topography. Good examples are found on the west face of Green Ridge, at 4400 ft (1340 m) in NE1/4NE1/4 Sec. 18, T.11S., R.10E., and at 3960 ft (1207 m) in NW1/4NE1/4 Sec.19, T.11S, R.10E. Similar deposits are also found west of the Metolius River, at 2860 ft (880 m) in NW1/4NW1/4 Sec. 12 T.11S., R.9E.

Aphyric Lavas (TDF 8)

Aphyric lavas enriched in FeO* and TIO_2 are an important component of the Deschutes Formation. Mapable exposures in the thesis area are limited to the Whitewater Canyon, and a sample from one of these has been dated at 5.9$\pm$0.6 ma (Hales, 1975, recalculated by Fiebelkorn, et al, 1983). Scattered float on Green Ridge and west of the Metolius River, near the canyon bottom, indicate the presence of aphyric lavas in those areas. Flows in the Whitewater Canyon show normal magnetic polarity.

Aphyric lavas form flows less than 20 ft (6 m) thick. Most aphyric lava flows have well-developed platy joints, usually spaced less than 2 cm apart. Due to the jointing, most outcrops tend to be low and rubbly.

Hand specimens are dark gray, and nearly aphyric. Sparse phenocrysts of plagioclase are present, along with very sparse olivine and clinopyroxene. Thin sections reveal plagioclase as the

most common phenocryst, making up less than 2% of the mode. Olivine and clinopyroxene phenocrysts are less common, and opaque oxide microphenocrysts are sparse. The groundmass of aphyric lavas has a distinctive fine-grained pilotaxitic texture.

Aphyric lavas tend to be enriched in FeO*, TiO_2, and alkalais, and low in MgO, CaO and Al_2O_3 compared to other Deschutes lavas. Appendix 2d indicates that this is also true of the aphyric lavas in the thesis area.

Composition

Deschutes Formation rocks are compositionally distinct from the underlying Castle Rocks volcanics. Analyses of Deschutes rocks straddle the calc-alkaline/tholeiitic dividing line on the AFM diagram (Fig. 6), with aphyric lavas falling in the tholeiitic field. Rocks from the Deschutes Formation are slightly enriched in alkalais, FeO*, and TiO_2 compared to Castle Rocks andesites, with the aphyric lavas showing much greater Fe and Ti-enrichment. Deschutes Formation rocks are depleted in CaO and MgO, compared to those from the Castle Rocks volcano.

Discussion

In addition to the compositional differences discussed above, Deschutes lavas in the thesis area are much less phyric than Castle Rocks Andesites, and lack the hydrous minerals characteristic of them. These comnpositional and petrographic differences represent a

return to more tholeiitic, probably extension-related volcanism after the strongly calc-alkaline Castle Rocks episode.

Hales (1975) dated a basaltic andesite at 5000 ft (1524 m) elevation in SE1/4 Sec. 19, T.11S., R.10 at 5.4±0.7 ma (recalculated by Fiebelkorn, et al, 1983). This is very near the top of the section in the thesis area. Farther south, deposition continued somewhat longer, with a basaltic andesite at 3250 ft (990 m) in NE1/4 Sec. 27, T.12S., R9E. dated by Hales at 4.7±0.4 ma (recalculated by Fiebelkorn, et al, 1983).

Hales did not report the magnetic polarity of the dated sample in Sec. 19, but mapping from this study indicates that it is part of the thin (less than 150 ft) normal polarity interval at the top of Green Ridge. If the radiometric date is accurate, this is probably Polarity Chron 3A of the magnetostratigraphic time scale (Harland, et al, 1982). Beneath this, the magnetic stratigraphy is unclear. All the samples collected on the face of Green Ridge below this point have reverse magnetic polarity. Accumulating 1000 ft (305 m) of Deschutes Formation lavas during a single interval of reverse polarity would require accumulation rates on the order of 2500 ft (762 m) per million years. Estimates of accumulation rates on Green Ridge based on more complete sections are much lower; 700-800 ft (210-240 m) per million years (Conrey, 1985). The discrepancy may be due, in part, to faulting increasing the apparent thickness of the Deschutes Formation in the field area. In addition, polarity reversals have probably gone unrecognized beneath the talus and forest cover in the field area. Still, the bulk of the Deschutes Formation in the field area shows reverse magnetic polarity and

probably extends back to at least the 3Br Chron, which began about 6.8 ma (Harland, et al, 1982).

As Hales (1975) and Conrey (1985) have pointed out, Deschutes Formation units on Green Ridge are often confined to east-trending paleovalleys. In the thesis area, lava flows dip eastward at less than 3°, with dips decreasing away from the crest of Green Ridge. Apparently, the source of the Deschutes Formation was to the west, and the section at Green Ridge has not been tilted eastward by faulting.

Conrey (1985) noted that not all Deschutes-age basaltic andesites are confined to paleo-valleys. He interpreted steeply-dipping autobreciated lavas in Sec. 36, T.11S., R.9E., 1.2 mi (2.4 km) south of the field area as the eastern flank of a Deschutes Formation shield volcano. Basaltic airfall pyroclastic deposits in the thesis area also suggest that at least some Deschutes Formation source volcanoes were nearby.

Working in the area to the south, Conrey (1985) reported that the uppermost 400 ft (122 m) of the Deschutes section is composed mainly of basaltic lava flows, and is nearly devoid of ash-flow tuffs and silicic lavas. The same is true in the thesis area, with basal ash-flow tuffs overlain by basaltic andesite lavas. Conrey attributed this change to the onset of normal faulting, which provided structural pathways for the ascent of mafic magmas. Continued normal faulting would, of course, cut the crest of Green Ridge off from its source of lava flows, and this appears to have happened about 5.4 ma in the thesis area.

One of the objectives of the thesis was to determine the amount

of displacement on the Green Ridge fault system. Some evidence gathered from the Deschutes Formation bears on the subject. Samples 184 and 185 are taken from 4450 ft (1356 m) in NW1/4NW1/4, Sec. 17, T.11S., R.10E., and 2640 ft (805 m) in SW1/4SE1/4, Sec. 12, T.11S., R.9E. Both compositionally and petrographically, they appear to be from the same basaltic andesite lava flow. It would be fortuitous indeed, if limited mapping of very poor exposures were to reveal two outcrops of the same lava flow on opposite sides of the Metolius River. If this is the case, however, then the two segments of this lava flow are offset by 1810 ft (552 m). Allowing for a 3° eastward dip increases the offset to about 2200 ft (670 m). Paleomagnetic stratigraphy may offer a check on estimates of offset across the fault system. The main paleomagnetic feature of the thesis area is the change from reverse to normal polarity near the crest of Green Ridge. In SW1/4, Sec.17 and NW1/4, Sec.20, T.11S., R.10E., the polarity change is found at 4700 ft (1433 m). Conrey (1985) observed the same reverse-to-normal polarity change at 4700 ft. In SW1/4, Sec. 8, 1.2 mi (2 km) to the north the change is found at 4850 ft (1478 m). The difference may be due to faulting, or to the presence of a constructive high during the period of reverse polarity.

West of the Metolius River, a reverse-to-normal polarity change is found among basaltic andesites in SE1/4, Sec.12, at about 3000 ft (915 m). If this is the same polarity change observed at the crest of Green Ridge, displacement across the Green Ridge fault zone must be 2100-2250 ft (640-685 m), allowing for a 3° eastward dip.

Estimates of displacement based on magnetic stratigraphy agree well with those based on the tentative correlation of lava flows.

Other field evidence, however, appears to be inconsistent with this estimate. The subject will be treated in greater detail in the section on structural geology.

High Cascades

Rocks of the High Cascade platform were erupted after early
Pliocene normal faulting terminated deposition of the Deschutes
Formation. In the thesis area, most High Cascade rocks are found
west of the Metolius River, "ponded" against the Green Ridge
escarpment. High Cascade volcanism east and south of Green Ridge
produced Squawback and Little Squawback volcanoes, Black Butte, and
Garrison Buttes (Fig. 1). Any hiatus between Deschutes and High
Cascades volcanism in the northern Green Ridge area was apparently
brief, as Yogodzinski (1985) dated the base of the High Cascades
section in the lower Whitewater River at 4.3 ±0.8 Ma.

High Cascade rocks in the thesis area are predominantly basaltic
andesite lava flows, similar in appearance to those from the
Deschutes Formation. The major distinction between the two is that
High Cascade units are not displaced by the Green Ridge fault.
Instead, the distribution of High Cascade units is controlled by
current topography. This is especially well demonstrated by the dik-
tytaxitic lavas confined to the Metolius River canyon.

High Cascade rocks exposed in the thesis area are divided into
five map units. The bulk of the High Cascade sequence is composed of
sparsely phyric olivine-bearing basaltic andesite lavas. These
apparently had their source in the Bald Peter volcano (fig. 1), and
are mapped together as unit THC 1. The "Sheep Creek Lavas", mapped
as unit THC 2, are basaltic andesites with sparse quartz xenocrysts.
Diktytaxitic basalts are a common rock type in the High Cascade
sequence, and two units are distinguished in the thesis area. Map

unit THC 3 is a sheet of diktytaxitic basalt which forms Metolius Bench (fig. 1). Diktytaxitic intracanyon basalts confined to the canyon of the Metolius River are mapped as unit THC 4, although they may actually be Quaternary in age. The youngest High Cascade deposit in the field area is an unconsolidated airfall pumice mapped as unit QHC 5. Several lines of evidence suggest that this pumice vented near Mt. Jefferson.

Basaltic Andesite Lava Flows

Bald Peter Lavas (THC 1)

Basaltic andesite lavas of unit THC 1 apparently issued from the Bald Peter shield volcano and are informally referred to as "Bald Peter Lavas". Use of this term is not meant to preclude the possibility that some of these basaltic andesites may have come from other unrecognized vents. The summit of Bald Peter is 6574 ft (2004 m) and shows a typical vent facies of bedded cinders, dikes, steeply dipping lavas, and a central plug (Hales, 1975; Yogodzinski, 1985). Bald Peter is 3.5 mi (5.6 km) west of the thesis area (fig. 1), and analyses of rocks collected higher on its flanks by Hales (1975) and Yogodzinski (1985) are included in Appendix 2e. Hales (1975) dated the summit of Bald Peter at 2.2 ±0.2 Ma (recalculated by Fiebelkorn, et al, 1983). Both Hales and Yogodzinski reported that Bald Peter lavas show reverse magnetic polarity. Nearly all the samples collected in this study, however, are normally polarized. These normally polarized rocks forming the rim of the Metolius canyon are probably older, apparently formed during the period of normal

polarity lasting from 3.4 to 2.5 Ma (Harland, et al, 1982).

Bald Peter lavas form thin flows, usually less than 50 ft (15 m) thick, although a few units are up to 120 ft (36 m) in thickness. Most flows have well developed platy jointing, with crude columnar joints in the upper parts of thicker flows.

Hand specimens are dark gray and sparsely porphyrytic, with phenocrysts of olivine and plagioclase. Bald Peter lavas are similar in appearance to Deschutes Formation basaltic andesites, and the distinction between them is not always easy to make. Bald Peter lavas tend to show less olivine-to-iddingsite alteration than Deschutes rocks, and their groundmass lacks the incipient alteration often seen in the Deschutes Formation.

In thin section, most Bald Peter lavas have less than 5 % phenocrysts. Subhedral olivine crystals less than 1 mm in diameter are the most common phenocryst phase. Olivine phenocrysts range from fresh to completely iddingsitized. Some olivine phenocrysts show partial alteration to iddingsite, inside a rim of clear olivine. Sheppard (1962), studying basalts in Washington, showed that the clear outer rim of such olivine phenocrysts was richer in iron than the core. Sheppard believed that the outer rim was formed after the iddingsitization of the core, implying a high-temperature origin for the iddingsite. This inference was disputed by Baker and Haggerty (1967), who believed that all iddingsite is formed under low temperature, oxidizing conditions.

Plagioclase phenocrysts are less common than olivine, and are also usually less than 1 mm in diameter. Most plagioclases have normally zoned cores with thin, clear, more sodic rims. A few

plagioclase phenocrysts have sieve-textured cores charged with inclusions of glass and pyroxene granules; these plagioclases tend to be larger than the others. Sparse anhedral clinopyroxenes are found in some thin sections. Some lavas are nearly aphanitic, and have a strongly developed pilotaxitic texture, with intergranular clinopyroxene, opaque oxides and sparse orthopyroxene.

Sheep Creek Lavas (THC 2)

Distinctve, quartz xenocryst-bearing basaltic andesites are exposed on both sides of Sheep Creek (Plate 1), and are informally referred to as "Sheep Creek Lavas". The Sheep Creek Lavas are up to 530 ft (162 m) thick, and show pronounced platy jointing. The distribution of float indicates that the Sheep Creek Lavas overlie the basaltic andesites of unit THC 1. Good exposures are rare, except on the north side of Sheep Creek canyon where the unit thins abrubtly to the east, apparently filling a north-south valley. The paleomagnetic polarity of the unit is ambiguous, as roughly equal numbers of samples show normal and reverse polarity, even when collected from a single outcrop.

Hand samples are distinctly more porphyritic than those from the Bald Peter lavas, and contain 10-15 % phenocrysts. Plagioclase is the most common phenocryst, followed by olivine and clinopyroxene. Many hand samples contain rounded, clear crystals rimmed with another, darker mineral.

In thin section, plagioclase phenocrysts up to 3 mm in length make up at least 10 % of the mode. Sheep Creek lavas show the usual two types of plagioclase phenocrysts; clear, tabular crystals, and

larger, sieve-textured anhedra. Relatively fresh, subhedral olivines up to 1.5 mm in diameter make up about 2 % of the mode and most thin sections contain a few anhedral clinopyroxene phenocrysts. Microscopic examination reveals that the rounded clear grains seen in hand specimen are quartz, surrounded by rims of clinopyroxene. As seen in Figure 23, the rim-forming clinopyroxene is usually granular and irregularly distributed around the quartz grain. The quartz grains appear to be xenocrysts which have reacted with the enclosing magma.

No evidence of a vent for the Sheep Creek lavas has been found. Petrographic characteristics of the Sheep Creek lavas indicate that they are not part of the main Bald Peter sequence. Yogodzinski (1985) reports porphyritic, late-stage basaltic andesites near the summit of Bald Peter. The phenocryst assemblage reported for these rocks is plagioclase + orthopyroxene, with trace amounts of olivine and clinopyroxene, therefore they are probably not related to the Sheep Creek lavas.

Diktytaxitic Basalts

Metolius Bench Basalts (THC3)

The diktytaxitic basalts forming Metolius Bench unconformably overlie Pre-Castle Rocks, Castle Rocks, and Deschutes Formation strata north of the Metolius River (Plate 1). In the thesis area, the Metolius Bench basalts are less than 100 ft (30 m) thick, and consist of as many as ten flows. The basal contact is gently undulating; apparently the basalts flowed onto a surface of very low relief. Just west of the thesis area, in the walls of the Whitewater
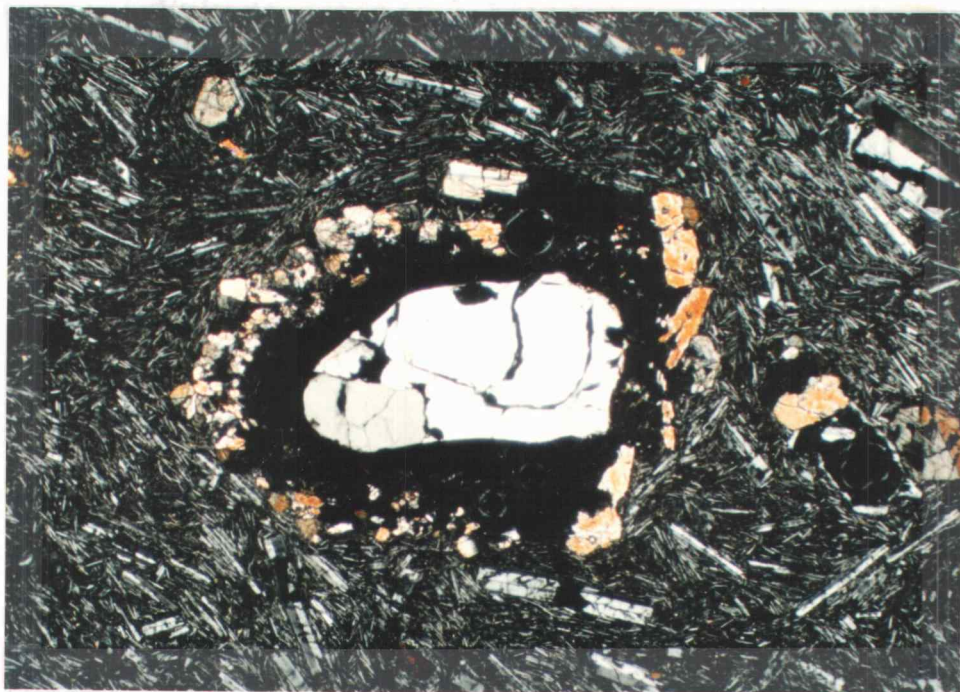
Figure 23.   Photomicrograph of a quartz xenocryst with clinopyroxene reaction rim (map unit HC 2, sample 213). SE1/4 Sec. 11, T.11S., R.9E. Field of view 3.3 mm., crossed polars.

Canyon, Metolius Bench basalts fill an east-trending paleovalley 500 ft (152 m) deep (Yogodzinski 1985). The vent for the Metolius Bench basalts has not been located, but must lie somewhere to the west of Green Ridge. Diktytaxitic basalts also form Tenino Bench, Schoolie Flat and Mill Creek Flat, prominent benches about 8 mi (13 km) to the north. Like Metolius Bench, these benches dip away from the Cascades, and may be stratigraphically equivalent.

Metolius Bench basalts are slightly porphyrytic and diktytaxitic, with up to 15 % void space. Olivine is about 12 % of the mode, and has a seriate size distribution from 1.25 to 0.25 mm in diameter. Plagioclase, at 35-45 % of the mode is the most abundant mineral, with 25-35 % intergranular clinopyroxene. Opaque oxides are about 5 % of the mode, and some samples contain intersertal brown glass.

Samples 215 and 216 were collected 3.2 mi (5.2 km) apart and are compositionally similar (Appendix 2e). Yogodzinski (1985) analyzed basalts farther west on Metolius Bench with a different composition (Table 3). Apparently the Metolius Bench basalts represent more than one episode of volcanism. The exact age of these basalts is unknown, but they overlie basaltic andesites dated at 4.3 ±0.7 Ma (Yogodzinski, 1985). Field relationships indicate that Metolius Bench basalts are older than the Metolius canyon basalts, placing them somewhere in the interval 4.3-1.7 Ma (age of the intracanyon basalts is discussed in the next section). Given their uniformly reversed magnetic polarity, it is likely that they were emplaced between 3.9 and 3.4 Ma ; during the active period of the Bald Peter shield volcano.

TABLE 3
Comparative Composition of Mafic Rocks

	AVNB	AVBP	MW	NS	SC	DEVGAR
SiO_2	49.8	55.2	55.4	55.6	58.1	48.8
TiO_2	1.48	1.17	1.16	0.93	0.88	0.9
Al_2O_3	17.3	18.0	17.9	18.5	18.6	17.2
$FeO*$	9.7	7.9	7.5	6.9	6.4	9.2
CaO	8.8	7.7	7.7	7.5	7.3	11.0
MgO	8.3	4.4	4.8	4.9	3.3	9.2
Na_2O	3.3	3.8	4.2	4.0	4.3	2.4
K_2O	0.71	0.90	1.14	0.94	0.85	0.29

	HAOT	LAMB	DWMB	MCn	MCr	JC
SiO_2	47.7	50.3	50.0	50.7	50.1	50.5
TiO_2	1.00	1.30	1.97	1.30	1.50	1.56
Al_2O_3	16.9	16.2	15.6	14.8	16.9	16.3
$FeO*$	9.9	11.0	10.6	11.6	10.5	10.7
CaO	11.2	8.4	8.4	9.4	9.4	10.1
MgO	9.1	9.9	8.6	8.4	7.3	7.8
Na_2O	2.5	2.6	3.1	2.8	3.1	2.8
K_2O	0.23	0.21	0.54	0.24	0.24	0.34

AVNB   "Normal" High Cascade basalt. Average of 13 (Hughes, 1985).
AVBP   Bald Peter basaltic andesite. Average of 40 (Hales, 1975; Yogodzinski, 1985; this paper).
MW   "Mt. Washington type" basaltic andesite. Average of eight (Hughes & Taylor, 1986).
NS   "North Sister type" basaltic andesite. Average of eight (Hughes & Taylor, 1986).
SC   Sheep Creek lavas. Average of three (this study).
DEVGAR "Devils Garden" diktytaxitic basalts from southern Oregon and northern California. Average of six (McKee, et al, 1983).
HAOT   "High Alumina Olivine Tholeiites" from the northwestern Great Basin. Average of 50 (Hart, et al, 1984).
LAMB   "Low Alkalai Metolius Bench". Average of six (Yogodzinski, 1985)
DWMB   Metolius Bench basalts. Average of two (this paper).
MCn   Normally polarized diktytaxitic benches in the Metolius River Canyon. Average of 12 (this paper and T. Dill, pers. comm.)
MCr   Reverse polarized diktytaxitic basalt from tops of normally polarized Metolius Canyon benches. Average of three (this paper).
JC   Reverse polarity diktytaxitic basalt from intracanyon bench in Jefferson Creek (Hales, 1975).

Intracanyon Basalts (THC 4)

Wedge-shaped benches of diktytaxitic olivine basalt follow the course of the Metolius River from near Jefferson Creek (Plate 1) almost to The Cove Palisades State Park (Tom Dill, pers. comm.), a distance of 20 mi (32 km). Composition of the basalts is similar over the entire distance, indicating that the benches represent a single group of lava flows. Elevation of the bench tops decreases downstream at 45 ft/mi (8 m/km), the same gradient as that of the modern Metolius River. Benches are up to 240 ft (73 m) thick, and composed of flow units less than 20 ft (6 m) thick. Their geometry and the fan jointing seen in Figure 24 indicate that they filled channels.

The basalts are diktytaxitic, with about 10 % void space. Olivine makes up 15-20 % of the mode, with a seriate size distribution from 3.5 to 0.25 mm. Olivines are relatively fresh, with only thin iddingsite rims. Plagioclase is more abundant than in the Metolius Bench basalts, making up 45-50 % of the mode. Clinopyroxene is correspondingly less abundant, at less than 20 % of the mode. Clinopyroxene is usually intergranular, often with subophitic domains in the same slide. Wedge-shaped intergranular opaque oxides make up less than 5 % of the rock.

A bench of diktytaxitic basalt in sections 25 and 36, T.11S., R.10E. appears to be the southernmost (upstream) end of the flow. Conrey (1985) reports a basalt dike in the NW1/4 Sec. 30, T.11S., R.10E. which has a composition similar to that of the bench (appendix 2e), and may be the source of these flows.

Previous descriptions of these intracanyon benches report a
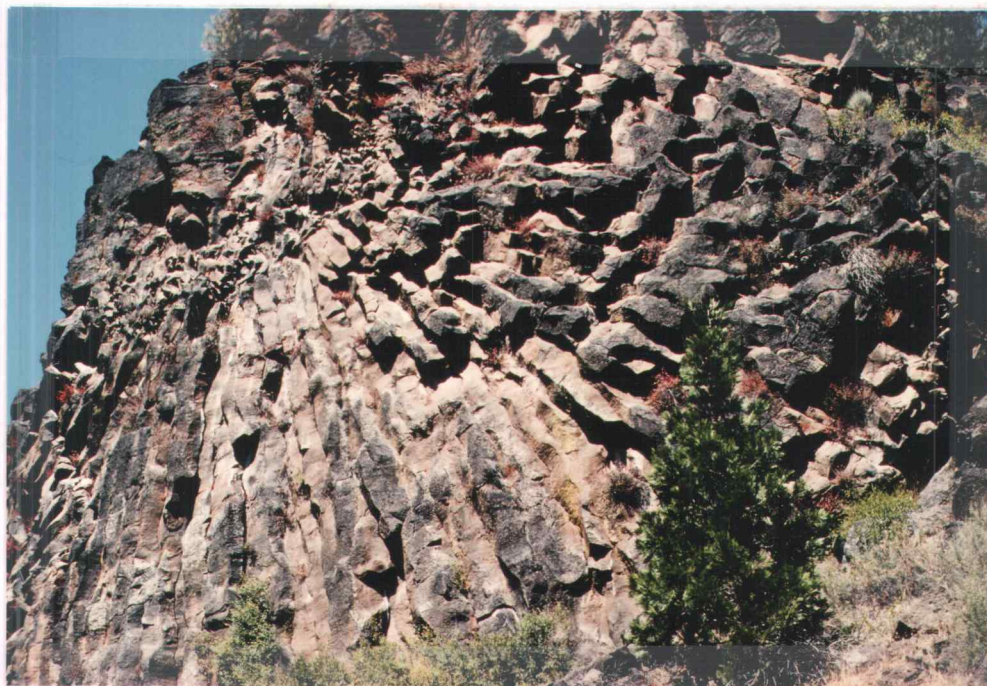
Figure 24. Fan jointing in intracanyon bench (map unit THC 4).
SE1/4, Sec. 36, T.10S., R.9E.

uniform composition and normal magnetic polarity. This study reveals a break in the section, although the break is not recognizable in the field. The lower part of each bench has normal polarity and a composition similar to that reported by Hales (1975) and Conrey (1985) (Appendix 2e, samples 217-224). Flows at the top of the benches have reverse polarity and a distinctly different composition. Rocks with reverse polarity are richer in TiO_2, Al_2O_3 and Na_2O, and poorer in MgO and FeO* (Appendix 2e, samples 225-227).

The age of the Metolius intracanyon benches is questionable. Conrey (1985) estimated the age of the benches in the Metolius valley by extrapolation from an intracanyon bench in the Jefferson Creek valley ("JCB" on Table 3), dated by Hales (1975) at 1.6 ±0.3 Ma (recalculated by Fiebelkorn, et al, 1983). Conrey assumed that the age of the two benches must be proportional to the height of their tops above river level (560 ft for the Metolius bench vs 330 ft for the Jefferson Creek bench), arriving at an estimate of about 2.7 Ma. Conrey noted that comparing the elevations at the bottom of the benches would yield a more accurate estimate of relative age, and the discovery of an outcrop of intracanyon bench east of the Metolius River (sample 219) makes this possible. Both the Metolius River and Jefferson Creek benches extend to about 80 ft (24 m) above river level. One of the benches may, of course, have originally extended below its currently exposed base, but not by more than 80 feet. Based on this new information, it appears that the Metolius River and Jefferson Creek benches are roughly the same age, an estimate consistent with the paleomagnetic stratigraphy. The Metolius River intracanyon benches show a consistent change from normal to reverse

polarity near the top. This is probably the change from Polarity

Chron 2 to Chron 1r (Fig. 3), dated at 1.67 Ma (Harland, et al,

1982). It seems likely that the Metolius River intracanyon lavas

were emplaced at about the Pliocene/Pleistocene boundary. Only one

analysis is available from the reverse polarity bench in Jefferson

Creek (Hales, 1975), and it is identical in composition to the upper,

reverse polarity portions of the Metolius River benches (Table 3).

Thorough sampling of the intracanyon benches will be required to

determine the significance, if any, of this similarity.

Airfall Deposits

Hornblende Pumice (QHC 5)

The youngest High Cascade unit in the thesis area is an airfall-

pumice deposit of apparent late Pleistocene age. Pumice lapilli of

this unit are distinctly fresh and silky, with conspicuous hornblende

crystals up to 4 mm in length. Patches of pumice-rich soil are found

throughout the thesis area and, as seen in Figure 25, hornblende

pumice is found in the tailings piles of underground workings. The

best exposures are found in roadcuts, and these are the only

locations mapped as QHC 5 on Plate I. The hornblende pumice is

distributed over a distance of at least 25 mi (41 km) from the upper

Whitewater canyon (Yogodzinski, 1985) to Lake Simtustus (Jay, 1982).

In the upper Whitewater canyon, hornblende pumice is found in an ash-

flow tuff and associated air-fall tuffs, with clast sizes up to 25 cm

(Yogodzinski, 1985). Maximum size of the pumice lapilli decreases

from 10 cm in the thesis area, to about 5 cm in Fly Creek

Figure 25.   Tailings pile containing hornblende pumice of map unit
QHC 5.   NE1/4 Sec. 12, T.11S., R.9E.

Canyon (fig. 1), and 2 cm near Wizard Falls (Conrey, 1985). Most of
the pumice in the thesis area is white with conspicuous hornblende
phenocrysts. Plagioclase is the dominant phenocryst phase, with
subordinate orthopyroxene and hornblende. As seen in Table 4, the
white pumice has a constant composition wherever it is found. Tom
Dill (pers. comm.) also reports an andesitic gray pumice (Table 4)
and a mixed white and gray pumice in the lower Metolius River Valley.
Gray and mixed pumices are also found in the soil below Metolius
Bench.

The westward increase in clast size, and the presence of ash-
flow tuffs in the upper Whitewater Canyon suggest that the vent for
the pumice was somewhere on Mt. Jefferson. Two hornblende dacite
domes are likely candidates: Goat Peak, on the southern flank of Mt.
Jefferson, and the "North Complex" (Sutton, 1974) on its northeast
slope. Both are compositionally similar to the white pumice (Table
4). The "North Complex" is the more likely source, as ash flows
venting there would be easily directed down the Whitewater canyon.

The hornblende pumice is probably Late Pleistocene in age, as it
is interbedded with glacial till in the Whitewater Canyon
(Yogodzinski, 1985). Ash-flow tuff outcrops high on the walls of the
Whitewater canyon also suggest that the canyon was ice-filled at the
time of eruption. Based on glacial stratigraphy, Yogodzinski (1985)
estimates the age of the hornblende pumice at 20,000-60,000 years.

TABLE 4
Composition of hornblende pumice and hornblende dacite domes from Mount Jefferson

	YWP	MWP	FCP	GRP	DWP
SiO_2	69.7	70.4	69.3	66.5	70.4
TiO_2	0.45	0.47	0.43	0.47	0.47
Al_2O_3	14.2	15.8	15.7	17.9	15.8
$FeO*$	3.2	3.4	2.9	3.3	3.4
CaO	2.9	3.0	3.0	3.2	3.00
MgO	1.0	1.0	1.0	1.1	1.0
Na_2O	4.6	4.3	4.4	4.4	4.3
K_2O	1.90	1.72	2.03	1.73	1.72

	LSP	LGP	QDD	QPF	QGP
SiO_2	69.7	61.0	65.9	72.2	67.5
TiO_2	0.41	0.82	0.64	0.43	0.46
Al_2O_3	15.4	18.6	17.0	14.2	15.3
$FeO*$	3.1	6.3	4.5	3.2	3.1
CaO	3.0	6.5	4.5	3.2	1.3
MgO	1.2	3.2	1.8	0.9	3.1
Na_2O	5.0	4.1	4.3	4.6	5.1
K_2O	2.32	1.16	1.53	2.04	1.70

YWP White pumice from upper Whitewater canyon. Average of three (Yogodzinski, 1985).

MWP White pumice from lower Metolius River canyon. Average of three (T. Dill, pers. comm.).

FCP White pumice from Fly Creek Canyon. Sample RC-276 of Conrey (1985).

GRP White pumice from west face of Green Ridge. Sample RC-114 of Conrey (1985).

DWP White pumice along Metolius River road. Average of two (this study).

LSP White pumice near Lake Simtustus (Jay, 1982).

LGP Light gray pumice from lower Metolius River canyon. Average of ten (T. Dill, pers. comm.).

QDD Hornblende dacite dome, northeast flank of Mt. Jefferson (Sutton, 1974).

QPF Plutonic fragment from ash-flow tuff in upper Whitewater canyon (Yogodzinski, 1985).

QGP Hornblende dacite from Goat Peak, southeast flank of Mt. Jefferson (Sutton, 1974).

Composition

Except for the tholeiitic diktytaxitic basalts, most High Cascade rocks in the thesis area plot within the Calc-Alkaline field on the AFM diagram (Fig. 6). Major-element composition of the basaltic andesites is quite similar to that of Deschutes Formation basaltic andesites, with High Cascade rocks being slightly enriched in MgO and K_2O, and depleted in FeO* and Al_2O_3.

Both Bald Peter and Sheep Creek basaltic andesites are high-alumina (averaging 18.2 wt %), and quartz normative. Both rock types fall within the high-alumina field of Kuno (1966). Average TiO_2 content is 1.17 wt %, with up to 1.5 wt % in the most mafic members (Appendix 2e).

Hughes and Taylor (1986) studied the central High Cascade platform of Oregon, and distinguished "normal" basalts from two types of basaltic andesite. Basalts are subphyric to porphyritic, and often diktytaxitic. Olivine phenocrysts make up about 20 % of the mode, with subordinate plagioclase. Normal basalts are high in alumina, and are olivine-normative. TiO_2 content averages 1.48 wt % (Table 3), high for a convergent plate margin (Green, 1980), but typical of continental rifting environments.

Hughes and Taylor recognize two types of basaltic andesites: a "Mount Washington type" (MW), and a "North Sister type" (NS). Both are porphyritic, with plagioclase in excess of olivine, and average about 55.5 wt % SiO_2 (Table 3). TiO_2 content of both types is lower than for the basalts, and is typical of mafic rocks from orogenic regions. As seen in Table 3, the Mount Washington type is higher in

TiO_2 and alkalis. Bald Peter basaltic andesites, however, are not plagioclase-phyric, nor does their composition fit the pattern described above. Although their TiO_2 contents are the same as the MW basaltic andesites, they are lower in alkalis than either the MW or NS type. Fe' (the molar ratio FeO*/FeO* + MgO) for Bald Peter basaltic andesites varies from 0.42 to 0.66, while Fe' for the MW and NS basaltic andesites ranges from 0.40 to 0.53 and 0.32 to 0.50, respectively. Mineralogically the Sheep Creek lavas resemble the High Cascade basaltic andesites of Hughes and Taylor (1986), and their composition approximates that of the NS type basaltic andesite (Table 3).

Diktytaxitic basalts in the thesis area are high-alumina olivine tholeiites containing normative olivine and hypersthene, but no quartz or nepheline (Yoder & Tilley, 1962). The composition of these basalts is similar to the "Normal High Cascade basalt" composition of Hughes & Taylor (1986), but with less K_2O and Al_2O_3, and greater FeO*. The Metolius Bench basalts are unusual in their high TiO_2 content.

Diktytaxitic olivine-tholeiite basalts are widespread in the northwestern Great Basin, and range in age from late Miocene to Holocene (McKee, et al, 1983; Hart, et al, 1984). Diktytaxitic basalts are also common in the late High Cascade sequence, suggesting that similar processes were operating in the Great Basin and behind the Cascade arc.

Table 3 compares diktytaxitic lavas from the thesis area with those from the northwestern Great Basin ("HAOT" AND "DEVGAR"). High Cascade diktytaxitic rocks in the thesis area are quite similar to

those from the Great Basin, except for a higher TiO_2 content and a decrease in CaO and Al_2O_3. The Metolius Bench basalts are unusual for their high TiO_2 and K_2O contents and for their low CaO content, lower even than that of the Metolius canyon basalts.

Discussion

Field evidence indicates that High Cascade rocks post-date faulting on the Green Ridge system, but radiometric dating (Yogodzinski, 1985) shows essentially no hiatus between Deschutes and High Cascade volcanism. This is consistent with of Conrey's (1985) suggestion that upper Deschutes mafic lavas ascended along structural pathways opened by the onset of normal faulting.

Bald Peter volcanism lasted from about 4.3 Ma to 2.2 Ma Unlike most Bald Peter lavas (Hales, 1975; Yogodzinski, 1985), basaltic andesites in the field area are generally normally polarized. During the period of Bald Peter activity, magnetic polarity was predominantly normal between 3.4 and 2.5 ma, and the basaltic andesites in the field area were probably emplaced during this period.

Many of the "Metolius Bench basalts" of Yogodzinski (1985) are compositionally distinct from those collected to the east as part of this study ("LAMB" vs. "DWMB" on Table 3). These basalts are indistinguishable in the field but based on topographic relationships, it appears that the low-alkalai basalts are younger. One of Yogodzinskis' Metolius Bench basalts (sample #1093, Yogodzinski, 1985) is identical to those from this study, and

overlies a High Cascade basaltic andesite dated at 4.3 Ma (Yogodzinski, 1985). Field relationships and paleomagnetic stratigraphy discussed earlier in this paper indicate that the Metolius Bench basalts were probably erupted between 3.9 and 3.4 Ma; during the active period of the Bald Peter shield volcano. Diktytaxitic basalts at the base of Mill Creek Flat (Fig. 1) have been dated at 3.7 ±0.1 Ma (Smith, 1986), indicating that they are stratigraphically equivelant to the basalts of Metolius Bench.

Basaltic andesite volcanism, which had begun at about 4.3 ma, ceased at about 2.2 ma, the age of the Bald Peter plug. Bald Peter volcanism was followed at about 1.7 Ma by the eruption of the Metolius canyon basalts.

The pattern of volcanism was thus one of coeval or alternating eruptions of subduction-related basaltic andesites and high-TiO_2, extension-related basalts. Hughes and Taylor (1986) describe a central High Cascades tectonic setting in place since about 4.5 Ma, in which extension and subsidence-related basalts predominate over basaltic andesites produced by a waning calc-alkaline system. High Cascade volcanism in the thesis area fits this pattern, with the late Pleistocene eruption of hornblende pumice from Mt. Jefferson showing that calc-alkaline magmatism is still active.

Structural Geology

Regional structural relationships

The structural geology of the Green Ridge area includes north-south and northwest-southeast faults, both of which are important structural features of the Oregon Cascade Range.

The most obvious structural feature in the Green Ridge area is the Green Ridge fault system, a series of down-to-the-west normal faults with a total displacement of at least 2500 ft (760 m). The Green Ridge escarpment marks the eastern boundary of the postulated "Cascades volcano-tectonic depression" of Allen (1966). Later work has revealed that the structure is not the simple graben proposed by Allen, but that the Cascade crest does coincide with a generally linear gravity low extending from near Mt. Jefferson to Mt. Lassen (Blakely, et al, 1985). The gravity low is presumably due to low-density fill in a structural depression along the Cascade crest.

Other boundary faults have been recognized in the Cascade Range, and are shown on Figure 26. The Hood River fault has approximately 1800 ft (550 m) of down-to-the-west displacement, and is analogous to the Green Ridge fault. South of Green Ridge, scattered down-to-the-west normal faults are mapped as far as Klamath Falls (Priest and others, 1983). West of the Cascade crest, the Cougar Reservoir fault probably has at least 1400 ft (427 m) of down-to-the-east displacement. The Horse Creek fault, 10 mi (16 km) east of the Cougar Reservoir fault, has 2000 ft (610 m) of displacement (Flaherty, 1981). Near Waldo Lake, the Groundhog Creek and Waldo Lake faults
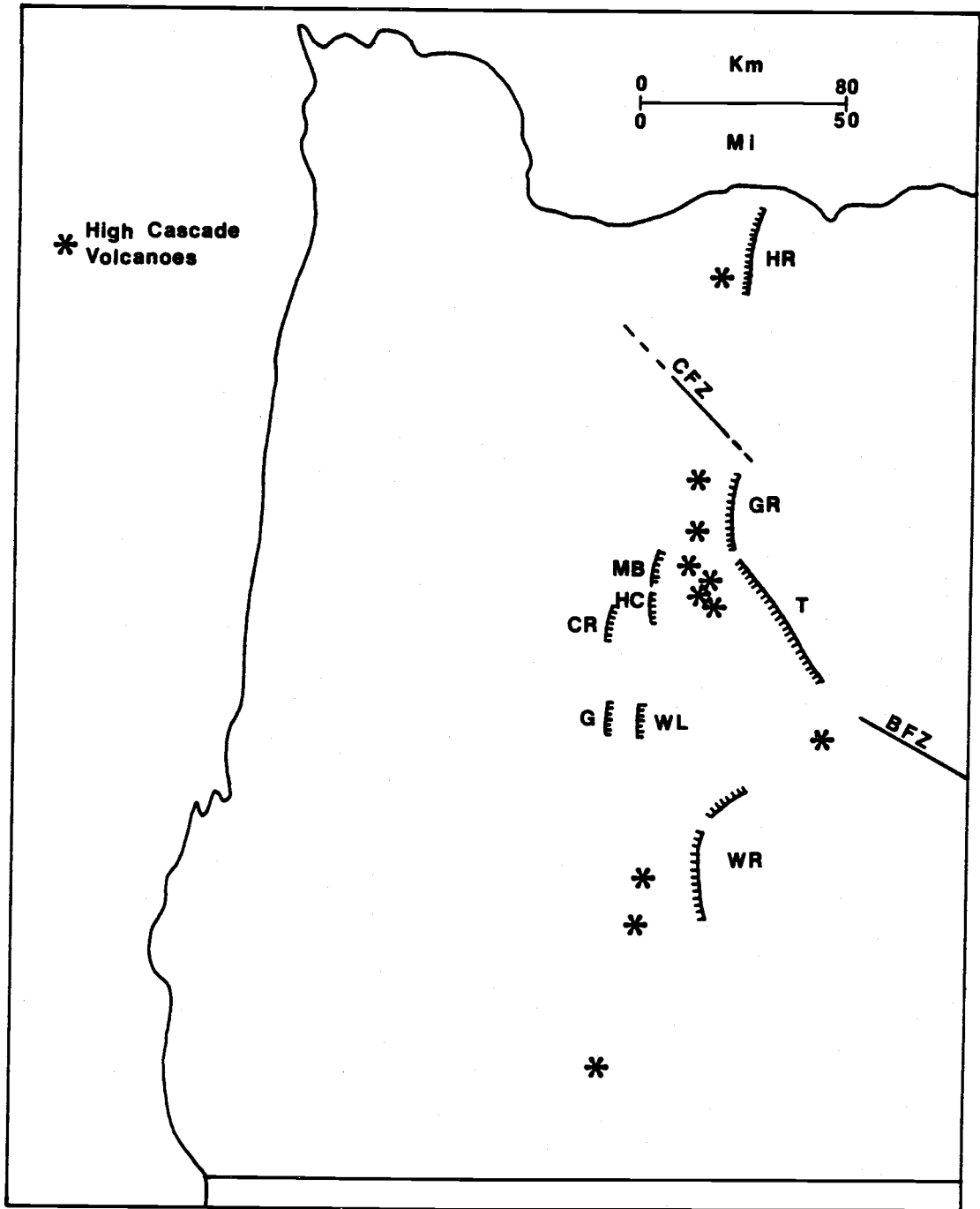
Figure 26. Major structural features of the Cascade Range in Oregon.
HR=Hood River fault, GR=Green Ridge fault, T=Tumalo
fault, MB=McKenzie Bridge fault, HC=Horse Creek fault,
CR=Cougar Reservoir fault, G=Groundhog Creek fault,
W=Waldo Lake fault, WR=Walker Rim fault system,
CFZ=Clackamas fault zone, BFZ=Brothers fault zone.
After Smith (1986b).

appear analogous to the Cougar Reservoir and Horse Creek faults farther north (Woller and Black, 1983).

The Cascades did not subside as a simple graben, because the boundary faults are discontinuous and were active at different times. The Green Ridge fault was active about 4.5 Ma, but subsidence on the Hood River fault continued until about 3 Ma (Priest and others, 1983). West of the Cascade crest, the Horse Creek fault was activated in early Pliocene, and motion apparently continued until about 1 Ma (Flaherty, 1981). Activity on the Cougar Reservoir fault began about 13 Ma (Priest and Woller, 1983), well before the early Pliocene subsidence episode recorded at Green Ridge.

Several lines of evidence indicate that the north-south graben is interrupted at about the latitude of Mt. Jefferson. West of Mt. Jefferson, Deschutes-equivelant rocks are found near the Cascade crest (Rollins, 1976; R.M. Conrey, pers. comm.). North of Mt. Jefferson, White (1980c) has mapped Pliocene Outerson Formation rocks at the Cascade crest. North of Green Ridge, on the east side of the Cascades, Pliocene basalts which cap the Deschutes Formation apparently flowed east unimpeded by a fault scarp (Smith, 1986b).

Geophysical studies also indicate a break in the graben at about the latitude of Mt. Jefferson. Gravity studies by Couch and others (1982) show that the strong north-south lineation found south of Mt. Jefferson does not continue to the north. Heat-flow studies reveal that the linear heat-flow high associated with the Cascade crest is also broken north of Mt. Jefferson (Black, 1980).

North of Mt. Jefferson, the north-south graben is interrupted by a northwest-trending fault system. One prominent structural zone

follows the course of the Clackamas River, and the entire zone of northwest trending faults is known as the "Clackamas fault zone". Faults within the zone trend about N45°W, and show both normal and strike-slip motion. Mapping by Hammond and others (1980) indicates that motion on the Clackamas fault zone began in mid Miocene, and continued until at least the Pliocene. White (1980c) inferred offset of Quaternary units along some northwest trending faults.

Toward the southern end of Green Ridge, displacement on the Green Ridge fault system decreases as it approaches a zone of northwest-trending faults about 12 mi (20 km) wide. This northwest-trending fault zone extends from the south end of Green Ridge to Newberry Caldera, and is known as the "Tumalo fault zone" (Hales, 1975). The sense of motion on individual faults is variable, producing small horsts and grabens. Lawrence (1976) used the term "Sisters Fault Zone", and contended that it connected the Green Ridge faults with the Brothers fault zone. Faults of the Tumalo fault zone cut Pleistocene and Holocene lavas from Newberry Crater, while those of the Brothers fault zone do not (Smith, 1986b), indicating that the Tumalo fault zone has been active more recently.

The relationship between the Green Ridge and Tumalo fault zones is uncertain. North-south normal faulting may continue southward toward the Three Sisters, as postulated by Conrey (1985). If so, the southern end of Green Ridge marks the intersection of major north-south and northwest-southeast fault systems. Smith (1986b), on the other hand, believes that the Green Ridge fault zone turns southeast and merges with the Tumalo fault zone. In Smiths' view, the southern end of Green Ridge marks a transition from north-south to northwest-

southeast faulting.

Many mafic vents of Late Miocene to Holocene age are located within the Tumalo fault zone. The cinder cones of Garrison Buttes may be as young as Pleistocene (Leudke and Smith, 1982), and are aligned on a N40°W trend (Fig. 1). In the Deschutes Basin, vents for the Late Miocene Tetherow Butte member of the Deschutes Formation are aligned on a N35°W trend. Near Lower Bridge on the Deschutes River, dikes feeding the Early Pliocene Steamboat Rock Member of the Deschutes Formation have a N15°W alignment (Smith, 1986b).

This northwest structural trend extends west beyond Green Ridge, as a N15°W-trending fault is presumed to be responsible for the alignment of Quaternary cinder cones south of Abbot Creek (Fig. 1). The Late Pliocene Bald Peter and Lionshead vents are on the northwest extension of this trend, but the alignment may be coincidental. Yogodzinski (1985) reports evidence of faulting and dike emplacement along a N30°W trend near the Lionshead eruptive center.

Structural geology of the thesis area

All of the faults mapped in the field area trend north-south and have down-to-the-west displacement. Recognized fault segments are short, due in part to poor exposures. Four faults are mapped (Plate 1), with three of the four in the southern part of the field area.

The most prominent fault passes just east of Reservation Point, and juxtaposes hornblende dacites against aphyric andesites in the saddle which marks its trace. Hornblende dacite is exposed east of the fault, as seen on Plate 1, and the top of Reservation point

appears to have been down-dropped about 225 ft (68 M) relative to the top of this outcrop. To the south, in NE1/4 Sec. 19, the top of the aphyric andesite is offset by about 200 ft (60 m). The fault cannot be followed further south because its trace is buried by basaltic andesite float, but it may be responsible for the shape of the ridgetop in SE1/4 Sec. 19, one mile (.62 km) south of Reservation point.

Another normal fault produces the prominent slope break in SW1/4 Sec. 19, T.11S., R.10E., where Deschutes Formation basaltic andesites are in contact with hornblende andesite tuff breccias. Offset is difficult to estimate, because the geometry of the tuff breccia unit is unknown. Offset is at least 400 ft (120 m), and possibly as much as 1000 ft (305 m). This is the only fault which can be traced south into the area mapped by Conrey (1985). Conrey estimates the displacement there to be at least 300 ft (91 m), and possibly as much as 800 ft (244 m).

A small fault scarp cuts basaltic tuff breccias in the center of Sec. 24, T.11S., R.9E. Displacement across the fault is between 20 ft (6 m) and 120 ft (36 m). The only fault in the northern part of the field area is in NW1/4, Sec. 1, T.11S., R.9E. The base of the down-dropped block of hornblende dacite is not visible, but offset is probably about 100 ft (30 m).

The total offset across the faults in the southern part of the field area is probably less than 1300 ft (400 m). This estimate does not include a correction for dip because the dip of the affected units is unknown. Evidence from Deschutes Formation rocks exposed north of Reservation Point suggests a substantially greater offset.

Paleomagnetic and lithologic correlations discussed in the section on
the Deschutes Formation require an offset of about 2200 ft (670 M).
The simplest explanation for the discrepancy is an inferred fault
with the required displacement, somewhere in the Metolius River
canyon. No such fault is shown on Plate 1 because hornblende dacites
of unit TCR 10 and mudflows of unit TPDF 3 are found at about the
same elevation on both sides of the Metolius River (Plate 1). If
there is no unexposed fault in the area, then displacement across the
mapped faults must be variable. If this is the case, total displace-
ment must increase from about 1300 ft (400 m) in the southern part of
the thesis area to at least 2200 ft (670 m) near Reservation Point.
It is possible that other north-south normal faults exist west of the
Metolius River. The existance of such faults must remain speculative
because, if present, their traces are buried beneath High Cascade
platform lavas. North of Reservation point, faulting decreases to a
total offset of about 100 ft (30 m) near Castle Rocks. There is no
evidence for significant normal faulting north of Castle Rocks,
although faulting cannot be ruled out entirely because of poor
exposures and lack of marker horizons. The orthopyroxene andesites
of unit TCR 7 appear to be undisturbed, and any faults in the area
must be minor. Yogodzinski (1985), mapping in the area immediately
to the north, reported no evidence of north-south normal faulting.
This northward decrease in normal faulting is consistent with the
observation that the north-south boundary faults die out north of the
latitude of Mt. Jefferson.

Many workers (Wells and Peck, 1961; Waters, 1968, Venkatakrish-
nan and others, 1982) map a northwest trending fault along the lower

Metolius River. Mapping from this study shows no offset of Pre-Castle Rocks or Castle Rocks strata across the presumed fault. The work of Yogodzinski (1985) and T. Dill (pers. comm.) demonstrates that Deschutes and High Cascade rocks are not displaced across the Metolius River. Smith (1986b) has noted that this lower Metolius lineament lines up with the Clackamas fault zone. Whatever its significance may be, the lineation is not a fault.

PETROLOGY

Pre-Castle Rocks

Pre-Castle Rocks units are tholeiitic, as shown by the AFM diagram (Fig. 6). Tholeiitic rocks in general are higher in TiO_2, K_2O and FeO* than calk-alkaline rocks, and lower in CaO, MgO and Al_2O_3. As seen in Figs. 7-10, this is true of Pre-Castle Rocks samples, compared to those from the overlying Castle Rocks units. The petrography of Pre-Castle Rocks samples is also typical of intermediate rocks of the tholeiitic trend, with few phenocrysts and no hydrous minerals.

Pre-Castle Rocks samples are unusual for their high degree of iron enrichment (Fig. 10), and for the presence of olivine phenocrysts in dacites. The high degree of iron enrichment in Pre-Castle Rocks samples is reflected in their Fe', which ranges from 0.61 for basaltic andesites to 0.89 for dacites. Microprobe analyses (Table 1) reveal that olivine phenocrysts in the dacites are fayalitic (Fo_{32}), and the coexisting clinopyroxene phenocrysts are ferroaugite. Both olivine and clinopyroxene are normally zoned, with their rims enriched in iron (Table 1).

The mineralogy and major-element composition of these rocks are consistent with a high degree of differentiation along a tholeiitic trend. Their high content of the incompatible elements Zr, Nb and Ba also suggests that Pre-Castle Rocks samples are highly differentiated.

Assuming that magma differentiation results from crystal

fractionation, major- and minor- element composition can be an indicator of the minerals involved. Two-element plots are commonly used to show differentiation trends, and several fractionation indices are available. In this study both the Pre-Castle Rocks and Castle Rocks groups have compositions which range from basaltic andesite to dacite, and it is desirable to chose an index which is appropriate for viewing the entire compositional range on one plot.

The Harker index (SiO_2 on the abscissa) is probably the most familiar fractionation index. In basaltic rocks however, SiO_2 content often shows little increase in the early stages of magmatic evolution. TiO_2-content may be used to indicate the degree of differentiation because Ti tends to be concentrated in the residual melt during crystal fractionation, especially in the tholeiitic trend. Eventually TiO_2 content should begin to decrease with increasing fractionation, as an iron oxide mineral comes onto the liquidus. As seen in Figure 9 the behavior of TiO_2 changes at about 58% SiO_2, making it less suitable as a fractionation index. MgO, or the ratio FeO*/MgO are also used as fractionation indices, especially in mafic rocks. In the more silicic rocks examined in this study, MgO-content is so low that analytical error becomes a significant factor, and its use is restricted to basalts. SiO_2 is used as the fractionation index in compositions other than basalt. More complicated fractionation indices are available, such as the Differentiation Index or the Solidification Index, but the simpler MgO and SiO_2 indices used here show the same information.

Ni-contents of Pre-Castle Rocks are about 6 ppm in a basaltic andesite and 2 ppm in an andesite (Appendix 2a). This is very low,

compared to the 30 ppm in a Castle Rocks andesite. Such a low Ni-content indicates extensive fractionation of forsteritic olivine, a mineral which is found in Pre-Castle Rocks basaltic andesites. Fe' shows a strong negative correlation with MgO, also suggesting fractionation of olivine.

Plagioclase has a very high CaO/FeO^*, and Figure 27 is consistent with the fractionation of plagioclase. The fractionation of a Ca-pyroxene would also lower CaO/FeO^*, and no simple treatment can separate the effects of the two processes.

The variation of CaO/Al_2O_3 is a good measure of clinopyroxene fractionation because clinopyroxene is rich in CaO, and contains very little Al_2O_3. As seen in Figure 27, CaO/Al_2O_3 shows a strong negative correlation with SiO_2, suggestive of clinopyroxene fractionation. Fractionation of calcic plagioclase would have little effect on CaO/Al_2O_3. Because of this, the CaO/Al_2O_3 vs SiO_2 plot in Fig. 27 does not preclude plagioclase fractionation, but does indicate that clinopyroxene must also be a factor.

V-content drops sharply, from 204 ppm in basaltic andesite, to 32 ppm in dacite. Since V is strongly partitioned into Fe-Ti oxides, some magnetite fractionation must have taken place in spite of the over-all trend toward iron enrichment. There is a strong positive correlation between TiO_2 and FeO^*, indicating that most TiO_2 is contained in Fe-Ti oxides. Pre-Castle Rocks basaltic andesites contain about 31 ppm Cr, but andesites and dacites do not contain measurable amounts. Mg-rich pyroxenes fractionate significant Cr, as do spinel group minerals. Othropyroxene phenocrysts are found in
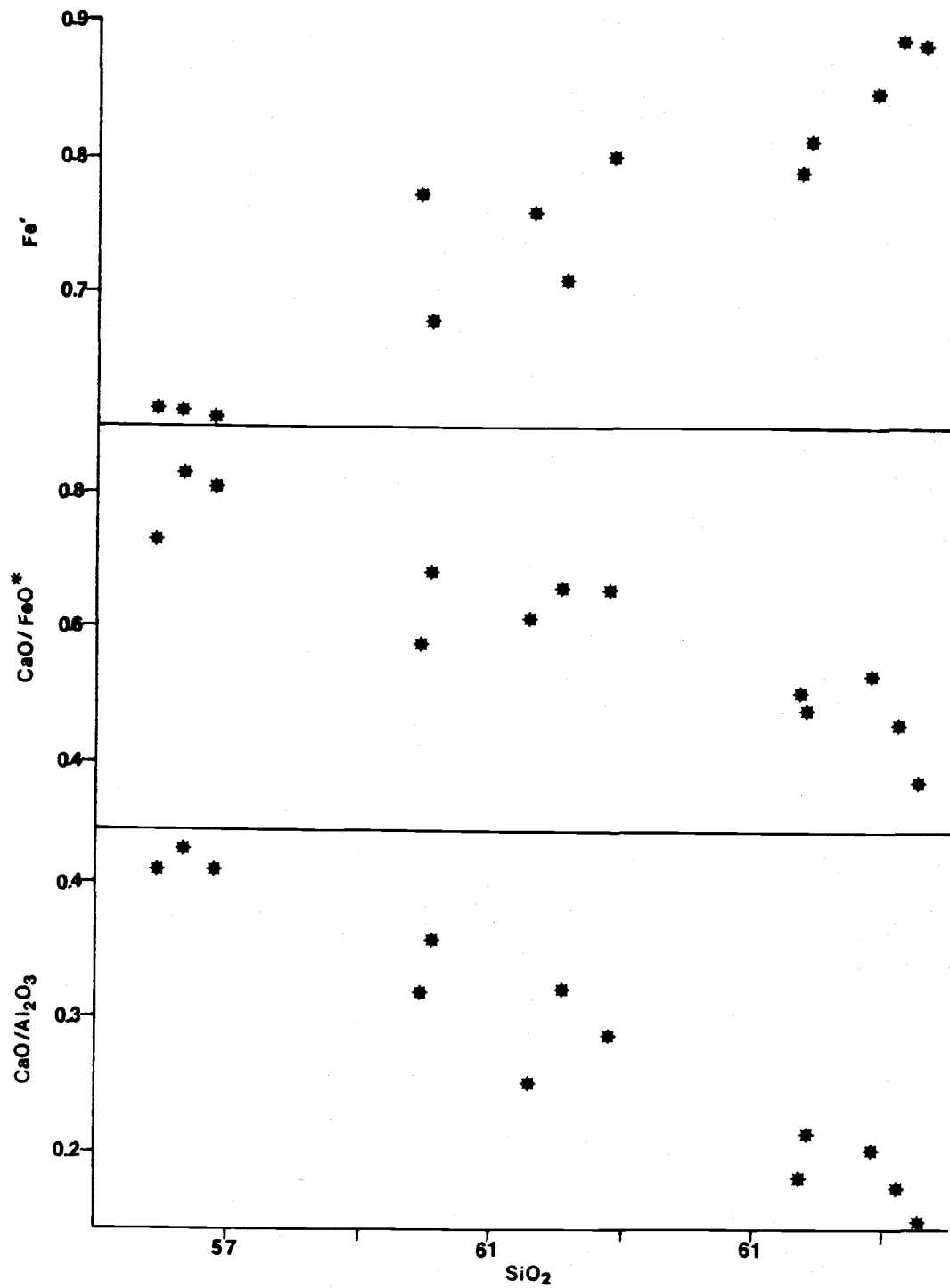
Figure 27. Variation of Fe', CaO/FeO* and CaO/Al₂O₃ with silica
content in Pre-Castle Rocks Samples.

Pre-Castle Rocks samples, and commonly contain opaque inclusions.
The composition of these inclusions is unknown, but they may contain
significant amounts of Cr.

Compositional data indicate that Pre-Castle Rocks andesites and
dacites could be derived from the basaltic andesites by the
fractional crystallization of olivine, clinopyroxene, plagioclase and
Fe-Ti oxides. All of these minerals are found as phenocryst or
microphenocryst phases in Pre-Castle Rocks samples.

More complete examples of tholeiitic fractionation series are
found in several parts of the world. The best-known example is the
Skaergaard Intrusion, summarized by Wager and Brown (1967). In the
Skaergaard, fractional crystalization of olivine, pyroxene and
plagioclase has produced late silicic rocks highly enriched in iron.
Pre-Castle Rocks dacites are in many ways analagous to subzone "a" of
the Upper Zone ("UZa") of Wager and Brown. The Upper Zone of the
Skaergaard Intrusion is marked by the appearance of fayalitic olivine
as a cumulus phase, and contains the mineral phases olivine (Fo_{31}),
ferroaugite ($Wo_{35}/En_{33}/Fs_{32}$), and plagioclase (An_{45}-An_{50}), plus some
apatite and magnetite. The similarities with Pre-Castle Rocks
mineralogy (Tables 1 & 2) are striking.

Pre-Castle rocks basaltic andesites contain forsteritic olivine,
but olivine is absent from andesites. In the Skaergaard intrusion,
cumulus forsteritic olivine disappears at the top of the Lower Zone,
apparently replaced by inverted pigeonite. The composition of
groundmass pyroxenes in Pre-Castle Rocks andesites is unknown because
of their fine grain size, but one clinopyroxene phenocryst has a rim
of pigeonite (Fig. 4).

Of course it is possible to overstate the analogy between a huge, well-exposed, layered mafic intrusion and two small outcrops of volcanic breccia. Study of the Skaergaard Intrusion does demonstrate that continued fractionation along a tholeiitic trend can produce rocks similar to those found in the thesis area.

Thingmuli volcano in eastern Iceland is an example of an extrusive sequence which shows some of the features of the Skaergaard differentiation trend. At Thingmuli, tholeiitic fractionation has produced Fe-rich andesites ("icelandites") and fayalite- bearing "rhyolites" (rhyodacites, according to the classification scheme used in this paper). As seen in Table 5, Compositions of these rocks are quite similar to those from the thesis area. The few minor and trace element analyses available from the thesis area are comparable to those plotted for Thingmuli (Carmichael, Turner, and Verhoogen, 1974, Tables 3-1 and 3-2). Both the Thingmuli and Pre-Castle Rocks suites show much less iron-enrichment than the Skaergaard. Carmichael (1964) attributed the reduced iron-enrichment at Thingmuli to the appearance of Fe-Ti oxides on the liquidus.

Castle Rocks

Products of the Castle Rocks volcano have calc-alkaline compositions, as discussed in the previous chapter. Their high phenocryst content (35-45%) and the abundance of amphibole phenocrysts in andesites and dacites are also characteristic of calc-alkaline rocks. Differentiation trends are not obvious, in spite of the linear patterns seen on major-element variation diagrams. This

TABLE 5
Comparative Composition of Fe-Rich Rocks

	PCA	TA	PCD	TD	UZb
SIO_2	61.4	60.6	66.8	64.5	65.9
TiO_2	1.12	1.25	0.59	0.71	1.00
Al_2O_3	16.6	15.1	15.2	14.4	12.1
$FeO*$	7.9	8.0	5.8	6.1	10.8
CaO	5.0	4.9	2.7	3.5	3.7
MgO	1.5	1.7	0.6	0.7	0.2
Na_2O	3.7	4.3	4.3	4.1	3.7
K_2O	2.50	1.59	3.07	2.14	2.07

PCA Pre-Castle Rocks andesite. Average of 5 (this paper).
TA   Thingmuli andesite. From Carmichael (1967), Analysis #14, Table 4.
PCD Pre-Castle Rocks Dacite. Average of 5 (this paper).
TD   Thingmuli "andesite". From Carmichael (1967), Analysis #15, Table 4.
UZb Calculated liquid from UZb level of the Skaergaard Intrusion. From Hunter and Sparks (1987), Table 2.

is not surprising, in view of the complex mineralogy ofCastle Rocks samples. Amphiboles have a wide range of possible compositions, and no compositional data are available on the amphiboles from the thesis area.

Even small amounts of clinopyroxe fractionation should strongly lower the ratio CaO/Al_2O_3 of more evolved rocks. Castle Rocks samples show a slight negative correlation of CaO/Al_2O_3 with SiO_2 content, as seen in Fig 28. Sc and Cr are strongly fractionated by clinopyroxene, but Figure 29 shows that their abundances do not correlate with CaO/Al_2O_3. Both of these elements are also fractionated by amphiboles; therefore, amphibole fractionation is apparently involved here.

The ratio $CaO/FeO*$ should decrease as a result of any plagioclase fractionation. Castle Rocks samples plotted on Figure 28 show a scattered, but positive correlation with SiO_2, ruling out fractionation of plagioclase alone. Sr-contents are high (up to 1000 ppm) and show only a slight decrease with increasing SiO_2 content, also indicating a lack of plagioclase fractionation. The generally high Sr content probably reflects the abundance of plagioclase phenocrysts. Fractionation of olivine could conceivably raise $CaO/FeO*$, but Ni-contents decrease only slightly, and olivine is not a phenocryst in Castle Rocks samples. Orthopyroxene is a common phenocryst, and its removal would tend to increase $CaO/FeO*$.

The apparent lack of plagioclase fractionation may reflect the H_2O-content of the magma. Increasing the water content of a magma shifts the diopside-anorthite cotectic toward anorthite, reducing the stability field of plagioclase (Yoder, 1965). Increasing the water
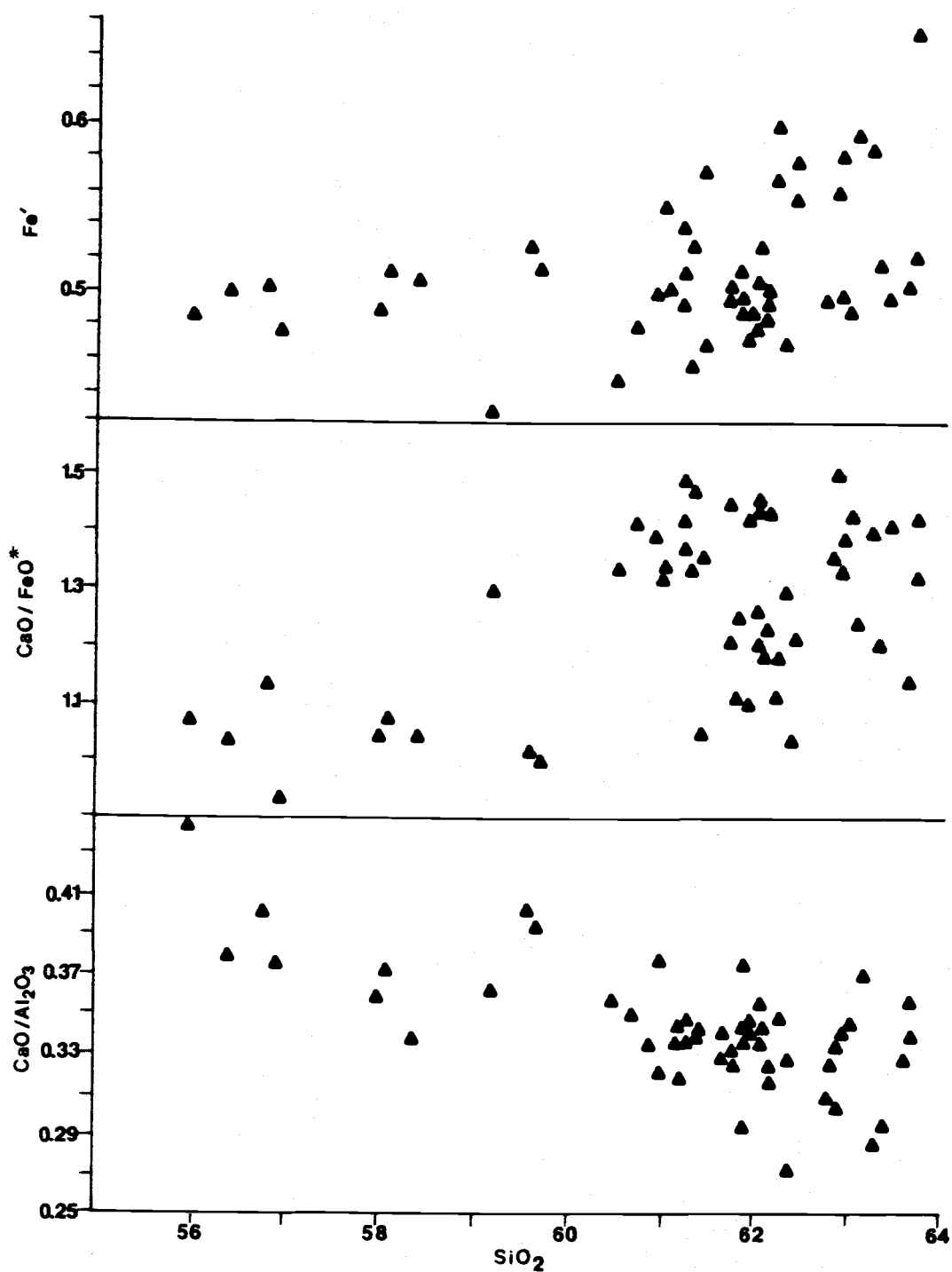
Figure 28. Variation of Fe', CaO/FeO* and CaO/Al$_2$O$_3$ with silica
content in Castle Rocks samples.
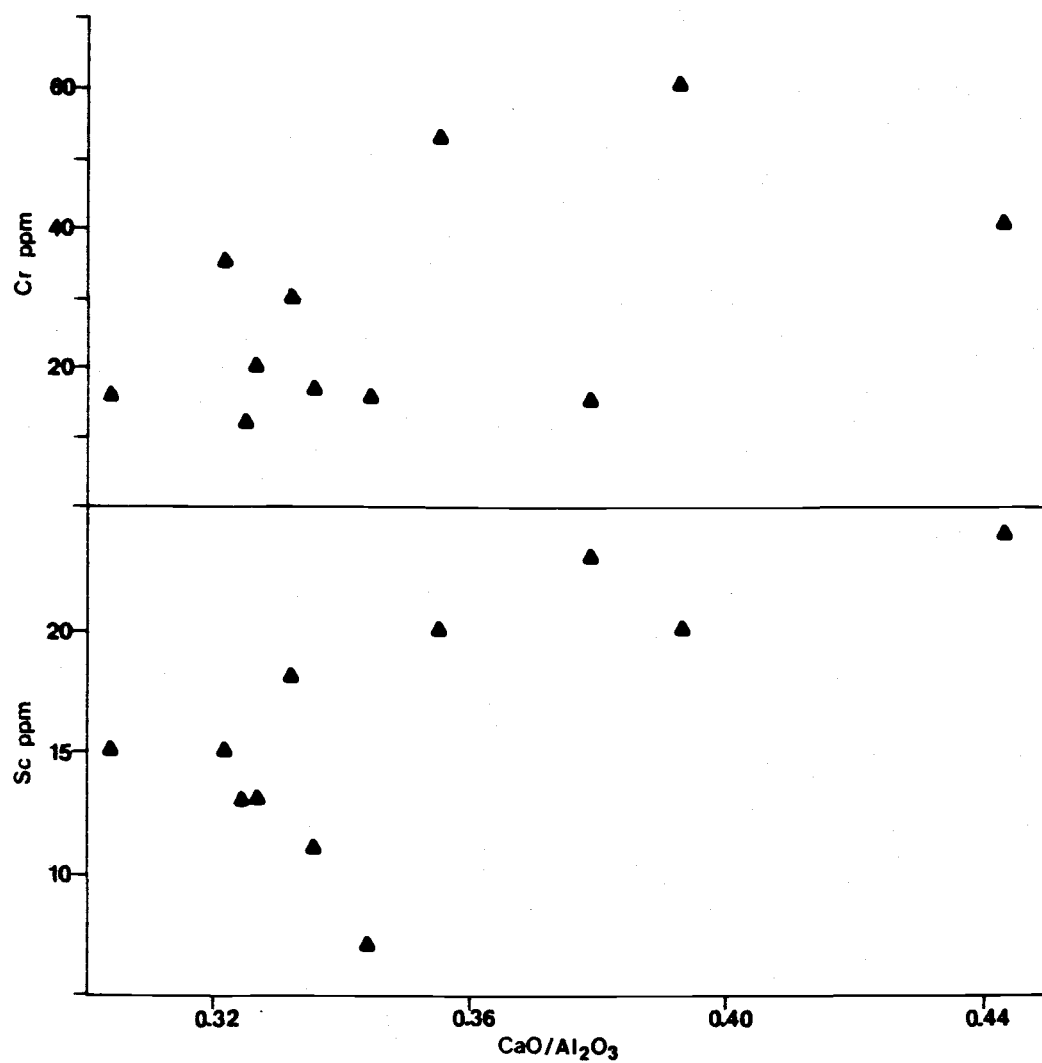
Figure 29. Variation of Cr and Sc with CaO/Al_2O_3 in Castle Rocks samples.

content of a magma also increases olivine.stability (Nicholls and Ringwood, 1973). Because of their abundant amphibole phenocrysts, it appears that Castle Rocks magmas formed under conditions of high water content. It should be pointed out that the abundance of plagioclase phenocrysts in Castle Rocks samples seems to contradict geochemical evidence for lack of plagioclase involvement in differentiation.

An obvious feature of the Castle Rocks trend is the lack of iron enrichment. This lack of iron enrichment is characteristic of calk-alkaline rocks, and must be a result of early removal of iron from the melt. Both Fe-Ti oxides and amphiboles are rich in iron and titanium, and the fractionation of either would suppress iron enrichment. In Castle Rocks samples, V decreases with increasing SiO_2 content. Because both Fe-Ti oxides and amphiboles fractionate V along with Fe and Ti, the removal of either mineral would decrease V and increase the SiO_2 content in residual melts. The limited compositional data available in this study are consistent with either possibility, especially as the composition of amphiboles in Castle Rocks samples is unknown. Amphibole is common as phenocrysts in silicic rocks of the Castle Rocks group, and as relicts in low-silica andesites. Early crystallization of opaque oxides is indicated by their presence as microphenocrysts, and as inclusions in pyroxene phenocrysts.

Trace element patterns are difficult to reconcile with any fractionation scheme. Zr, Nb and Rb are all highly incompatible, but do not increase with increasing SiO_2. Zr does show a strong positive correlation with P_2O_5. This suggests some form of fractionation, but

not one which increases SiO_2. Mineralogy of Castle Rocks samples is too complex, and compositional data are too sparse, to construct a unique fractionation scheme explaining Castle Rocks compositional trends. All that can be said is that the available data allow derivation of the most silicic members from the low-silica orthopyroxene andesites.

A discussion of calc-alkaline magma genesis is beyond the scope of this paper, but some mention should be made of the possible role of amphiboles in the process. Many authors (Holloway and Burnham, 1972; Boettcher, 1973; Cawthorn and O'Hara, 1976) have suggested that fractionation of iron-rich amphibole could suppress the iron enrichment trend, thus producing calc-alkaline magmas. Evidence from from inclusions and xenoliths in mafic rocks indicates that amphiboles may be in equilibrium with mantle-derived primary melts (Arculus and Willis, 1980; Conrad and Kay, 1980, 1981). Anderson (1980) cited experimental and petrographic evidence that hornblende can be stable in basaltic liquids.

An often-cited objection to this hypothesis is the general absence of amphibole from calc-alkaline basalts and andesites. Stewart (1975) proposed that two-pyroxene + plagioclase + magnetite clots in calc-alkaline volcanic rocks are the breakdown products of early-formed amphiboles. Garcia and Jacobson (1979) demonstrated that in many cases these clots are simply glomerocrysts.

Evidence from this study suggests that some crystal clots cannot be glomerocrysts, and probably are the products of amphibole breakdown instead. Crystal clots from Castle Rocks consist of plagioclase + clinopyroxene + orthopyroxene + opaque oxide, or (less

commonly) plagioclase + clinopyroxene + opaque oxide. True glomerocrysts are common, but the term "crystal clots" is reserved for those aggregates with properties which are inconsistent with formation as glomerocrysts. These properties are: 1), smooth outer boundary, suggestive of a crystal margin; 2), no included glass or groundmass material; 3), smooth and interlocking grain boundaries within the clot, as in a plutonic rock; 4), no oscillatory zoned plagioclase within the clot. The fine-grained, hypidimorphic granular texture of the clots indicates that they formed slowly, and are not simply a near-surface phenomenon. One of these clots is shown in Figure 30, and has a shape suggestive of a hornblende crystal. In the thesis area, crystal clots are most common in andesites although some are found in rocks with SiO_2 contents as low as 58%. This is not proof that amphiboles are involved in calc-alkaline magma genesis, but the evidence is at least consistent with that hypothesis.

Miyashiro (1974) noted that in the Japanese arc, calc-alkaline andesites are erupted on thicker crust while tholeiites are found on thin crust. Kay and Kay (1982) observed that in the Aleutian arc, calc-alkaline volcanic centers are smaller than tholeiitic centers, apparently indicating a more difficult ascent for calc-alkaline magmas. Green's (1980) discussion of petrogenic models suggests that calc-alkaline magmas may result from relatively shallow, hydrous fractionation within thickened crust. In Green's model the parent magma is a mantle-derived tholeiitic melt. The zoned hornblende pseudomorphs found in Castle Rocks samples also suggest several pressure-related stages in their magmatic evolution.
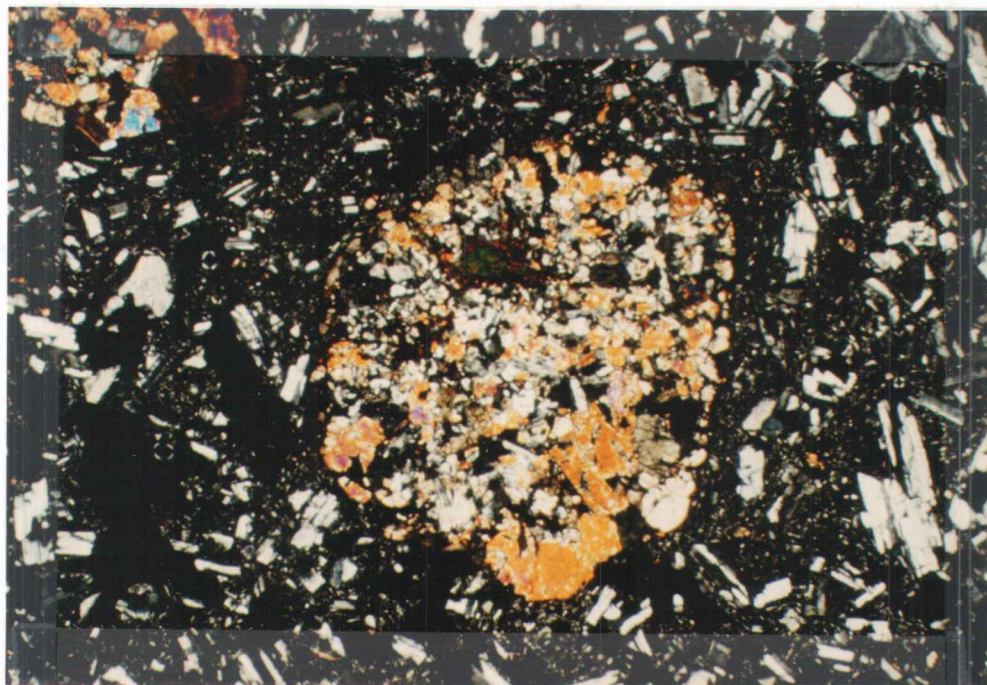
Figure 30. Crystal clot with hornblende-shaped outline. (map unit
TCR 5, sample #124). Crossed polars, field of
view 3.3 mm.

Pre-Deschutes Rocks

Pre-Deschutes basaltic andesites occupy a stratigraphic position above Castle Rocks units and below those of the Deschutes Formation. As discussed in the unit description, they seem to have issued from a satellite vent on the flanks of the Castle Rocks volcano. The only phenocryst mineral in Pre-Deschutes basaltic andesites is olivine, while low-silica rocks from the Castle Rocks volcano are characterized by orthopyroxene phenocrysts. Olivine phenocrysts in Deschutes Formation basaltic andesites are usually associated with plagioclase and clinopyroxene.

Major-element composition of Pre-Deschutes basaltic andesites (Appendix 2c) is fairly typical of basaltic andesite in the thesis area, except for their high K_2O and, to a lesser extent, Na_2O contents (Fig. 7). Watson (1982) demonstrated experimentally that basaltic melts contaminated with "crustal" components could be enriched in K_2O, Zr, and Nb. Pre-Castle Rocks samples are enriched in these elements but are also enriched in Na_2O, which Watson suggests should not be increased by contamination. P_2O_5, Ba and Sr contents are also unusually high for basaltic andesites.

As seen in Figure 31, the ratio $CaO/FeO*$ shows no change with increasing SiO_2 content, suggesting that plagioclase fractionation is not a dominant factor. The ratio $CaO/FeO*$ shows a marked negative correlation with SiO_2 in Deschutes samples, suggesting that the two groups are not related.

The ratio CaO/Al_2O_3 shows a negative correlation with
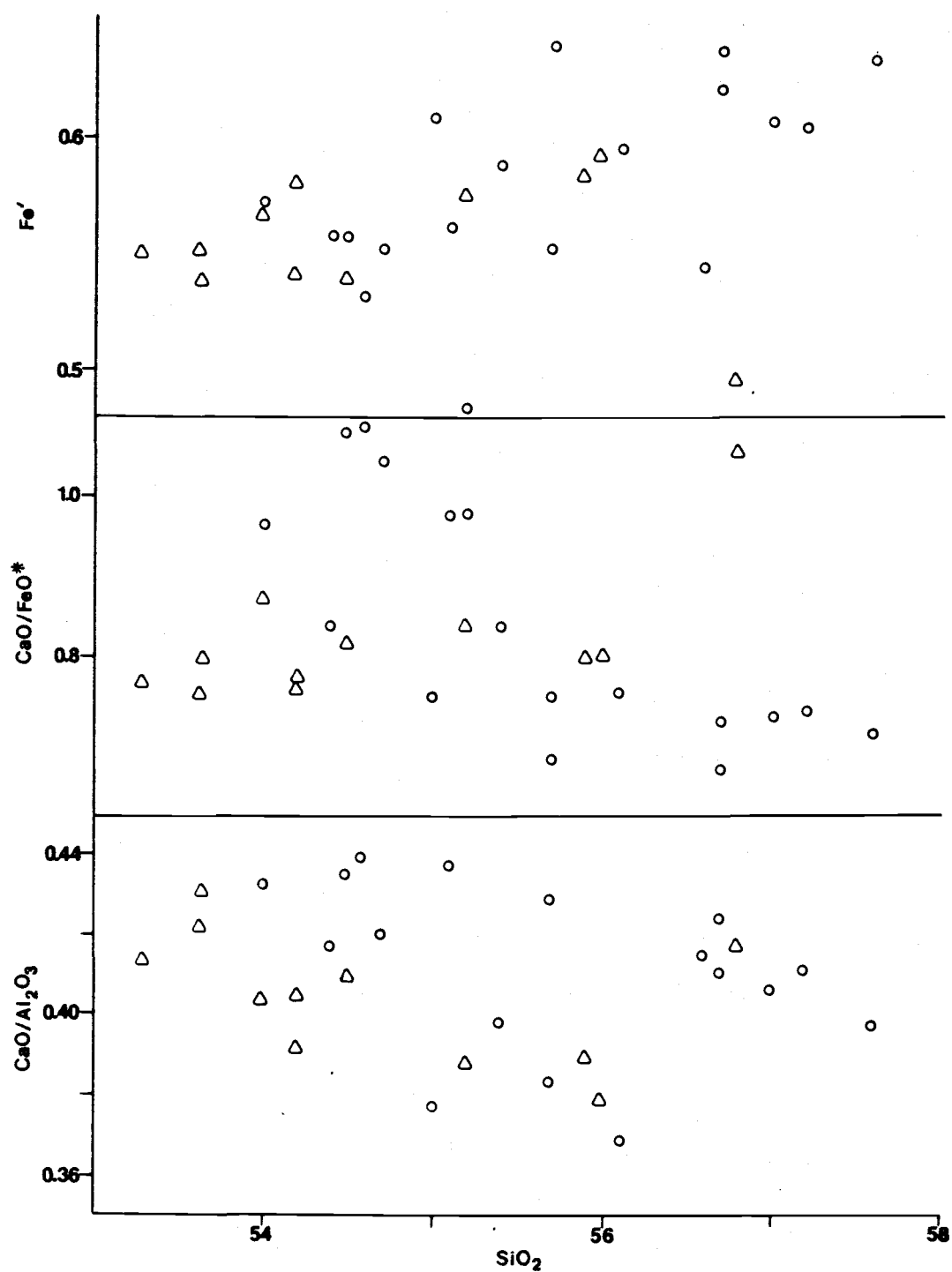
Figure 31. Variation of Fe', CaO/FeO* and CaO/Al₂O₃ with silica content in Pre-Deschutes and Deschutes Formation samples. Symbols as in Figure 6.

SiO_2. This is difficult to reconcile with the lack of clinopyroxene phenocrysts, because clinopyroxene is the only common mineral which can effect this ratio. Deschutes Formation samples also show a negative correlation but the ratio is lower in Pre-Deschutes rocks, again suggesting no relationship between the two.

Both FeO/MgO and Fe' increase with SiO_2 content, indicating a tholeiitic iron enrichment trend. Trace-element data are sparse for Deschutes Formation rocks from Green Ridge (see Conrey, 1985). Available data do not suggest any petrogenetic relationship between Pre-Deschutes and Deschutes rocks. Although Ni and Cr contents are about the same, Pre-Castle Rocks samples are enriched in the incompatible elements Rb, Ba, and Sr. Another incompatible element, Zr, shows no enrichment in Pre-Castle Rocks samples. Available evidence indicates that Pre-Castle Rocks basaltic andesites are not directly related to either the Castle Rocks series or the Deschutes Formation. Instead, they appear to represent an isolated batch of magma from a unique source. Their trend toward iron enrichment and the lack of phenocrysts suggest that their tectonic affinities are extensional.

Deschutes Formation

Analyzed Deschutes Formation rocks from the thesis area have a limited compositional range. Except for one analysis of the Whitewater Tuff (#178), all Deschutes samples are basaltic andesites. No trace element data are available for Deschutes Formation rocks in the thesis area.

Deschutes Formation analyses straddle the line between the calc-alkaline and tholeiitic fields shown on Fig. 6. Figs. 8 and 9 show a trend toward Fe and Ti enrichment which is especially pronounced in aphyric varieties. The ratio CaO/Al_2O_3 declines with increasing SiO_2 as seen in Figure 31, suggesting fractional crystalization of clinopyroxene. $CaO/FeO*$ also declines with increasing SiO_2, consistent with the fractional crystalization of plagioclase. Progressive iron enrichment reflects the fractionation of ferromagnesian minerals, probably forsteritic olivine. Fractional crystalization of forsteritic olivine (or orthopyroxene) would be expected to raise $CaO/FeO*$, but the effect is apparently masked by plagioclase fractionation. All of the presumed fractionating phases (olivine, plagioclase, and augite) are present as phenocrysts in basaltic andesites.

TiO_2 content is an important indicator of fractionation trends in Deschutes Formation rocks, but shows no correlation with SiO_2 in the compositional range reported here. Smith (1985), studying Deschutes Formation basaltic andesites in the Deschutes Basin, reported that TiO_2 content increases until about 57% SiO_2, and then begins to decrease. Yogodzinski (1985) reported a similar change in TiO_2 behavior at about 56% SiO_2. The lack of correlation seen here may reflect the small number of samples, or the narrow range of SiO_2 concentrations sampled.

Table 6 compares the average composition of Deschutes Formation basaltic andesites in the field area with the average "primitive" Deschutes Formation basalt of Conrey (1985).

Table 6
Average compositions of primitive basalt
and basaltic andesite.

	AVPB	AVBA
SIO_2	50.9	55.4
TiO_2	0.88	1.43
Al_2O_3	16.9	17.7
FeO^*	8.9	8.8
CaO	11.5	7.7
MgO	9.0	3.8
Na_2O	2.4	3.8
K_2O	0.19	0.95

"AVPB"= average primitive basalt.
"AVBA"= average basaltic andesite

The trends in CaO/Al_2O_3, CaO/FeO^*, and FeO^*/MgO discussed above are consistent with the derivation of the basaltic andesites from basalts by fractionation. K_2O content shows a great increase from basalt to basaltic andesite, and mass balance considerations require the fractionation of about 65% K_2O-free material in order to derive basaltic andesite from basalt. This degree of fractionation would raise the TiO_2 content of basaltic andesite content to about 2.1%. Because basaltic andesites average only 1.43% TIO_2, the fractionation hypothesis requires removal of a Ti-bearing phase. Conrey (1985) discusses the problem in detail, and favors a magma mixing hypothesis.

High Cascade Basaltic Andesites

Basaltic andesites discussed in this section include both the Bald Peter and Sheep Creek lavas. Most analyses plot within the calc-alkaline field on the AFM diagram (Fig. 6) and are generally more iron-rich than the Castle Rocks Andesites. Although basaltic

andesite analyses plot within the calc-alkaline field, they lack the abundant phenocrysts and hydrous minerals considered typical of calc-alkaline rocks.

Figures 6 and 10 show a typically calc-alkaline lack of iron enrichment among High Cascade basaltic andesites. It is not clear how this is achieved, because the rocks lack Fe-Ti oxide or amphibole phenocrysts. The ratio CaO/Al_2O_3 shows a negative correlation with SiO_2, which suggests clinopyroxene fractionation. Clinopyroxene, however, is not a common phenocryst phase. $CaO/FeO*$ increases with SiO_2 content, as seen in Figure 32. Fractionation of plagioclase is apparently not a factor, since it should decrease the ratio. Fractionation of olivine with the proper composition could produce the observed increase in $CaO/FeO*$.

Figures 7-10 show that the average normal High Cascade basalt falls on the major element trend lines established in this study for basaltic andesites. This suggests that the basaltic andesites are derived from the basalts by fractionation. The minerals which could produce these trends, however, are not all found as phenocryst phases. The lack of Fe and Ti enrichment among basaltic andesites is especially difficult to explain, because of the lack of Fe-Ti oxide or amphibole phenocrysts. The decrease in CaO/Al_2O_3 requires fractionation of clinopyroxene, but augite phenocrysts are scarce. The lack of the minerals needed to produce the observed compositional trends seems to require very efficient crystal fractionation of early phases.
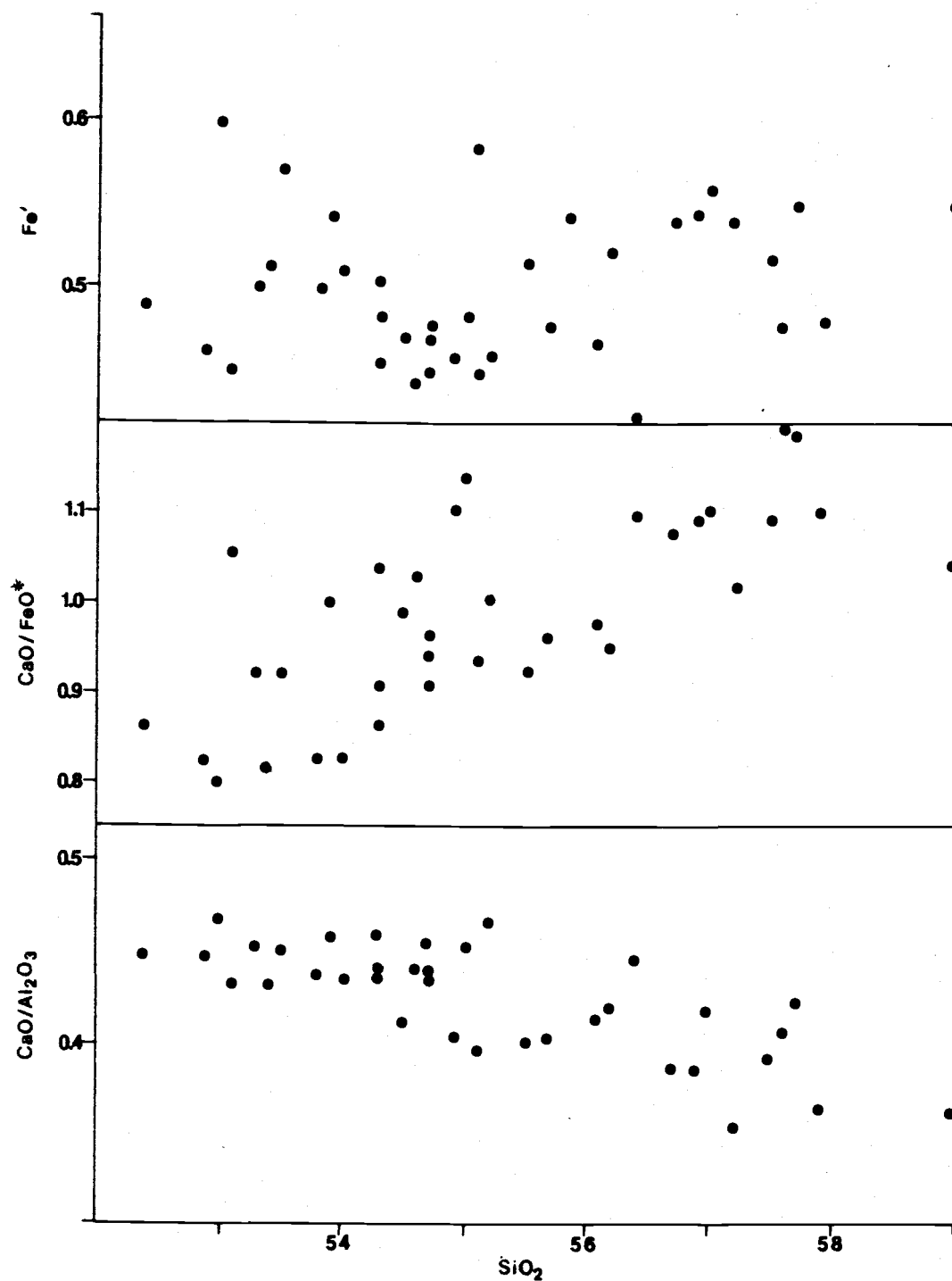
Figure 32.   Variation of Fe', CaO/FeO* and CaO/Al₂O₃ with silica content in High Cascade basaltic andesites.
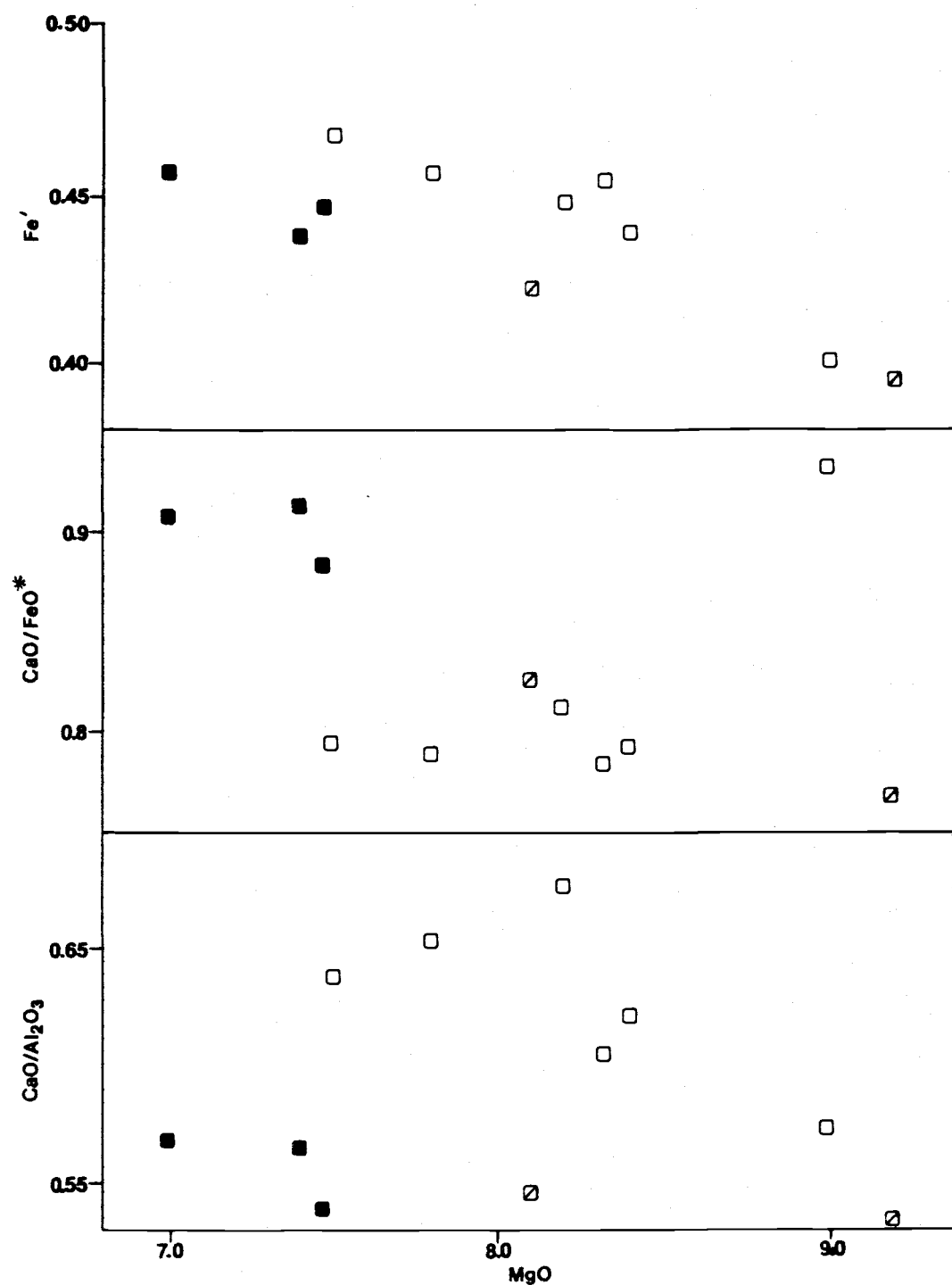
Figure 33. Variation of Fe', CaO/FeO* and CaO/Al$_2$O$_3$ with MgO content in diktytaxitic basalts. Open symbols are Metolius canyon normal polarity. Solid symbols are Metolius canyon reverse polarity. Slashes are Metolius Bench.

Diktytaxitic basalts

Although all of the diktytaxitic basalts are similar in hand sample, there are three compositional types in the field area. Normal and reverse polarity intervals within Metolius Canyon benches correspond to different compositions, as seen in Appendix 2e. The basalts of Metolius Bench are enriched in TiO_2 and alkalais, and appear to represent a more evolved magma.

Major element composition of the diktytaxitic basalts is similar to that of the "normal High Cascade basalt" (AVNB) shown on Table 3. Diktytaxitic basalts in the field area are higher in alkalais and Ca than the normal basalts, and lower in Al_2O_3 and FeO*. TiO_2 is lower than in the normal basalts, but still high for a convergent plate margin (Green, 1980).

Smith (1985) stated that Al_2O_3 content is an indicator of provenance among mafic rocks in the Deschutes basin. According to Smith, basalts of High Cascade provenance have Al_2O_3 contents of at least 16.5 wt.%, while those erupted within the basin have Al_2O_3 contents between 15 and 16.5 wt.%. Appendix 2e, however, shows that the diktytaxitic basalts in the field area (obviously of High Cascade provenance) often have Al_2O_3 contents of less than 15 wt.%. Apparently alumina content is not an infallible indicator of provenance.

Plots of CaO/FeO* and CaO/Al_2O_3 vs MgO seen in Figure 33 show no obvious trends, presumably because of the low sample density. They do, however, suggest that the Metolius canyon normal and Metolius canyon reverse flows represent separate batches of magma. A plot of

Fe' vs MgO indicates fractionation of a ferromagnesian mineral. Oddly enough, the Metolius Bench basalts have the lowest Fe' among the three types. This is surprising, in view of their relatively evolved major and trace element composition.

Major element composition also indicates that normal High Cascade

basalts and diktytaxitic basalts are not related by fractionation, because the TiO_2 and alkalai contents of the normal basalts are too high. The diktytaxitic basalts are quite similar to the widespread high-alumina olivine tholeiites (HAOT) of the northwestern Great Basin. These basalts are believed to reflect a long-lived extensional regime in the area (McKee and others, 1983; Hart and others, 1984). The presence of diktytaxitic basalts in the Cascades is often taken as evidence of similar tectonic conditions there (Priest and others, 1983).

Table 3 compares the composition of diktytaxitic rocks in the thesis area with that of high-alumina olivine tholeiites in the Great Basin. Major element compositions are similar, with the Cascade rocks being enriched in TiO_2 and FeO*, and lower in MgO, CaO and Al_2O_3. Cascade rocks share the unusually low alkalai and incompatible element concentrations of HAOT.

McKee and others (1983) have attempted to more precisely establish the tectonic significance of these rocks. Cascades diktytaxitic lavas and HAOT are depleted in K (less than 0.4 wt %) and Rb (less than 2 ppm) similar to mid-ocean ridge basalts (MORB). Ni contents of Cascade diktytaxitic lavas and HAOT are higher than in MORB, and much higher than those of back-arc basin basalts or island-

arc tholeiites. In contrast to MORB, HAOT samples are enriched in Sr (about 250 ppm vs 140 ppm) and Ba (150 ppm vs 10 ppm). Diktytaxitic basalts from the thesis area have even higher Ba and Sr contents than HAOT of the Great Basin (Appendix 2e). McKee and others (1983) find the exact tectonic affinities of HAOT uncertain, while Hart and others (1984) suggest that they represent back-arc spreading conditions. In any case, the diktytaxitic basalts in the field area represent extensional conditions east of the Cascade crest. Diktytaxitic basalts are also common in the Deschutes Formation, indicating similar conditions east of the Cascades crest during the Pliocene (Conrey, 1985; Smith, 1985).

Summary

Rocks in the thesis area record alternating periods of tholeiitic and calc-alkaline volcanism. Tholeiitic volcanism is represented by Pre-Castle Rocks, Pre-Deschutes, Deschutes Formation and diktytaxitic basalt strata. The Castle Rocks Andesites and High Cascade basaltic andesites, on the other hand, are calc-alkaline. Differences between the two types are not always petrographically obvious, but compositional trends are distinct.

Pre-Castle Rocks and Deschutes Formation units have the most obvious tholeiitic affinities. Tholeiitic rocks show a consistent decline in CaO/Al_2O_3 with increased SiO_2 content, suggesting clinopyroxene fractionation. $CaO/FeO*$ declines over the same SiO_2-range, probably due to a combination of plagioclase and clinopyroxene fractionation. Fe' shows a strong negative correlation with total

MgO. This, coupled with a decline in Ni-content, suggests fractionation of olivine.

Rocks from the Castle Rocks volcano are the more obviously calc-alkaline, because of their highly porphyrytic character and the abundance of hornblende phenocrysts. Both Castle Rocks and High Cascade basaltic andesite samples show a negative correlation between CaO/Al_2O_3 and SiO_2. As in the tholeiitic rocks, this is interpreted as evidence of clinopyroxene fractionation. An important difference between the tholeiitic and calc-alkaline rocks is in the behavior of CaO/FeO^* with increasing SiO_2. In calc-alkaline rocks CaO/FeO^* increases with SiO_2, suggesting little plagioclase fractionation and the influence of opaque oxide or Fe-rich amphibole fractionation instead. High Cascade basaltic andesites lack either opaque oxide or amphibole phenocrysts, and a mechanism for suppressing iron enrichment is not clear. The lack of iron enrichment is easier to explain in Castle Rocks andesites, because of their abundant amphibole phenocrysts.

Summary and Conclusions

Volcanic rocks in the thesis area range in age from late Miocene or earlier to Quaternary. The informal stratigraphic nomenclature used in the thesis corresponds to a pattern of alternating tholeiitic and calc-alkaline volcanism. This alternating pattern reflects four changes in the tectonic setting of the central Oregon Cascade Range.

The oldest rocks in the thesis area are a series of basaltic andesite to dacite lava flows, breccias and dikes, referred to as Pre-Castle Rocks units. Their source vent apparently was near the northern end of the modern Green Ridge. This Pre-Castle Rocks volcano formed a topographic high which was downfaulted in the Pliocene, and buried by lavas of the High Cascade platform. Pre-Castle Rocks samples are high in K_2O, P_2O_5, Zr, Nb and Rb, suggesting extreme fractionation. A phenocryst assemblage of fayalitic olivine, ferroaugite, plagioclase and Fe-Ti oxides is also consistent with a high degree of differrentiation along a tholeiitic trend.

An unconformity above the Pre-Castle Rocks units marks a change from extensional to compressional tectonics. Calc-alkaline rocks loosely referred to as Castle Rocks Andesites issued from a strato-volcano centered on the present north end of Green Ridge. This former volcanic center is represented by interbedded hornblende-pyroxene andesite lava flows and pyroclastic rocks, dikes, and a pyroxene andesite plug. A radiometric date of 8.1 Ma probably represents the top of the Castle Rocks section. Similar porphyrytic calc-alkaline andesites are common in the Western Cascades, but none are found on the eastern flanks of the central Oregon Cascades.

Apparently correlative rocks in the Western Cascades have been assigned to the Late Western Cascades Episode by Priest and others (1983), an episode which lasted from 18 to 9 Ma. The composition of Castle Rocks Andesites is characterized by a lack of iron enrichment which was probably produced by hornblende fractionation. Other compositional trends suggest fractionation of clinopyroxene and a ferromagnesian mineral.

The Castle Rocks Andesites are unconformably overlain by K_2O-rich basaltic andesites. These "Pre-Deschutes" basaltic andesites apparently erupted from a satellite vent on the west flank of the Castle Rocks volcano, and their eruption triggered extensive mud-flows. The unique composition of these rocks indicates that they are not directly related to either the underlying Castle Rocks Andesites or the overlying Deschutes Formation. Their sparsely phyric nature and tendency toward iron enrichment suggest that they reflect a change from compressional to extensional tectonics.

Deschutes Formation volcanism began at about 7.6 Ma, but the base of the section in the thesis area is somewhat younger. Ash-flow tuffs and basaltic andesite lava flows of the Deschutes Formation bank against the southern flank of the Castle Rocks volcano, but never covered it. Deschutes Formation lavas in the thesis area are sparsely porphyrytic basaltic andesites. Their tholeiitic compositional trend reflects a return to extensional tectonics. Compositional trends suggest that the basaltic andesites formed from more primitive basalt by fractionation of olivine, clinopyroxene and plagioclase. Conrey (1985) has examined a more extensive section of the Deschutes Formation and favors a magma-mixing hypothesis to

explain compositional changes.

Deposition of the Deschutes Formation in the thesis area ended at about 5.4 Ma, as normal faulting at Green Ridge down dropped the source volcanoes to the west. Correlation of rock and magneto-stratigraphic units across the Metolius River indicates a maximum displacement of about 2200 ft (670 m) across the Green Ridge fault. Faulting dies out northward, and no significant normal faults are recognized north of the Castle Rocks plug.

High Cascade volcanic rocks erupted shortly after the episode of normal faulting. Most High Cascade rocks in the thesis area are basaltic andesites from the Bald Peter shield volcano. Yogodzinski (1985) dated the base of the Bald Peter sequence at 4.3 Ma, and the summit plug of Bald Peter is dated at 2.2 Ma (Hales, 1975). Bald Peter basaltic andesites have a generally calc-alkaline composition, with compositional trends similar to those of the Castle Rocks Andesites.

Tholeiitic, diktytaxitic basalts related to extension were coeval with the subduction-related basaltic andesites. The basalts of Metolius Bench are the oldest of these diktytaxitic basalts. Field and paleomagnetic relationships indicate that they were erupted between 3.9 and 3.4 Ma. Intracanyon basalts followed the present course of the Metolius River almost to the Cove Palisades State Park. These intracanyon benches have an inferred age of about 1.7 Ma, demonstrating that the Metolius River has followed its present course since at least the late Pliocene.

The youngest volcanic unit in the thesis area is a late Pleistocene air-fall pumice. Its source was apparently the north flank of

Mt.Jefferson, indicating that calc-alkaline volcanism has recently been active.

Bibliography

Anderson, A.T., 1980, Significance of hornblende in calk-alkaline andesites and basalts: Amer. Mineral., v. 65, p. 837-851.

Arculus, R.J., and Willis, K.A., 1980, The petrology of plutonic blocks and inclusions from the Lesser Antilles arc: Jour. Petrol., v. 21, p. 743-799.

Armstron, R.L., Taylor, E.M., Hales, P.O., and Parker, D.J., 1975: K-Ar dates for volcanic rocks, central Cascade Range of Oregon, Isochron/West, No. 13, p. 5-10.

Armstrong, R.L., 1978, Cenozoic igneous history of the U.S. cordillera from lat 42 to 49 N.: Geol. Soc. Amer. Mem. 152, p. 263-282.

Atwater, T., 1970, Implications of plate tectonics for the Cenozoic tectonic evolution of western North America: Geol. Soc. Amer. Bull., v. 81, p. 3513-3536.

Baker, I., and Haggerty, S., 1967, The alteration of olivine in basaltic and associated lavas, Part II: intermediate and low temperature alteration: Contr. Min. and Petrol., v. 16, p. 258-273.

Black, G.L., 1983, Heat flow in the Oregon Cascades, in, Priest, G.W.,and Vogt, B.F., eds., Geology and geothermal resources of the central Oregon Cascade Range: Oreg. Dept. Geol. Min. Ind.Spec. Paper 15, p. 3.28.

Bates, R.L., and Jackson, J.A., 1980, Glossary of geology: Amer. Geol. Inst., 749 p.

Boettcher, A.L., 1973, Volcanism and orogenic belts - the origin of andesites: Tectonophysics, v. 17, p. 223-240.

Carmichael, I.S.E., 1964, The petrology of Thingmuli, a Tertiary volcano in eastern Iceland: Jour. Petrol., v. 5, p. 435-460.

_____, Turner, F..J., and Verhoogen, J., 1974, Igneous Petrology: McGraw Hill, New York, 739 p.

Cady, W.M., 1975, Tectonic setting of the Tertiary volcanic rocks of the Olympic Peninsula, Washington: U.S. Geol. Surv. Jour. Res., v. 3, p. 573-582.

Carmichael, I.S.E, 1964, The petrology of Thingmuli, a Tertiary volcano in eastern Iceland: Jour. Petrol., v. 5, p. 435-460.

_____, Turner, F.J., and Verhoogen, J., 1974, Igneous Petrology: McGraw-Hill, 739 p.

Cawthorn, R.G., and O'Hara, M.J., 1976, Amphibole fractionation in calc-alkaline magma genesis: Am. Jour. Sci., v. 276, p. 309-329.

Christiansen, R.L., and Lipman, P.W., 1972, Cenozoic volcanism and plate-tectonic evolution of the western United States. II. Late Cenozoic: Phil. Trans. Royal Soc. London, v. A271, p. 249-284.

Coney, P.J., and Reynolds, S.J., 1977, Cordilleran benioff zones: Nature, v. 270, p. 403-406.

Conrad, W.K., and Kay, R.W., 1980, Petrology and significance of olivine and amphibole bearing xenoliths in Aleutian andesites: EOS, v. 61, no. 7, p. 400.

_____, 1981, Xenoliths from Adak Island: evidence for hydrous basaltic primary magmas in the Aleutian arc: EOS, v. 62, no. 45, p. 1092.

Conrey, R.M., 1985, Volcanic stratigraphy of the Deschutes Formation, Green Ridge to Fly Creek, north-central Oregon: Corvallis, Oregon State Univ. M.S. thesis (unpub.), 349 p.

Couch, R.W., Pitts, G.S., Gemperle, M, Braman, D.E., and Veen, C.A., 1982, Gravity anomalies in the Cascade Range in Oregon: structural and thermal implications: Oreg. Dept. Geol. Min. Ind. Open-file Rept. 0-82-9, 43 p.

Dickinson, W.R., 1976, Sedimentary basins developed during evolution of Mesozoic-Cenozoic arc-trench system in western North America: Can. Jour. Earth Sci., v. 13, p. 1268-1287.

Dutton, C.E., 1889, U.S. Geol. Surv. Ann. Rept. no. 8, p. 156-165.

Ewart, A., Green, D.C., Carmichael, I.S.E., and Brown, F.H., 1971, Voluminous low temperature rhyolite magmas in New Zealand: Contr. Min. Petrol., v. 33, p. 128-144.

Ewing, T., 1980, Paleogene tectonic evolution of the Pacific Northwest: Jour. Geol., v. 88, p. 619-638.

Enlows, H.E., and Parker, D.J., 1972, Geochronology of the Clarno igneous activity in the Mitchell quadrangle, Wheeler County, Oregon: Ore Bin, v. 34, p. 104-110.

Ewing, T., 1980, Paleogene tectonic evolution of the Pacific Northwest: Jour. Geol., v. 88, p. 619-638.

Farooqui, S.M., Bunker, R.C., Thoms, R.E., Clayton, D.C., and Bella, J.L., 1981, Dalles Group: Neogene formations overlying the Columbia River Basalt Group in north-central Oregon: Oregon Geology, v. 43, p. 131-140.

Fiebelkorn, R.B., Walker, G.W., MacLeod, N.S., McKee, E.H., and Smith, J.G., 1983, Index to K-Ar determinations for the State of Oregon: Isochron/West, no. 37, p. 3-60.

Fisher, R.V., 1966, Rocks composed of volcanic fragments: Earth-Science Rev., v. 1, p.287-298.

Francis, P.W., Roobol, M.J., Walker, G.P.L., Cobbold, P.R., and Coward, M., 1974, The San Pedro and San Pablo volcanoes of northern Chile and their hot avalanche deposits: Geol. Rundsch., v. 63, p. 357-388.

Garcia, M.O., and Jacobson, S.S., 1979, Crystal clots, amphibole fractionation and the evolution of calc-alkaline magmas: Contr. Mineral. Petrol., v. 69, p. 319-327.

Green, T.H., 1980, Island arc and continent-building magmatism: a review of petrogenic models based on experimental petrology and geochemistry: Tectonophysics, v. 63, p. 367-385.

Hales, P.O., 1975, Geology of the Green Ridge area, Whitewater River quadrangle, Oregon: Corvallis, Oregon State Univ. M.S. thesis (unpub.), 90 p.

Hammond, P.E., 1979, A tectonic model for evolution of the Cascade Range, in, Armentrout, J.M., Cole, M.R., and Terbest, H., Jr., eds., Cenozoic Paleogeography Symposium No. 3, Anaheim Calif., Society of Economic Paleontologists and Mineralogists, Pacific Section, 335 p.

Harland, W.B., Cox, A.V., Llewellyn, A.C., Pickton, C.A.G., Smith, A.G., and Walters, R., 1982, A Geologic Time Scale: Cambridge, Cambridge University Press, 131 p.

Hart, W.K., Aronson, J.L., and Mertzman, S.A., 1984, Areal distribution and age of low-K, high alumina olivine tholeiite magmatism in the northwestern Great Basin: Geol. Soc. Amer. Bull., v. 95, p. 186-195.

Hodge, E.T., 1928, Framework of Cascade Mountains in Oregon: Pan American Geologist, v. 49, p. 341-357.

_____, 1938, Geology of the lower Columbia River: Geol. Soc. Amer. Bull., v. 49, p. 831-930.

_____, 1942, Geology of north central Oregon: Oregon State Monographs, Studies in Geology no. 3, 76 p.

Holloway, J.R., and Burnham, C.W., 1972, Melting relations of basalt with equilibrium water pressure less than total pressure: Jour. Petrol., v. 13, p. 1-29.

Hughes, S.M., and Taylor, E.M., 1986, Geochemistry, petrogenesis and tectonic implications of central High Cascade mafic platform lavas: Geol. Soc. Amer. Bull., v. 97, p. 1024-1036.

Hunter, R.H., and Sparks, R.S.J., 1987, The differentiation of the Skaergaard Intrusion: Contr. Min. Petrol., v. 95, p. 451-461.

Jay, J.B., 1982, The geology and stratigraphy of the Tertiary volcanic and volcaniclastic rocks, with special emphasis on the Deschutes Formation, from Lake Simtustus to Madras in central Oregon: Corvallis, Oregon State Univ. M.S. thesis (unpub.), 119 p.

Kay, S.M., Kay, R.W., and Citron, G.P., 1982, Tectonic controls on tholeiitic and calc-alkaline magmatism in the Aleutian arc. Jour. Geophys. Res., v. 87, p. 4051-4072.

Kuno, H., 1966, Lateral variation of basalt magmas type across continental margins and island arcs: Bull. Volc., v. 29, p. 195-222.

Lawrence, R.D., 1976, Strike-slip faulting terinates the Basin and Range province in Oregon: Geol. Soc. Amer. Bull., v. 87, p. 486-850.

Leudke, R.G., and Smith, R.L., 1982, Map showing distribution, composition and age of Late Cenozoic volcanic centers in Oregon and Washington: U.S. Geol. Surv. Map I-1091-D.

Lipman, P.W., Prostka, H.J., and Christiansen, R.L., 1972, Cenozoic volcanism and plate-tectonic evolution of the western United States. I. Early and middle Cenozoic: Phil. Trans. Royal Soc. London, v. A271, p. 217-248.

Lux, D.R., 1982, K-Ar and ^{40}Ar-^{39}Ar ages of mid-Tertiary volcanic rocks from the Western Cascade Range, Oregon: Isochron/West, no. 33, p. 27-32.

MacLeod, N.S., Walker, G.W., and McKee, E.H., 1975, Geothermal Significance of eastward increase in age of upper Cenozoic rhyolite domes in southeast Oregon: in, Proceedings of the second United Nations symposium on the development and use of geothermal resources, v. 1, p. 465-474.

Magill, J., and Cox, A., 1981, Post-Oligocene tectonc rotation of the Oregon Western Cascade Range and the Klamath Mountains: Geology, v. 9, p. 127-131.

McBirney, A.R., Sutter, J.F., Naslund, H.R., Sutton, K.G., and White, C.M., 1974, Episodic volcanism in the central Oregon Cascade Range: Geology, v. 2, p. 585-589.

McKee, E.H., Duffield, W.A., and Stern, R.J., 1983, Late Miocene and early Pliocene basaltic rocks and their implications for crustal structure, northeastern California and south central Oregon: Geol. Soc. Amer. Bull., v. 49, p. 292-304.

Miyashiro, A., 1974, Volcanic rocks series in island arcs and active continental margins: Amer. Jour. Sci., v. 274, p. 321-355.

Nicholls, I.A., and Ringwood, A.E., 1973, Effect of water on olivine stability in tholeiites and the production of silica saturated magmas in the Island-Arc environment: Jour. Geol., v. 81, p. 285-300.

Noble, D.C., 1970, Stratigraphy and geochronology of Miocene volcanic rocks in northwestern Nevada: U.S. Geol. Surv. Prof. Paper 700-D, p. 23-32.

Peck, D.L., Griggs, A.B., Schlicker, H.G., Wells, F.G., and Dole, H.M., 1964, Geology of the central and northern parts of the Western Cascade Range in Oregon: U.S. Geol. Surv. Prof. Paper no. 449, 56 p.

Priest, G.A., Woller, N.M., and Black, G.W., 1983, Overview of the geology of the central Oregon Cascade Range, in, Priest, G.W., and Vogt, B.F., eds., Geology and geothermal resources of the central Oregon Cascade Range: Oreg. Dept. Geol. Min. Ind.Spec. Paper 15, p. 3.28.

Robinson, P.T., Brem, G.M., and McKee, E.H., 1984, John Day Formation of Oregon: a distal record of early Cascade volcanism: Geology, v. 12, p. 229-232.

Rogers, J.W., and Novitsky-Evans, J.M., 1977, The Clarno Formation of centra Oregon, U.S.A. - volcanism on a thin continental margin: Earth & Planet. Sci. Lett., v. 34, p. 56-66.

Russel, I.C., 1897, The volcanoes of North America: New York, The MacMillan Co., 346 p.

Sheppard, R.A., 1962, Iddingsitization and recurrent crystallization of olivine in basalts from the Simcoe Mountains, Washington: Amer. Jour. Sci., v. 260, p. 67-74.

Smith, G.A., and Snee, L.W., 1983, Revised stratigraphy of the Deschutes basin, Oregon: implications for the Neogene development of the central Oregon Cascades: EOS, v. 65, p. 330.

Smith, G.A., 1986a, Simtustus Formation: Paleogeographic and stratigraphic significance of a newly defined Miocene unit in the Deschutes Basin, central Oregon: Oregon Geology, v. 48, p. 63-72.

_____, 1986b, Stratigraphy, sedimentology, and petrology of Neogene rocks of the Deschutes basin, central Oregon: a record of continental-margin volcanism and its influence on fluvial sedimentation in an arc-adjacent basin: Corvallis, Oregon State Univ. Ph. D. dissertaion (unpub.). 467 p.

Smith, J.G., 1980, An important lower Oligocene welded-tuff marker bed in the Western Cascade Range of southern Oregon: Geol. Soc. Amer. Abs. Prog., v.12, no. 3, p. 153.

Snavely, P.D. Jr., MacLeod, N.S., and Wagner, H.C., 1968, Tholeiitic and alkalic basalts of the Eocene Siletz River Volcanics, Oregon Coast Range: Amer. Jour. Sci., v. 266, p. 454-481.

_____, and MacLeod, N.S., 1974, Yachats Basalt, an Upper-Eocene differentiated volcanic sequence in the Oregon Coast Range: U.S. Geol. Surv. Jour. Res., v. 2, p. 395-403.

Stewart, D.C., 1975, Crystal clots in calc-alkaline andesites as breakdown products of high-Al amphiboles: Contr. Mineral. Petrol., v. 53, p. 195-204.

Streckeisen, A.L., 1979, Classification and nomenclature of volcanic rocks, lamprophyres, carbonatites, and melitic rocks: reccomendations and suggestions of the IUGS subcommission on the systematics of igneous rocks: Geology, v. 7, p. 331-335.

Sutton, K.G., 1974, The geology of Mount Jefferson: Eugene, Univ. of Oregon M.S. thesis (unpub.), 120 p.

Swanson, D.A., Wright, T.L., Hooper, P.R., and Bentley, R.D., 1979, Revisions in stratigraphic nomenclature of the Columbia River Basalt Group: U.S. Gel. Surv. Bull. 1457-G, 59 p.

Taubeneck, W.H., 1970, Dikes of Columbia River Basalt in northeastern Oregon, western Idaho, and southeastern Washington, in, Gilmore, E.H., and Stradling, D., eds, Proceedings of the second Columbia River Basalt Symposium: Cheny, Eastern Washington State Press, p. 73-96.

Taylor, E.M., 1978, Field geology of the s.w. Broken top quadrangle, Oregon: Oregon Dept. Geol. Min. Ind. Spec. Paper 2. 50 p.

_____, 1981a, A mafic dike systemin the vicinity of Mitchell, Oregon, and its bearing on the timing of Clarno-John Day volcanism and Early Oligocene deformation in central Oregon: Oregon Geology, v. 43, p. 107-112.

_____, 1981b, Central High Cascades roadside geology: Bend, Sisters, McKenzie Pass, and Santiam Pass, Oregon, in Johnston, D.A., and Donnelly-Nolan, J., eds, Guides to some volcanic terranes in Washington, Idaho, Oregon, and northern California: U.S. Geol. Surv. Circ. 838, p. 55-58.

Thayer, T.D., 1939, Geology of the Salem Hills and the North Santiam River basin, Oregon: Oreg. Dept. Geol. and Min. Ind. Bull no. 15, 40 p.

Van der Plas, L., and Tobi, A. (1965), A chart for estimating the reliability of point counting results: Amer. Jour. Sci., V. 263, p. 87-90.

Venkatakrishnan, R., Bond, J.G., and Kauffman, J.D., 1980, Geologic linears of the northern part of the Cascade Range, Oregon: Oreg. Dept. Geol. Min. Ind. Spec. Paper 12, 25 p.

Wager, L.R., and Brown, G.M., 1967, Layered igneous rocks: San Francisco, W.H. Freeman and Co., 588 p.

Walker, G.W., 1970, Some comparisons of basalts in southeast Oregon with those of the Columbia River Basalt Group, in, Gilmore, E.H., and Stradling, D., eds, Proceedings of the second Columbia River Basalt Symposium: Cheny, Eastern Washington State Press, p. 73-96.

Waters, A.C., 1968, Reconnaissance geologic map of the Madras quadrangle, Jefferson and Wasco counties, Oregon: U.S. Geol. Surv. Misc. Invest. Map. I-555.

Watson, B., 1982, Basalt contamination by continental crust, some experiments and models: Contr. Min. Petrol. v. 80, p. 73-87.

Weidenheim, J.P., 1981, The petrography, structure, and stratigraphy of Powell Buttes, Crook Co., central Oregon: Corvallis, Oregon State Univ. M.S. thesis (unpub.), 95 p.

Wells, F.G., and Peck, D.L., 1961, Geologic map of Oregon west of the 121st meridian: U.S. Geol. Surv. Misc. Invest. Map I-325.

Wells, R.E., Engebretson, D.C., Snavely, P.D. Jr., and Coe, R.S., 1984, Cenozoic plate motions and the volcano-tectonic evolution of western Oregon and Washington: Tectonics, v. 3, p. 275-294.

White, C.M., 1980a, Geology and geochemistry of Mt. Hood volcano: Oreg. Dept. Geol. Min. Ind. Spec. Paper 9, 26 p.

_____, 1980b, Geology and geochemistry of volcanic rocks in the Detroit area, Western Cascade Range, Oregon: Eugene, Univ. of Oreg. Ph.D. dissertation (unpub.), 178 p.

_____, 1980c, Geology of the Breitenbush Hot Springs quadrangle, Oregon: Oreg. Dept. Geol. Min. Ind. Spec. Paper 9, 26 p.

Williams, H., 1957, A geologic map of the Bend quadrangle, Oregon, and a reconnaissance geologic map of the central portion of the High Cascade mountains: Oregon Dept. Geol. Min. Ind.

Woheletz, K.H., and Sheridan, M.F., 1979, A model of pyroclastic surge: Geol. Soc. Amer. Spec. Paper 180, p. 177-194.

Woller, N.M., and Black, G.L., 1983, Geology of the Waldo Lake-Swift Creek area, Lane and Klamath Counties, Oregon, in, Priest, G.W., and Vogt, B.F., Geology and geothermal resources of the central Oregon Cascade Range: Oreg. Dept. Geol. Min. Ind. Spec. Paper 15, p. 57-68.

Wright, J.B., Smith, A.L., and Self, S., 1980, A working terminology of pyroclastic deposits: Jour. Volc. Geotherm. Res., v. 8, p. 315-336.

Yoder, H.S., and Tilley, C.E., 1962, Origin of basalt magmas: an experimental study of natural and synthetic rock systems: Jour. Petrol., v. 3, p. 342-532.

_____, 1965, Diopside-anorthite-water at five and 10 kilobars and its bearing on explosive volcanism: Ann. Rept. Dir. Geophys. Lab., Carnegie Inst. Wash., v. 64, p. 82-89.

Yogodzinski, G.M., 1985, The Deschutes Formation-High Cascade transition in the Whitewater River are, Jefferson County Oregon: Corvallis, Oregon State Univ. M.S. thesis (unpub.), 165 p.

APPENDICES

APPENDIX 1: Analytical Methods

Sample preparation

Samples were prepared for XRF by crushing a fist-sized sample. Chips showing weathered surfaces were discarded, and the remaining fresh sample was pulverized. A 3.00 gram split of pulverized sample was powdered in a ball mill using tungsten carbide balls. The powder was then furnace dried at 600° C for one hour. A 2.00 gram split of dried sample was thoroughly mixed with 10.00 grams of lithium tetraborate flux, placed in a graphite crucible, and fused at 1050° C for one hour, producing a homogeneous glass button. XRF analyses are reported as weight percent of the appropriate oxide. Iron content was determined as total iron, and reported as FeO^*.

For AA analysis, the button used for XRF was pulverized in a ball mill. A 0.10 gram split of powdered glass was dissolved in 200 ml of 0.5N HNO_3 to produce the AA solution.

Calibration curves used in the XRF procedure were revised periodically. Artificial "rocks" made with measured amounts of the various oxides, and USGS standards were used for this purpose.

Analytical precision for major oxides is estimated (E.M. Taylor, pers. comm.) to be:

SiO_2	1.0%
Al_2O_3	0.5%
FeO^*	0.2%
CaO	0.1%
K_2O	0.05%
TiO_2	0.05%
Na_2O	0.2%
MgO	0.2%.

Minor element analyses were performed by R.M. Conrey, using XRF methods, and have a reported analytical precision of: Va & Ba, ±15 ppm; Cr & Ni, ±10 ppm; Sc, ±3 ppm; Rb, Sr, Zr, Y, Nb, Ga, Cu, Zn, ± 1

ppm.

Duplicate analyses may be used to assess the accuracy of analytical procedures. DW366a and DW366b are analytical results from 2 buttons, made from separate 3 gram splits of the same crushed sample. The rock was a diktytaxitic olivine basalt.

	DW366a	DW366b
FeO^*	10.2	10.2
TiO_2	1.29	1.28
CaO	9.3	9.1
K_2O	0.26	0.27
SiO_2	49.7	50.0
Al_2O_3	16.5	17.1
Na_2O	3.1	3.2
MgO	7.4	7.7
	98.06	99.30

Another diktytaxitic olivine basalt, DW415a was taken from the same flow unit as POH329, analyzed by Hales (1975).

	DW415a	POH329
FeO^*	11.6	11.7
TiO_2	1.36	1.32
CaO	9.2	9.3
K_2O	0.29	0.30
SiO_2	51.8	52.4
Al_2O_3	14.1	14.6
Na_2O	3.0	2.9
MgO	7.8	7.5
	99.14	100.00

DW93a and DW93b were made from two hand samples taken from the same outcrop. The rock is a porphyritic two-pyroxene andesite.

	DW93a	DW93b
FeO^*	8.8	8.8
TiO_2	1.29	1.28
CaO	7.1	7.2
K_2O	1.60	1.62
SiO_2	54.1	54.5
Al_2O_3	17.3	17.5
Na_2O	4.1	4.1
MgO	4.0	4.2
	98.29	99.20

Appendix 2: Chemical Analyses

Major element compositions are reported as weight % of their
oxide. Minor and trace elements are reported in ppm. Volume
percents of phenocryst phases were determined by point-counting, and
are rounded off to the nearest 0.5%

Appendix 2a
Chemical Analyses of Pre-Castle Rocks Units

Unit	TPCR1	TPCR2	TPCR3				TPCR4	TPCR5	
Sample	101	102	103	104	105	106	107	108	109
SiO_2	56.8	55.9	59.9	60.1	61.6	62.8	62.1	65.7	65.8
TiO_2	1.44	1.64	1.22	1.25	1.02	1.01	1.18	0.63	0.68
Al_2O_3	17.4	17.8	16.6	16.0	17.0	16.9	15.3	15.2	14.4
FeO*	8.8	9.9	9.2	8.3	6.8	7.3	7.4	5.4	6.3
CaO	7.1	7.3	5.3	5.7	4.2	4.8	4.9	2.7	3.0
MgO	3.2	3.5	1.5	2.2	1.2	1.0	1.7	0.8	0.8
Na_2O	3.4	3.2	3.5	3.8	3.7	3.9	3.8	4.5	4.3
K_2O	1.56	1.69	2.56	2.20	2.88	2.32	2.36	2.89	2.88
P_2O_5		0.34	0.52						
Total	99.70	100.97	100.20	99.55	99.60	100.03	98.74	97.82	98.16
Ni		7	2						
Cr		31	0						
Sc		26	26						
V		204	62						
Ba		548	658						
Rb		65	77						
Sr		375	357						
Zr		181	225						
Y		36	50						
Nb		12	15						
Ga		22	26						
Cu		44	34						
Zn		104	123						
Plag	21	10	3	13	5	13	21	7	10
Cpx	4	0	tr	2	1	2	4	tr	1
Opx	3	0	tr	0	0	2	2	0	0
Oliv	2	3	tr	0	0	0	0	1	1
Mag	0.5	0	tr	tr	0	tr	1	tr	tr
Gnd	69.5	87	97	85	94	83	72	92	88

Appendix 2a (cont.)
Chemical analyses of Pre-Castle Rocks Units

Unit   TPCR5.............

Sample	110	111	112
SiO_2	66.8	67.2	67.5
TiO_2	0.69	0.38	0.55
Al_2O_3	16.5	15.1	14.8
Feo*	6.1	5.7	5.6
CaO	3.3	2.6	2.1
MgO	0.6	0.4	0.4
Na_0	3.4	4.4	5.1
K_2O	3.31	3.01	3.25
P_2O5	0.18		
Total	100.88	98.79	99.30

Ni	2		
Cr	0		
Sc	13		
V	32		
Ba	771		
Rb	115		
Sr	266		
Zr	271		
Y	43		
Nb	20		
Ga	22		
Cu	8		
Zn	93		

Plag	6	4	N.A.
Cpx	1	tr	-
Opx	0	0	-
Oliv	2	3	-
Mag	1	tr	-
Gnd	90	93	-

101 Lava flow: elev. 2190 ft, SE1/4SW1/4, Sec. 25, T.10S., R.10E.
102 Lava flow: elev. 2400 ft, SE1/4NW1/4, Sec. 3, T.11S., R.10E.
103 Breccia Clast: elev. 2400 ft, NW1/4NW1/4, Sec. 28, T.10S., R.10E.
104 Dike: elev. 2560 ft, SW1/4NE1/4, Sec. 26, T.10S., R.10E.
105 Breccia clast: elev. 2520 ft, SE1/4NE1/4, Sec. 26, T.10S., R.10E.
106 Breccia clast: elev. 2450 ft, SE1/4NW1/4, Sec. 34, T.10S., R.10E.
107 Lava flow: elev. 3400 ft, NW1/4NE1/4, Sec. 7, T.11S., R.10E.
108 Lava flow: elev. 2700 ft, SW1/4NW1/4, Sec. 3, T.11S., R.10E.
109 Lava flow: elev. 2500 ft, NE1/4SE1/4, Sec. 29, T.11S., R.10E.

Appendix 2a (cont.)

<u>110</u> Breccia clast: elev. 2550 ft, NE1/4SW1/4, Sec. 29, T.10S.,
     R.10E.
<u>111</u> Lava flow: elev. 3040 ft, SE1/4SE1/4, Sec. 21, T.10S., R10E.
     Anal. #1002 from Yogodzinski (1985).
<u>112</u> Lava flow: elev 2600 ft, NW1/4NE1/4, Sec. 28, T.10S., R10E.
     Anal. #298 from Hales (1975).

Appendix 2b
Chemical Analyses of Castle Rocks Units

Unit	TCR3						TCR4		
Sample	113	114	115	116	117	118	119	120	121
SiO_2	61.2	62.9	62.0	61.7	62.1	63.0	61.3	61.4	62.0
TiO_2	0.63	0.65	0.64	0.64	0.64	0.63	0.68	0.71	0.72
Al_2O_3	18.4	19.0	18.5	19.2	18.3	18.3	18.3	18.7	19.0
$FeO*$	4.3	4.6	4.4	4.4	4.3	4.4	4.3	4.7	5.1
CaO	6.3	6.3	6.2	6.3	6.1	6.2	6.3	6.3	6.5
MgO	2.3	2.6	2.4	2.5	2.5	2.6	2.9	3.0	2.6
Na2O	4.1	4.1	4.1	4.0	4.0	4.1	4.0	3.9	3.9
K_2O	0.93	0.93	0.97	0.95	0.97	0.98	1.10	1.16	1.09
Total	98.16	98.08	99.21	99.59	98.41	100.21	98.88	99.87	100.91
Plag	31	31	32	30	31	32	34	38	26
Cpx	1.5	1.5	1	1.5	1.5	1.5	1.5	2.5	1
Opx	4.5	6	5	4.5	4	4.5	4.5	4.5	3.5
Hb	2.5	4.5	5	2.5	5	5	4	7.5	5
Mag	tr	tr	tr	tr	tr	0	0	tr	0
Gnd	60.5	57.0	57.0	61.5	58.5	57.0	56.0	48.0	65.0

Appendix 2b (cont.)
Chemical Analyses of Castle Rocks Units

Unit   TCR5...

Sample	122	123	124	125	126	127	128	129	130
SiO_2	59.2	60.5	60.7	60.9	61.0	61.2	61.2	61.3	61.7
TiO_2	0.80	0.76	0.71	0.68	0.70	0.69	0.65	0.72	0.80
Al_2O_3	18.5	18.2	18.4	19.0	18.5	19.5	18.8	19.6	17.8
FeO*	5.2	4.9	4.6	4.6	4.4	4.5	4.5	4.9	5.0
CaO	6.7	6.5	6.4	6.4	6.00	6.2	6.3	6.6	6.1
MgO	3.9	3.4	2.8	2.6	2.5	2.2	2.6	2.5	2.8
Na_2O	4.7	3.9	4.1	4.2	4.0	3.9	4.0	3.9	4.1
K_2O	1.01	0.99	1.03	1.05	1.35	1.32	0.99	1.02	1.12
P_2O_5					0.17		0.14		
Total	100.01	99.15	98.74	99.43	98.62	99.51	99.18	100.54	99.42

Ni					39		24		
Cr					35		17		
Sc					15		11		
V					109		93		
Ba					335		248		
Rb					19		12		
Sr					1029		1012		
Zr					158		147		
Y					12		10		
Nb					6		4		
Ga					20		20		
Cu					19		32		
Zn					50		47		

Plag	24.5	35	34	28	15	30	29.5	31	22.5
Cpx	2	1	1.5	2	2	2	2	1.5	0.5
Opx	3.5	3.5	3	8.5	2	3.5	4.5	4	7.5
Hb	7.5	4	4	5	1	1	1.5	4	1
Bio	tr	tr	tr	0	0	0	0	tr	tr
Mag	tr	0	tr	tr	0	0	0.5	tr	0
Gnd	62.5	55.5	57.5	56.5	80.0	63.5	62.5	59.5	69.5

Appendix 2b (cont.)
Chemical analyses of Castle Rocks Units

Unit	TCR5								
Sample	131	132	133	134	135	136	137	138	139
SiO_2	61.8	61.8	61.9	61.9	62.0	62.0	62.1	62.3	62.4
TiO_2	0.83	0.80	0.72	0.68	0.81	0.70	0.67	0.69	0.78
Al_2O_3	19.0	17.7	18.1	18.1	18.1	18.7	17.2	18.0	18.0
FeO*	5.1	5.2	4.8	4.9	5.2	4.4	4.8	4.8	4.8
CaO	6.3	5.8	6.8	5.4	6.2	6.4	5.9	6.3	5.9
MgO	2.9	2.8	3.0	2.9	3.2	2.6	2.9	3.1	2.2
Na_2O	3.7	4.0	3.8	3.6	4.1	4.0	4.0	3.9	4.0
K_2O	1.23	1.22	0.97	1.40	1.13	1.08	1.15	1.01	1.13
P_2O_5	0.11								
Total	100.97	99.32	100.09	99.14	100.74	99.88	98.72	100.10	99.31
Ni	28								
Cr	30								
Sc	18								
V	103								
Ba	325								
Rb	12								
Sr	852								
Zr	118								
Y	11								
Nb	4								
Ga	19								
Cu	38								
Zn	56								
Plag	22.5	25.5	30	32	11	33	32	20	11
Cpx	1	1	2.5	0	tr	3	1	0.5	2.5
Opx	4.5	1.5	3.5	13	4	7.5	6	3	1.5
Hb	0.5	2.5	tr	6	3	1	tr	2.5	1.5
Mag	tr	0	tr	0	0	tr	0	tr	0
Gnd	71.5	69.5	64.0	49.0	82.0	55.5	61.0	74.0	83.5

Appendix 2b (cont.)
Chemical Analyses of Castle Rocks Units

Unit	TCR5..TCR6							TCR7.......	
Sample	140	141	142	142	144	145	146	147	148
SiO$_2$	62.8	62.9	63.3	63.4	63.6	63.7	62.8	56.0	56.4
TiO$_2$	0.68	0.71	0.68	0.58	0.68	0.68	0.66	1.00	1.04
Al$_2$O$_3$	19.1	19.3	19.1	17.5	17.5	17.7	18.7	17.6	19.3
FeO	4.4	4.4	4.5	3.7	5.0	4.4	4.1	7.3	7.1
CaO	5.9	5.9	5.5	5.1	5.7	6.3	6.1	7.8	7.3
MgO	2.5	1.8	2.4	2.1	2.8	2.3	1.8	4.4	4.0
Na$_2$O	4.2	3.5	4.0	4.5	3.8	4.0	3.9	3.5	3.6
K$_2$O	1.33	0.99	1.29	1.31	1.41	1.16	1.07	0.65	0.74
P$_2$O$_5$		0.11			0.11			0.14	0.13
Total	100.91	99.61	100.77	98.19	100.60	100.24	99.13	98.39	99.61
Ni		13			30			45	26
Cr		16			20			41	15
Sc		15			13			24	33
V		84			114			175	174
Ba		225			349			176	225
Rb		11			19			9	12
Sr		935			818			704	680
Zr		132			128			127	138
Y		9			13			18	17
Nb		5			5			5	6
Ga		20			19			21	21
Cu		22			85			40	46
Zn		47			64			63	72
Plag	24	25	22	17.5	32	28.5	49	N.A.	28.5
Cpx	1	1.5	0.5	1	0.5	2.5	1	-	tr
Opx	5	5.5	4	1.5	9.5	1.5	3.5	-	6.5
Hb	2	0	1	2.5	2.5	0.5	1	-	0
Mag	0	0	0	0	tr	1	2	-	tr
Gnd	68	68	72.5	77.5	55.5	66	43.5	-	65

Appendix 2b (cont.)
Chemical Analyses of Castle Rocks Units

Unit	TCR7						TCR8	TCR9	TCR10
Sample	149	150	151	152	153	154	155	156	157
SiO2	56.8	56.9	58.0	58.1	58.4	59.6	59.7	61.0	62.1
TiO2	1.02	1.07	1.05	1.04	1.05	0.86	0.87	0.65	0.66
Al2O3	18.6	18.3	19.5	19.1	19.6	17.4	17.8	17.5	17.5
FeO*	6.6	7.4	6.7	6.7	6.3	6.9	6.7	5.0	5.2
CaO	7.5	6.9	7.0	7.1	6.6	7.0	7.0	6.6	6.2
MgO	3.7	4.6	4.0	3.6	3.5	3.5	3.7	2.3	2.9
Na2O	3.5	3.6	3.7	3.6	3.6	3.6	3.1	3.9	4.0
K2O	0.71	0.77	0.83	0.76	0.86	0.67	0.64	1.18	1.12
P2O5							0.14		0.12
Total	98.33	99.54	100.78	100.00	99.91	99.83	99.65	98.13	99.80
Ni							41		32
Cr							61		53
Sc							20		20
V							162		98
Ba							238		321
Rb							11		21
Sr							669		656
Zr							129		136
Y							15		14
Nb							7		7
Ga							20		20
Cu							6		32
Zn							59		59
Plag	25	29	30	40.5	27	28	30	N.A.	25
Cpx	0.5	0.5	0.5	0.5	1	0.5	1	-	0.5
Opx	7.5	6	7.5	8.5	7	13	12	-	8
Hb	tr	0	0	tr	0	0	0	-	0
Mag	tr	tr	0	tr	0	0	0	-	0.5
Gnd	67.5	64.5	62.0	50.5	72.0	58.5	53.0	-	62.0

Appendix 2b (cont.)
Chemical Analyses of Castle Rocks Units

Unit	TCR10....................TCR11					TCR12......	
Sample	158	159	160	161	162	163	164
SiO_2	62.2	63.0	63.2	63.7	62.4	61.4	62.2
TiO_2	0.64	0.64	0.60	0.64	0.68	0.69	1.03
Al_2O_3	18.6	17.8	17.0	18.5	19.4	17.5	17.6
FeO*	5.1	4.9	4.5	4.8	5.1	5.7	5.0
CaO	6.0	6.1	6.3	6.3	5.3	6.0	5.6
MgO	2.2	1.9	1.8	1.4	2.1	2.4	1.9
Na_2O	3.8	3.7	3.8	2.6	4.0	4.2	4.2
K_2O	1.21	1.40	1.50	1.40	1.13	0.90	1.09
P_2O_5	0.15	0.16					
Total	99.90	99.36	98.70	99.34	100.11	98.79	98.18
Ni	14	26					
Cr	12	16					
Sc	13	7					
V	94	97					
Ba	296	312					
Rb	16	19					
Sr	907	895					
Zr	143	142					
Y	14	14					
Nb	6	5					
Ga	19	17					
Cu	10	33					
Zn	39	58					
Plag	27	24	N.A.	20	15	0	0
Cpx	0	0	-	0	0	tr	0
Opx	0	0	-	0	0	1.5	tr
Hb	12.5	11	-	10.5	6	tr	0
Mag	1.5	1	-	1.5	tr	0	0
Gnd	59.0	64.5	-	68.0	79.0	98.5	100

Appendix 2b (cont.)
Castle Rocks Sample Locations

113 Breccia clast: elev. 3940 ft on Castle Rocks traverse,
     NE1/4NE1/4, Sec. 7, T.11S, R.10E.
114 Breccia clast: elev. 4000 ft on Castle Rocks traverse.
115 Breccia clast: elev. 4100 ft on Castle Rocks traverse.
116 Breccia clast: elev. 4310 ft on Castle Rocks traverse.
117 Breccia clast: elev. 4400 ft on Castle Rocks traverse.
118 Breccia clast: elev. 4460 ft on Castle Rocks traverse.
119 Breccia clast: elev. 3250 ft, NW1/4NE1/4, Sec. 33, T.10S.,
     R.10E.
120 Breccia clast: elev. 4100 ft, SE1/4SE1/4, Sec. 33, T.10S.,
     R.10E.
121 Breccia clast: elev. 3030 ft, NW1/4SW1/4, Sec. 3, T.10S.,
122 Lava flow: elev. 3520 ft, NE1/4NW1/4, Sec. 6, T.11S., R.10E.
123 Lava flow: elev. 4360 ft, SE1/1SW1/4, Sec. 33, T.10S., R.10E.
124 Lava flow: elev. 3420 ft, NW1/4NE1/4, Sec. 33, T.10S., R.10E.
125 Lava flow: elev. 3550 ft, SW1/4SW1/4, Sec. 34, T.10S., R.10E.
126 Lava flow: elev. 3000 ft, NE1/4SW1/4, Sec. 34, T.10S., R.10E.
127 Lava flow: elev. 3380 ft, NW1/4NE1/4, Sec. 4, T.11S., R.10E.
128 Lava flow: elev. 3780 ft, SW1/4NE1/4, Sec. 33, T.10S., R.10E.
129 Lava flow: elev. 3190 ft, SW1/4NE1/4, Sec. 4 T.11S., R.10E.
130 Lava flow: elev. 2560 ft, NW1/4SE1/4, Sec. 34, T.10S., R.10E.
131 Lava flow: elev. 2380 ft, SW1/4NE1/4, Sec. 31, T.10S., R.10E.
132 Dike: elev. 3720 ft, NE1/4NE1/4, Sec. 6, T.11S., R.10E.
133 Lava flow: elev. 3920 ft, SW1/4NE1/4, Sec. 6, T.11S., R.10E.
134 Lava flow: elev. 2680 ft, NW1/4NE1/4, Sec. 20, T.10S., R.10E.
     Anal. # 1008 from Yogodzinski (1985).
135 Lava flow: elev. 2200 ft, SW1/4NE1/4, Sec. 34, T.10S., R.10E.
136 Lava flow: elev. 3880 ft, SW1/4NW1/4, Sec. 33, T.10S., R.10E.
137 Lava flow: elev. 2680 ft, NW1/4SW1/4, Sec. 35, T.10S., R.10E.
138 Lava flow: elev. 4350 ft, NW1/4NW1/4, Sec. 4, T.11S., R.10E.
139 Lava flow: elev. 2990 ft, NE1/4NE1/4, Sec. 4, T.11S., R.10E.
140 Lava flow: elev. 2700 ft., SE1/4 SE1/4 sec. 28, T.10S., R.10E.
141 Lava flow: elev. 4640 ft., NW1/4 NW1/4 sec. 8, T.11S., R.10E.
142 Lava flow: elev. 2800 ft., SW1/4 SW1/4 sec. 27, T.10S., R.10E.
143 Lava flow: elev. 3650 ft., SE1/4 NW1/4 sec. 32, T.10S., R.10E.
144 Lava flow: elev. 2560 ft., SW1/4 NW1/4 sec. 21, T.10S., R.10E.
145 Lava flow: elev. 3660 ft., NW1/4 NE1/4 sec. 9, T.11S., R.10E.
146 Lava flow: elev. 4220 ft., NE1/4 NW1/4 sec. 5, T.11S., R.10E.
147 Dike, elev. 2400 ft., SW1/4 NE1/4 sec. 31, T.10S., R.10E.
     Analysis # 162 from Hales (1975).
148 Lava flow: elev. 2800 ft., NE1/4 NE1/4 sec. 1, T.11S., R.10E.
149 Dike: elev. 3200 ft., SW1/4 SW1/4 sec. 32, T.10S., R10E.
150 Lava flow: elev. 3240 ft., NW1/4 SW1/4 sec. 6, T.11S., R.10E.
151 Lava flow: elev. 2810 ft., NW1/4 NW1/4 sec. 31, T.10S., R.10E.
152 Lava flow: elev. 3250 ft., NE1/4 SE1/4 sec. 3, T.10S., R.10E.
153 Lava flow: elev. 2770 ft., NE1/4 NE1/4 sec. 36, T.10S., R.9E.
154 Lava flow: elev. 3690 ft., SE1/4 SE1/4 sec. 18, T.10S., R.10E.
155 Lava flow: elev. 4200 ft., NE1/4 SE1/4 sec. 18, T.10S., R.10E.
156 Plug: elev. 4000 ft., NE1/4 NE1/4 sec. 6, T.11S., R.10E.
157 Dike: elev. 4200 ft., NW1/4 NW1/4 sec. 5, T.11S., R.10E.

Appendix 2b (cont.)
Castle Rocks Sample Locations

158 Lava flow (dome): elev. 3160 ft, SE1/4SW1/4, Sec. 18, T.11S.,
     R.10E.
159 Lava flow: elev. 2580 ft, SW1/4NWW1/4, Sec. 1, T.11S., R.9E.
160 Lava flow (dome): elev. 3900 ft, SW1/4SE1/4, Sec. 18, T.11S.,
     R.10E.
161 Lava flow (dome): elev. 3800 ft, SW1/4SE1/4, Sec. 18, T.11S.,
     R.10E.
162 Breccia clast: elev. 3520 ft, SW1/4NW1/4, Sec. 19, T.11S.,
     R.10E.
163 Lava flow: elev. 4040 ft, NE1/4SE1/4, Sec. 18, T.11S., R.10E.
164 Lava flow: elev. 4480 ft, SE1/4SE1/4, Sec. 17, T.11S., R.10E.

Appendix 2c
Chemical Analyses of Pre-Deschutes Units

Unit	TPDF1	TPDF2..						
Sample	165	166	167	168	169	170	171	172	173
SiO_2	53.6	53.6	54.0	54.2	54.2	54.5	55.2	55.9	56.0
TiO_2	1.21	1.23	1.25	1.34	1.39	1.28	1.27	1.31	1.29
Al_2O_3	17.2	17.0	17.5	17.4	18.0	17.5	18.3	18.3	18.5
$FeO*$	9.3	9.5	9.0	9.1	9.3	8.8	8.5	8.9	8.8
CaO	7.4	7.2	7.4	7.0	7.0	7.2	7.1	7.1	7.0
MgO	4.5	4.3	3.4	3.7	4.4	4.2	3.5	3.6	3.4
Na2O	3.8	4.0	4.2	4.1	4.0	4.1	4.3	4.3	4.3
K_2O	1.9	1.56	1.55	1.68	1.54	1.62	1.47	1.65	1.55
P_2O_5	0.79	0.87							
Total	99.70	99.26	98.30	98.82	99.83	99.20	99.54	101.06	100.84

Ni	43	39
Cr	50	59
Sc	17	22
V	165	177
Ba	791	810
Rb	20	14
Sr	842	772
Zr	184	181
Y	29	30
Nb	11	13
Ga	18	20
Cu	101	42
Zn	117	105

Plag	0	N.A.	0	0	0	0	0	0	0
Cpx	0	-	0	0	0	0	0	0	0
Opx	0	-	0	0	0	0	0	0	0
Oliv	2.5	-	2	3	1.5	3	3	2	3
Mag	0	-	0	0	0	0	0	0	0
Gnd	97.5	-	98.0	97.0	98.5	97.0	97.0	98.0	97.0

Appendix 2c (cont.)
Chemical Analyses of Pre-Deschutes Units

Unit	TPDF3	TPDF4
Sample	174	175
SiO_2	56.0	56.8
TiO_2	1.29	1.00
Al_2O_3	18.5	18.1
$FeO*$	8.7	7.2
CaO	7.0	7.6
MgO	3.4	4.1
Na_2O	4.3	3.5
K_2O	1.55	1.59
Total	100.74	99.89
Plag	0	19.5
Cpx	0	3
Opx	0	2
Oliv	3.5	tr
Mag	0	0
Bio	0	tr
Gnd	96.5	75.5

Appendix 2c (cont.)
Pre-Deschutes Sample Locations

165 Breccia Clast: elev. 2700 ft, NW1/4NE1/4, Sec. 12, T.11S., R.9E.
166 Lava flow: elev. 2900 ft, NW1/4SW1/4, Sec. 7, T.11S., R.10E.
Anal #319 from Hales (1975).
167 Lava Flow: elev. 3100 ft, NE1/4NW1/4, Sec. 7, T.11S., R.10E.
168 Lava flow: elev. 3100 ft, SE1/4NW1/4, Sec. 7, T.11S., R.10E.
169 Lava flow: elev. 3250 ft, SE1/4NW1/4, Sec. 7, T.11S., R.10E.
170 Lava flow: elev. 3640 ft, NW1/4SE1/4, Sec. 7, T.11S., R.10E.
171 Lava flow: elev. 3600 ft, NW1/4NE1/4, Sec. 7, T.11S., R.10E.
172 Lava flow: elev. 3200 ft, NE1/4NW1/4, Sec. 7, T.11S., R.10E.
173 Lava flow: elev. 3550 ft, SE1/4SW1/4, Sec. 6, T.11S., R.10E.
174 Clast from Mudflow: elev. 2440 ft, NE1/4NW1/4, Sec. 12, T.11S.,
R.9E.
175 Dike: elev. 3000 ft, SE1/4SW1/4, Sec. 31, T.10S., R.10E.

Appendix 2d
Chemical Analyses of Deschutes Formation Units

Unit	TDF1	TDF2	TDF3	TDF6	..........TDF7......................				
Sample	176	177	178	179	180	181	182	183	184
SiO_2	55.2	50.7	66.7	55.0	56.1	54.0	54.4	54.5	54.6
TiO_2	1.26	1.22	0.97	1.40	1.32	1.33	1.37	1.17	1.18
Al_2O_3	18.1	16.6	16.1	19.1	18.6	18.5	17.5	19.3	19.0
FeO^*	8.3	9.9	5.3	9.6	9.1	8.3	8.7	7.8	7.6
CaO	8.1	7.2	2.9	7.2	6.8	8.0	7.3	8.4	8.4
MgO	5.0	3.9	1.1	3.5	3.5	3.5	3.9	3.5	3.8
Na_2O	3.8	3.9	4.8	3.8	4.1	3.7	4.1	3.8	3.7
K_2O	0.96	1.16	2.51	0.63	0.71	0.95	1.04	0.62	0.80
Total	100.82	94.58	100.38	100.83	100.23	98.28	98.31	99.09	99.08
Plag	0	2	N.A.	1	tr	N.A.	N.A.	N.A.	21.5
Cpx	0	0	-	0	0	-	-	-	0
Opx	0	0	-	0	0	-	-	-	0
Oliv	2	2.5	-	0	0	-	-	-	1
Mag	0	0	-	0	0	-	-	-	tr
Gnd	98.0	95.5	-	99.0	100	-	-	-	77.5

Appendix 2d (cont.)
Chemical Analyses of Deschutes Formation Units

Unit	TDF7					TDF8			
Sample	185	186	187	188	189	190	191	192	193
SiO_2	54.7	55.1	55.4	55.7	56.6	55.7	56.7	56.7	57.0
TiO_2	1.22	1.45	1.34	1.32	1.15	1.91	1.72	1.71	1.65
Al_2O_3	19.5	19.2	18.1	18.0	18.8	15.6	16.1	15.8	16.0
FeO*	7.9	8.6	8.6	9.2	7.8	10.0	9.2	10.2	9.0
CaO	8.2	8.4	7.2	6.9	7.8	6.7	6.6	6.7	6.5
MgO	3.6	3.8	3.4	4.2	3.7	3.2	3.2	3.3	3.3
Na_2O	3.8	3.6	3.9	4.2	3.7	4.1	4.1	4.1	4.1
K_2O	0.82	0.82	1.00	0.75	0.77	1.02	1.18	1.15	1.25
Total	99.64	100.97	98.94	100.27	100.32	98.23	98.80	99.66	98.80
Plag	17.5	18.5	N.A.	N.A.	1	0.5	1.5	1.5	1
Cpx	0	0	-	-	0	0	0	0	0
Opx	0	0	-	-	0	0	0	0	0
Oliv	0.5	1	-	-	0.5	tr	tr	tr	tr
Mag	tr	tr	-	-	0	0	tr	tr	tr
Gnd	82.0	80.5	-	-	98.5	99.0	98.5	98.5	99.0

Appendix 2d (cont.)
Chemical Analyses of Deschutes Formation Units.

Unit	TDF8........	
Sample	194	195
SiO_2	57.2	57.6
TIO_2	1.67	1.71
Al_2O_3	15.8	16.1
FeO*	8.9	9.1
CaO	6.5	6.4
MgO	3.3	3.0
Na_2O	4.2	4.1
K_2O	1.24	1.22
Total	98.81	99.23
Plag	1	1
Cpx	tr	tr
Opx	0	0
Oliv	tr	tr
Mag	tr	tr
Gnd	99.0	99.0

Appendix 2d (cont.)
Deschutes Formation Sample Locations

176 Dike: elev 3710 ft, NW1/4SW1/4, Sec.19, T.11S., R10E.
177 Breccia Clast: elev. 3170 ft, NW1/4NW1/4, Sec.19, T.11S., R.10E.
178 Clast from ash-flow tuff: elev. 3200 ft, SE1/4NW1/4, Sec. 17, T.10S., R.10E. Anal. #1053 from Yogodzinski (1985).
179 Megacryst-bearing lava: elev. 3560 ft, NW1/4SW1/4, Sec.22, T.11S., R.10E. Anal. #QB-1 from Conrey (1985).
180 Megacryst-bearing lava: elev. 3570 ft, NW1/4SW1/4, Sec. 22, T.11S., R.10E. Anal. #J-2 from Conrey (1985).
181 Lava flow: elev. 5000 ft, NW1/4NE1/4, Sec. 19, T.11S., R.10E. Anal. #246 from Hales (1975).
182 Lava flow: elev. 4520 ft, NW1/4NW1/4, Sec. 20, T.11S., R.10E. Anal. #244 from Hales (1975).
183 Lava flow: elev. 4400 ft, NW1/4NW1/4, Sec.17, T.11S., R.10E. Anal. #241 from Hales (1975).
184 Lava flow: elev. 4450 ft, SW1/4NW1/4, Sec. 17, T.11S., R.10E.
185 Lava flow: elev. 2640 ft, SW1/4SE1/4, Sec. 12, T.11S., R.9E.
186 Plagioclase phyric lava flow: elev. 3380 ft, SW1/4SW1/4, Sec.14, T.11S., R.10E.
187 Lava flow: elev. 4850 ft, SW1/4SW1/4, Sec. 17, T.11S., R.10E. Anal. #243 from Hales (1975).
188 Lava flow: elev. 3190 ft, NW1/4SE1/4, Sec. 23, T.11S., R.10E. Anal. #202 from Hales (1975).
189 Lava flow: elev. 2700 ft, SW1/4SE1/4, Sec. 12, T.11S., R.9E.
190 Aphyric lava: elev. 3120 ft, NW1/4NW1/4, Sec. 27, T.10S., R.10E. Anal. #1033 from Yogodzinski (1985).
191 Aphyric lava: elev. 3020 ft, NW1/4SE1/4, Sec. 21, T.10S., R.10E. Anal. #1035 from Yogodzinski (1985).
192 Aphyric lava: elev. 3120 ft, SW1/4SW1/4, Sec. 22, T.10S., R.10E. Anal. #1037 from Yogodzinski (1985).
193 Aphyric lava: elev. 3050 ft, NW1/4NW1/4, Sec. 27, T.10S., R.10E.
194 Aphyric lava: elev. 2820 ft, NW1/4NW1/4, Sec. 27, T.10S., R.10E. Anal. #1038 from Yogodzinski (1985).
195 Aphyric lava: elev. 2800 ft, NE1/4NE1/4, Sec. 20, T.10S., R.10E. Anal. # 1036 from Yogodzinski (1985).R.10E.

Appendix 2e
Chemical Analyses of High Cascade Units

Unit   THC1...

Sample	196	197	198	199	200	201	202	203	204
SiO_2	53.0	53.4	53.5	53.5	54.3	54.6	54.7	54.7	54.7
TiO_2	1.70	1.42	1.31	1.33	1.38	1.05	1.19	0.85	1.28
Al_2O_3	17.8	17.4	17.5	18.0	17.1	18.0	17.4	16.1	17.7
$FeO*$	10.4	9.2	8.6	8.8	8.7	7.7	8.2	10.3	8.5
CaO	8.3	7.5	7.9	8.1	7.5	7.9	7.9	8.2	7.7
MgO	3.9	4.9	4.8	3.7	4.8	5.4	5.6	3.0	5.2
Na_2O	3.8	3.7	3.6	3.8	3.7	3.5	3.6	4.3	3.7
K_2O	0.60	0.92	0.99	0.95	0.88	0.90	0.94	1.30	0.85
Total	99.50	98.44	98.20	98.18	98.36	99.05	99.53	98.75	99.63
Plag	N.A.	2	3	N.A.	2	5	2	N.A.	3
Cpx	-	0	1.5	-	0	0	0	-	0
Opx	-	0	0	-	0	0	0	-	0
Oliv	-	2	2	-	2	2	3	-	1
Mag	-	0	tr	-	0	0	0	-	0
Gnd	-	96.0	93.5	-	96.0	93.0	95.0	-	96

Appendix 2e (cont.)
Chemical Analyses of High Cascade Units

Unit	THC1...................................THC2..............							
Sample	205	206	207	208	209	210	211	212	213
SiO_2	54.9	55.0	55.2	56.4	57.0	57.9	57.6	57.7	59.0
TiO_2	0.97	0.97	1.25	0.88	1.25	0.92	0.81	0.85	0.99
Al_2O_3	18.6	18.2	17.4	18.0	18.0	19.1	18.7	18.3	18.3
FeO*	6.8	7.2	8.1	7.3	6.8	6.3	6.3	6.5	6.3
CaO	7.5	8.2	8.1	8.0	7.5	6.9	7.5	7.7	6.6
MgO	4.5	4.3	5.3	5.6	3.0	3.8	3.9	3.0	2.9
Na_2O	4.0	3.5	3.6	3.7	4.1	4.0	4.5	4.1	4.4
K_2O	0.98	1.03	0.80	0.75	1.10	1.00	0.72	0.99	0.85
Total	98.25	98.40	99.75	100.63	98.75	99.92	100.03	99.14	99.34
Plag	73	N.A.	1	77	N.A.	0	7	N.A.	12
Cpx	7	-	0	4	-	0	1	-	1
Opx	11	-	0	13	-	0	0	-	0
Oliv	1	-	2	0	-	0	3	-	1.5
Mag	0	-	0	2	-	0	0	-	0
Kspar	8	-	0	4	-	0	0	-	0
Gnd	0	-	97.0	0	-	100.0	89.0	-	85.5

Appendix 2e (cont.)
Chemical Analyses of High Cascade Units

Unit	THC3		THC4						
Sample	214	215	216	217	218	219	220	221	222
SiO_2	50.0	50.1	48.0	49.4	50.1	50.2	51.1	51.5	51.8
TiO_2	2.04	1.91	1.37	1.24	1.32	1.19	1.31	1.31	1.36
Al_2O_3	15.4	15.9	17.4	16.0	14.2	15.4	15.4	14.9	14.1
FeO*	10.7	10.5	10.7	12.3	11.8	12.4	11.1	11.7	11.6
CaO	8.2	8.7	10.0	9.7	9.6	9.7	9.0	9.3	9.2
MgO	9.2	8.1	9.0	8.3	8.2	9.8	6.4	8.4	7.8
Na_2O	3.1	3.0	3.0	2.6	2.8	2.6	2.9	2.9	3.0
K_2O	0.54	0.55	0.17	0.14	0.20	0.26	0.20	0.25	0.29
P_2O_5		0.37	0.22	0.16					
Total	99.18	99.13	99.86	99.84	98.22	101.55	97.41	100.26	99.15

Ni		191	161	160					
Cr		420	248	321					
Sc		21	33	27					
V		211	212	241					
Ba		320	136	171					
Rb		2	2	1					
Sr		475	353	502					
Zr		171	102	83					
Y		30	25	22					
Nb		15	4	2					
Ga		18	15	17					
Cu		57	41	26					
Zn		115	69	93					

Plag	0	0	0	0	0	N.A.	N.A.	0	0
Cpx	0	0	0	0	0	-	-	0	0
Opx	0	0	0	0	0	-	-	0	0
Oliv	12	12	17	18	18	-	-	11	18
Mag	0	0	0	0	0	-	-	0	0
Gnd	88.0	88.0	83.0	82.0	82.0	-	-	89.0	82.0

Appendix 2e (cont.)
Chemical Analyses of High Cascade Units

Unit	THC4.......................QHC5.......					
Sample	223	224	225	226	227	228
SiO_2	52.4	49.7	50.2	50.5	70.4	70.4
TiO_2	1.32	1.55	1.38	1.59	0.48	0.46
Al_2O_3	14.6	16.5	17.5	16.7	15.5	16.1
FeO*	11.7	10.2	10.7	10.7	3.5	3.2
CaO	9.3	9.3	9.4	9.5	2.9	3.1
MgO	7.5	7.4	7.5	7.0	1.0	1.0
Na2O	2.9	3.1	2.7	3.4	4.2	4.4
K_2O	0.30	0.26	0.16	0.30	1.55	1.90
P_2O_5		0.27	0.21			
Total	100.02	98.28	99.75	99.49	99.53	100.56
Ni		135	139			
Cr		252	294			
Sc		30	30			
V		223	206			
Ba		216	361			
Rb		2	2			
Sr		394	348			
Zr		124	106			
Y		29	26			
Nb		4	4			
Ga		18	18			
Cu		103	59			
Zn		97	79			
Plag	N.A.	0	0	0	N.A.	N.A.
Cpx	-	0	0	0	-	-
Opx	-	0	0	0	-	-
Oliv	-	18	17	18	-	-
Mag	-	0	0	0	-	-
Gnd	-	82.0	83.0	82.0	-	-

196 Lava flow: elev. 3700 ft, SW1/4NE1/4, Sec. 20, T.11S., R.9E. Anal. #276 from Hales (1975).

197 Lava flow: elev. 5758 ft, NE1/4SW1/4, Sec. 21, T.10S., R.9E. Anal. #1057 from Yogodzinski (1985).

198 Lava flow: elev. 5235 ft, NW1/4SE1/4, Sec. 1, T.11S., R.9E.

199 Lava flow: elev. 5200 ft, SW1/4SW1/4, Sec. 32, T.10S., R.9E. Anal. #311 from Hales (1975).

200 Lava flow: elev. 4740 ft, SW1/4SW1/4, Sec. 16 T.10S., R.9E. Anal. #1059 from Hales (1975).

201 Lava flow: elev. 5260 ft, NE1/4SW1/4, Sec. 21, T.10S., R.9E. Anal. #1074 from Yogodzinski (1985).

202 Lava flow: elev. 6300 ft, SE1/4NW1/4, Sec. 32, T.10S., R.9E. Anal. #1066 from Yogodzinski (1985).

203 Lava flow: elev. 5600 ft, NW1/4SW1/4, Sec. 21, T.10S., R.9E. Anal. #326 from Hales (1975).

204 Lava flow: elev. 5340 ft, NW1/4SW1/4, Sec. 32, T.10S., R.9E.

205 Bald Peter Plug: elev. 5320 ft, NW1/4SW1/4, Sec.32, T.10S., R.9E. Anal. #1076 from Yogodzinski (1985).

206 Porphyrytic lava flow: elev. 6650 ft, SE1/4SE1/4, Sec. 32, T.10S., R.9E. Anal. #309 from Hales (1975).

207 Subphyric lava flow: elev. 3480 ft, NW1/4SE1/4, Sec. 20, T.10S., R.10E.

208 Bald Peter plug: elev. 5240 ft, NW1/4SW1/4, Sec. 32, T.10S., R.9E. Anal. #1077 from Yogodzinski (1985).

209 Porphyrytic lava flow: elev. 6650 ft, SE1/4SE1/4, Sec.32 T.10S., R.9E. Anal. #308 from Hales (1975).

210 Subphyric lava flow: elev. 3330 ft, NE1/4NE1/4, Sec. 23, T.11S., R.10E.

211 Subphyric lava flow: elev. 3080 ft, SE1/4NE1/4, Sec. 14, T.11S., R.9E.

212 Porphyrytic lava flow: elev. 3400 ft, SW1/4NE1/4, Sec. 14, T.11S., R.9E. Anal. #309 from Hales (1975).

213 Subphyric lava flow: elev 3530 ft, SE1/4SE1/4, Sec. 11, T.11S.,

214 Lava flow from Metolius Bench: elev. 3100 ft, NW1/4NW1/4, Sec. 21, T.10S., R.10E.

215 Lava flow from Metolius Bench: elev. 3220 ft, SE1/4NW1/4, Sec. 35, T.10S., R.10E.

216 Intracanyon lava flow, normal polarity: elev. 2980 ft, NW1/4 NE1/4, Sec. 13, T.11S., R.9E.

217 Intracanyon lava flow, normal polarity: elev. 2940 ft, NW1/4 SW1/4, Sec. 29, T.10S., R.10E.

218 Intracanyon lava flow, normal polarity: elev. 2560 ft, NE1/4 SE1/4, Sec. 12, T.11S., R.10E.

219 Diktytaxitic dike: elev. 3700 ft, NW1/4, Sec. 30, T.11S., R.10E. Anal. #563b from Conrey (1985).

220 Intracanyon lava flow: elev. 3200 ft, NE1/4, Sec. 35, T.11S., R.9E. Anal. #120 from Conrey (1985).

221 Intracanyon lava flow, normal polarity: elev. 2920 ft, NW1/4 NE1/4, Sec. 29, T.10S., R.10E.

222 Intracanyon lava flow, normal polarity: elev. 2680 ft, NE1/4 NW1/4, Sec. 2, T.10S., R.10E., R.9E. Anal. #1062 from Yogodzinski (1985).

<u>223</u> Intracanyon lava flow, normal polarity: elev. 2700 ft, NW1/4
       NW1/4, Sec. 2, T.10S., R.10E.
<u>224</u> Intracanyon lava flow, reverse polarity: elev. 3000 ft, NW1/4
       SW1/4, Sec. 29, T.10S., R.10E.
<u>225</u> Intracanyon lava flow, reverse polarity: elev. 3020 ft, NE1/4
       NW1/4, Sec. 13, T.11S., R.10E.
<u>226</u> Intracanyon lava flow, reverse polarity: elev. 2340 ft, NE1/4
       SE1/4, Sec. 14, T.11S., R.9E.
<u>227</u> Hornblende pumice, white: elev. 2110 ft, SE1/4NE1/4, Sec. 3,
       T.11.S., R.10E.
<u>228</u> Hornblende pumice, white: elev. 2600 ft, SW1/4SE1/4, Sec. 13,
       T.11S., R.9E.